COMPOSITION, VARIATIONS AND EXCITATION OF THE AURORAL LUMINESCENCE SPECTRA

BY
L. VEGARD
(Manuscript received November 26th, 1955)

§ 1. Introduction.

The present paper deals with results of auroral spectrograms obtained at the Tromsø observatory during the winters 1951/52 and 1952/53. We have first of all used the two big glass-spectrographs «V» and «F», built by Société Générale d'Optique in Paris. The collimator lens of the «V» — and «F»-spectrographs had a diameter of 178 mm and 240 mm respectively and the two prisms had corresponding dimensions.

Light power and dispersion will be seen from table I.

Table I

Wavelength (Å)	Scale value (Å/mm)	
	Spectr.«V»(F:1,2)	Spectr.«F»(F:0,65)
4 000	40	77
5 000	99	205
6 000	188	395
7 000	308	650

The «V» spectrograph was put up at Tromsø in the summer 1950 and the «F» spectrograph one year later.

In dealing with the physical interpretation of the auroral spectrum and its great variability, we are now in the favourable position that we know the essential features and properties of the solar electric ray bundles, which produce the aurora.

The conception arrived at, that they consist of rapidly moving electrons neutralized by slower positive ions, dates back to 1916 (1).

A theory of the upper atmosphere based on certain results from the auroral spectral investigations led to a theory regarding the formation of such bundles and their connection with solar activity (2, 3, 4, 5, 6, 7, 8).

Regarding the properties of such bundles it was pointed out as early as 1916 that the mutual electro-magnetic attraction between the rapidly moving electrons helps to contract the bundle so that it maintains a somewhat limited cross section (cfr. paper 1, p. 871).

The bundle has a similar constitution as the long narrow electron ray bundles which are known to be emitted from a hot cathode in a discharge tube, e. g. like those used by Brüche for the illustration of Størmer's auroral theory (cfr. e.g. paper 6 p. 612).

These narrow bundles produced in laboratories are electrostatically neutralized by positive ions and maintain the small cross-section through the mutual electro-magnetic attraction between the moving electrons.

Thus the electro-magnetic focussing effect is an inherent property attached to the solar bundles which according to my view produce the auroral luminescence.

The correctness of the assumed constitution of the solar bundles was proved in 1939 (9), when it was found that showers of hydrogen occasionally entered into the atmosphere, and when, in 1940—41, it was found that auroral spectrograms showed hydrogen lines broadened and displaced towards shorter waves through Doppler effect (10, 11, 12, 13.)

The Doppler effect of auroral hydrogen lines has been studied in greater details from spectrograms obtained with the new «V» spectrograph at Oslo Feb. 23—24 1950 (15,16), and at Tromsø in the beginning of 1951 (17, 18, 19).

My detection and further studies of the Doppler effect were based on the H_β — and partly on the H_γ-line. On account of the small dispersion of our spectrographs in the long wave region the Doppler displacement of H_α was very small and likely to be masked by other spectral features, particularly by bands of $N_2$1P.

Meinel and Gartlein using grating spectrographs, succeeded in obtaining from an aurora on August 18—19, 1950, spectrograms showing the Doppler displacement of H_α (20, 21). This, however, is no discovery of the Doppler effect of auroral hydrogen lines; for many years earlier it had been found by means of H_β and on a number of spectrograms.

With regard to the history of the detection of the Doppler effect of auroral hydrogen lines, we may refer to a paper published in «Geof. Publ. 1952» (14) to the papers (16) and (19) and to reports and papers read at international meetings and congresses (17, 18).

A preliminary account of some results to be dealt with in the present paper was given at the meeting of the General Assembly of I. U. G. G. at Rome 1954. The account was based on a paper: «Intensity Variations of Hydrogen Lines and the influence of the Solar Proton Radiation on the Auroral Luminescence recently published in G. P. Oslo (22).

The best procedure will be to treat the spectrograms from the «V» and the «F» spectrograph separately.

The main interest of the «V» spectrograms is connected with wavelength measurements and identification of the bands and lines appearing in the auroral luminescence, the most accurate determination of ionospheric temperature, the appearance of hydrogen lines and the determination of the proton velocities from their Doppler-displacement.

The «F» spectrograms, which require much shorter exposure, may give information regarding the variability effects, e.g. variations of spectral features with altitude and latitude, with auroral types, and changes in auroral spectra possibly connected with the intensity of the hydrogen lines, meaning to investigate the influence of proton excitation on the auroral spectrum.

We have also found it important to determine the ionospheric temperature from N_2^+1N bands obtained with the much smaller dispersion of the «F»-spectrograph.

On account of the much greater light power of this instrument the F-spectrograms may help us to solve the important problem of finding out whether the ionospheric temperature increases very greatly towards greater altitudes e.g. those of the F_2-layers.

SECTION A

AURORAL SPECTROGRAMS TAKEN WITH THE «V»-SPECTROGRAPH

§ 2. General Remarks.

During the two winters 1951/52, 52/53, 8 «V»-spectrograms were obtained, 4 each winter, and they are reproduced on Pl. I. The most important data are given in the «Explanation to Pl. I» at the end of the paper.

We have tried different sorts of plates:

Spectrograms Nos. 1, 2, 7 were taken on Kodak 103a F

Spectrograms Nos. 5, 6, 8 were taken on Kodak 103a C

Spectrograms Nos. 3 were taken on Kodak 103a T

Spectrograms Nos. 4 were taken on Kodak 103a O.

The F-plate has the advantage of a great sensitiveness in red, and is the only one of the plates tried that can be used with advantage when we want to obtain H_α. From green towards shorter waves its sensitiveness does not seem to be so good as that of the plates T- and C.

The O-plate is only sensitive in the short wave region. We thought that it might be used with advantage for the study of H_β, but it is difficult to draw any definite conclusion from a single auroral spectrogram.

The main interest of spectrogram No 4 is connected with the nitrogen bands 4278 and 3914 which give good conditions for temperature measurements.

With the exposure of three of the spectrograms Nos. 1, 3 and 5 the spectrograph was all the time directed towards magnetic zenith - which means in the direction of the magnetic lines of force and of the auroral streamers.

This procedure is in many respects of great interest.

a. The protons and the emitting hydrogen atoms have the maximum velocity towards the observer under the conditions present during the exposure.
b. When by means of the condensor lens an image of the auroral radiation-point (magnetic zenith) is thrown on the slit of the spectrograph, there is a great chance that a considerable fraction of the auroral light entering the slit is emitted from near the top of the auroral ray streamers because they appear to meat at the radiation points.

In this convenient way we may be able to detect and study intensity variations of auroral features with increasing altitude, e.g. the variation of relative intensity of H-lines, the forbidden OI and NI lines, the possible change with altitude of the ionosperic temperature and of the intensity of many other lines and bands present in the auroral luminescence.

This method of studying altitude effects, however, has the disadvantage that it requires long exposure, and can therefore only give average effects for a certain period.

For the study of variation effects on a definite auroral type or situation it is essential to use spectrographs of the greatest possible light power, and at any moment direct the instrument in the direction wanted. For the study of altitude effects a method used with great advantage has been to compare spectrograms taken from near the upper limit of the aurora with such taken from near the bottom edge of the same auroral type. The procedures used in the study of variability effects will be further dealt with in connection with spectrograms obtained with the «F»-spectrograph.

As a matter of fact during the exposure of the three «V»-spectrograms Nos. 1, 4, 5 the instrument was directed towards magnetic zenith and No. 5 shows the H_β and H_γ with very pronounced doppler displacement towards shorter waves. No 1 shows the H_α line but the doppler displacement is masked by the band $N_2$1P (7—4), and the exposure is too weak to show H_β and H_γ.

With spectrogram No. 2 the instrument was kept directed towards the magnetic meridian and the light would mainly come from the lower part of the aurorae. In this case no H-lines appeared, but this may be partly due to weak exposure.

When the other «V»-spectrograms Nos. 3, 6, 7, 8 were taken, the spectrograph was directed towards the strongest part of the aurorae and preferably near the zenith.

No. 3 for which the plate was insensitive to H_α — shows a weak broadened and displaced H_β-line. Comparing Nos 1 and 7 taken on the same sort of plate and having about the same degree of exposure, it is seen that No. 1 shows the H_α-line quite marked, while no indication of the presence of H_β is to be noticed. The three spectrograms 6, 7 and 8 were obtained during my stay at Tromsø, January 1953.

The strongly exposed spectrogram No. 8, was obtained in a single night with intensive auroral displays. It was moonlight and although the instrument was directed far away from the moon, the Fraunhofer lines due to the moonlight appeared. Still a great number of auroral emission lines are clearly seen.

It is of particular interest to notice that the Fraunhofer absorption H_β — and H_γ = lines appear quite distinctly, while no trace of auroral H_β = or H_γ-emission lines can be detected in spite of the strong exposure. *This means that the proton flux of the solar bundles has been very small, and that the predominant part of the auroral luminescence was due to electron excitation.*

It is also of interest to notice, that the sodium D-doublet appears quite distinctly on all «V» spectrograms except No. 4 taken on a plate insensitive to yellow.

§ 3. Wavelength and Intensity Measurements from «V»-spectrograms.

On the spectrograms a number of features usually appears which are sufficiently strong to be measured directly on the negative by means

Table II a. The Long-wave part of Spectrograms Pl. I No. 1, 2, and 7.

No. 1		No. 2	No. 7	Previously measured	Interpretation
I	λ	λ	λ	λ	
1,6	6891,5	6888,8	6889,3	6895,5	N_2^+ 2N(2—0)
	80,1	78,6			N_2 1P(3—0)
				63,5	N_2 1P(3—0)
3,6	58,9	58,0	58,8	58,3	N_2 1P(3—0), N_2^+ 2N(2—0), NII(57,6)O_2^+ 1N(0—2)
	42,9		44,9	42,5	N_2 1P(3—0), V.K. (7—22)
	39,6			34,1	V.K. (3—19)
5,3	6786,1	6786,2	6786,6	6786,3	$N_2$1P(4—1) (16—15)
	80,2	79,1	78,1	80,8	N_2 1P(4—1) (16—15)
	61,2	60,1	58,2	51,3	N_2 1P(4—1)
				42,9	NI(41,3)
5,0	03,4	05,5	03,4	04,7	NI(06,2), $N_2$1P(5—2)
	6693,4	6695,8	6694,5	6693,5	N_2 1P(5—2)
	83,9			87,2	N_2 1P(5—2)
	74,8	76,3	75,1	74,5	$N_2$1P(5—2) OII(78,2)
				66,9	OII(66,9), NI(66.8)
				55,2	NI(53,4, 56,6), OI(53,8)N_2^+2N(6—3)
				49,0	NI(46,5), N_2 1P(6—2)
		38,2			V.K. (2—18) (6—21), O_2 S.R. (2—29)
				30,0	NII (30,5)
4,0	20,3	23,1	22,6	21,7	N_2^+2N(6—3), $N_2$1P(6—3), NI(22,5)
	13,2	11,8	12,0	(16,8)	$N_2$1P(6—3)
	07,5			08,0	$N_2$1P(6—3)
	6594,0	6594,9	6594,5	6592,6	$N_2$1P(6—3)
				83,3	NII(83,4)
		61,5		62,5	$H\alpha$
3,6	56,9		58,8	58,5	$H\alpha$ displaced
			54,7	54,5	NII(54,5)
				51,7	NII $2p^2(^3P_1—^1D_2)$
3,8	42,4	42,8	43,2	42,0	$N_2$1P(7—4), O_2 S.R. (1—28)
	34,0	34,5	33,7		«
				27,7	«
	10,5	10,6	14,0	12,1	NI(10,3)
				05,5	NI(06,), NII(04,9)
1,6	6480,5	6482,3	6482,4	6480,2	NII(82), N_2^+2N(5—2)
1,9	64,8	66,6	68,2	66,5	1P(8—5)
	55,2	57,7	57,1	53,9	$N_2$1P(8—5), OI(53,6, 54,5)
	39,4	39,5	41,5	37,9	V.K.(5—20), N_2^+2N(5—2), NI(37,3), 1P(8—5)
		27,9	26,8	(33)	NI(28)
	14,1			17,0	NI(17,1), O_2^+1N(0—1)
			04,1		NI(07,7)
	6398,8		6397,0	6398,0	$N_2$1P(9—6)
1,3	91,3	6392,7	91,0	91,0	OI$(^3P_0—^1D_2)$, 1P(9—6), O_2^+1N(0—1)
	87,6	82,1	82,0	79,8	$N_2$1P(9—6), NI(78) «
13,1	63,8	63,8	63,8	63,2	OI$(^3P_1—^1D_2)$, $N_2$1P(9—6), N_2^+2N(9—5)
		48,4			NII(47,1), 1P(11—8)
	25,7	28,5	30,2		NII(28,6)
	23,6			20,7	NI(21,7), $N_2$1P(10—7), S.R. (6—31)
	19,8			18,0	NI(18,8) «
	6300,3	6300,3	6300,3	6300,3	OI$(^3P_2—^1D_2)$, N_2^+2N(4—1)
	6277,3		6278,0		NI(76)
	71,0			6272,4	NI(72,8), N_2^+2N(4—1), V.K.(0—16), S.R.(2—28)
				67,0	OI(66,9)
			60,0	64,0	OI(64,4)
				52,0	$N_2$1P(11—8), V.K. (4—19)

Table II a. The Long-wave part of Spectrograms Pl. I No. 1, 2, and 7.

No. 1		No. 2	No. 7	Previously measured	Interpretation
I	λ	λ	λ	λ	
	6243,9	6241,8	6242,0	43,8	NI(43,2), $N_2 1P$(11—8)
		38,8	35,4	39,6	NI(37,5) «
	. 24,5	24,9		23,0	NI(24,0), S. R. (5—30)
	6198,9	6196,8			
	89,1		91,4	85,0	$N_2 1P$(4—0)
	79,5		78,5		«
	76,2			75,0	O_2 S.R. (1—27) (76,5), NII(73,4)
	69,8	67,1	65,7		$N_2 1P$(4—0) (12—9)
1,8	57,5		56,0	55,6	OI(56,0) (56,8)
	37,9			38,2	$N_2^+ 2N$(3—0), NII(36,9)
	27,6		27,0	27,0	«
	23,8				V.K. (7—21) (23), O_2 S.R. (4—29) (24)
	18,2	18,2	16,7	19,0	$N_2 1P$(5—1), S.R. (7—31)
	10,2		10,1	9,0	$N_2^+ 2N$(3—0) (10), $N_2 1P$(5—1)
2,1	07,2	08,1			OI(06,3)
			6082,8	6078,0	V.K. (3—18), O_2 S.R. (0—26)
			70,8	71,0	$N_2 1P$(6—2), NI(69,0)
2,0	6065,8	6066,8		67,3	«
	58,7		59,3	59,6	« NI(61,9)
2,4	43,0		41,7	44,3	NI(44,8)
	21,5		20,4	23,3	$O_2^+ 1N$(0—0)
3,0	10,1	10,7	12,0	11,2	NI(08,4, 12,0), $N_2 1P$(7—3)
	04,0	02,6		02,0	$O_2^+ 1N$(0—0) (1—1), NI(5999,6), $N_2^+ 2N$(7—3)
	5990,5	5989,2	5993,3	5990,5	$N_2 1P$(7—3), $O_2^+ 1N$(0—0), OI(95,3, 93,5)
3,1	74,8	75,9	74,2	75,5	$O_2^+ 1N$(11—1) (0—0), $N_2^+ 2N$(7—3), NI(72,1)
2,7	56,2	59,3	57,4	58,0	NI(58,8), $N_2 1P$(8—4), NII(60,9)
	52,4				NII(52,4)
	50,0		49,7	51,0	NI(51,1), $N_2 1P$(8—4), V.K. (6—20), NII(52,4)
				40,0	NI(41,9), NII(40,3), 41,7, $N_2 1P$(8—4)
2,3	32,8	33,7		34,0	O_2 S.R. (2—27) (32,7), $N_2 1P$(8—4)
	31,1	31,2		30,0	NI(31,2), NII(31,8)
				27,3	NI(27,5), NII(27,8), $O_2^+ 1N$(2—2)
		13,0	17,0		V.K. (2—17)
				03,3	$N_2 1P$(9—5), NI(05,07)
3,9	5892,3	5892,3	5892,3	5892,1	NaD_1, D_2, $N_2 1P$(9—5)

of a comparator. But usually structures can be noticed indicating the presence of lines so weak and closely packed that they cannot be seen in the microscope of the comparator. In that case we have to take our refuge in photometer curves. The procedure has been described in previous papers (16, 19) when a registering Moll-photometer was used.

By the wavelength and intensity measurements dealt with in this paper, we have mainly been using a Knorr-Albers registering photometer of much greater sensitivenes and magnification, which belongs to the Central Institute for Industrial Research.

The spectrograms Nos. 4 and 6 only show some of the strongest features, already well known and measured. On Nos 1, 2, 7, some lines and bands in the red part and on No. 1 also some weaker lines in the region of shorter waves appear and they were measured by means of photometer curves of great magnificatin. The results are given in the tables IIa and IIb.

The first column contains intensities (I) measured for some moderately strong lines.

The strongest bands of $N_2^+ 1N$ and the forbidden OI lines are too heavily exposed for accurate intensity measurements.

The last column gives possible interpretations.

Table II b.

The short wave part of «*V*» Spectrogram Pl. I No. 1.

Pl. I No. 1 I	Pl. I No. 1 λ	Previous obs. λ	Interpretation
	5875,6	5877,9	$O_2^+1N(3—3)$
	69,2	65,6	$N_2^+1N(0—4)$
	56,4	53,0	*NI*(54,1, 56,1), 1*P*(10—6)
	44,5		$O_2^+1N(4—4)$ »
	41,2	42,0	*NI*(41,1), $N_2^+1N(6—2)$ »
	33,8	31,8	*NI*(34,8) 1*P*(10—6)
2,2	26,4		*NI*(29,6)
	16,9		*NI*(16,5)
	09,0	09,0	$N_2^+2N(6—2)$
	05,9		1*P*(11—7), *NI*(03)
	5799,5	01,0	»
	96,5		»
	93,2	5790,0	» *NI*(90,4)
	82,8	0	*NI*(81,7)
	76,8		*V.K.*(5—19) (77,8)
	73,0	70,7	*NI*(72,8), $N_2^+2N(10—5)$
	66,9	66,0	*NII*(67,4), *NI*(68,6)
	63,9		*NI*(64,5), 1*P*(12—8)
	53,7	53,6	*NI*(52,7), *NII*($^1D_2—^1S_0$) 1*P*(12—8)
	49,5	45,0	*NII*(47,3), S.R. (0—25)
	38,7		1*P* (12—8), *NI*(35,6, 40,0)
	28,9	30,0	» *NI*(28,8)
	26,6	25,6	»
		10,5	*N*(10,5), *NII*(10,8)
	5690,3	5688,0	$N_2^+2N(5—1)$, *NII*(86,2)
2,4	80,0	79,5	*NII*(79,6)
	{70,1		$N_2^+1N(3—7)$
1,8	{68,2	66,2	*NII*(66,6)
	{64,1	58,0	$N_2^+2N(5—1)$, S.R.(8—30)
	{30,5	30,0	$O_2^+1N(1—0)$, 1*P*(5—0)
2,7	{23,6	21,4	» »
	{14,6	13,5	» »
	05,5	06,7	» *NI*(04,4)
	02,2	01,3	» *NI*(00,5)
V.str.	5577,35	5577,35	*OI*($^1D_2—^1S_0$)
	5554,8	5554,0	*OI*(54,9) 1*P*(7—2)
	43,0	43,0	*NI*(43,5) » $N_2^+2N(4—0)$
	5487,0	87,5	*OI*(86,6) $N_2^+1N(4—8)$
	76,8	77,0	*NI*(78,1) 1*P*(9—4)
	67,8	67,0	V.K.(3—17)
	61,9	61,8	*NII*(62,5), 1*P*(9—4)
	40,7	42,8	1*P*(10—5)
	37,0	37,3	*OI*(35,2, 35,8, 36,8), S.R.(0—24)
	25,5	26,0	S.R. (3—26)
	20,0	21,7	1*P*(10—5)
	10,0	11,0	*OI*(10,8)
	5366,0	5368,5	*NI*(67,3)
	61,8	60,0	*NI*(60,1)
	51,6	50,0	*NI*(51,2)
	30,2	30,5	*OI*(29,0, 26,6, 30,7) *NI*(28,8)

Table II b continued.

Pl. I No. 1 I	Pl. I No. 1 λ	Previous obs. λ	Interpretation
	5320,5	19,0	1*P*(13—8)
	5280,7	5281,2	$O_2^+1N(2—0)$, *NI*(81,2)
	71,8	73,5	$O_2^+1N(2—0)$, *NI*(75,1)
2,3	55,0	55,4	$O_2^+1N(4—2)$, *NOβ* (3—18)
2,6	27,0	27,8	$N_2^+1N(0—3)$
2,8	5199,5	5199,5	*NI* ($^4S_{3/2}$ $^2D_{3/2\ 5/2}$)
	5188,2	89,0	*NI* V.K. (1—15,) $N_2^+2N(6—1)$ *NII*(90.4), *NI*(89,3)
	48,2	48,2	*NI*(48,7), $N_2^+1N(1—4)$
	29,2	32,0	*OI*(30,5) *NI*(30)
	09,2	08,5	*NII*(05) ?
	05,0	05,0	*NII*(04,5)
	5093,0	5093,0	V.K. (4—17) (92,4)
	67,3	67,0	*NI*(68.)
	45,2	46,5	*NII*(45,1)
	18,8	18,5	*OI*(18,8, 19,3)
1,1	04,0	04,4	*NII*(05,1)
	4994,1	4995,0	*NII*(94,4)
	78,6	77,0	S.R. (1—23)
	4887,7	4886,0	*NI*(86,3) S. R. (0—22)
	64,7	64,5	*OII*(64,9)
	56,8	57,0	*OII*(56,8)
	4836,1	4835,9	V.K. (2—15), S.R. (11—28)
	4792,1	4792,0	*NOβ*(2—16), *NII*(93,7)
	79,8	79,9	*NII*(81,2)
	52,8	51,5	*OII*(52,7, 51,3), *NI*(50,3)
	33,2		S.R. (1—22) (31)
12,5	4709,	4709,	$N_2^+1N(0—2)$
	4686,6	86,0	*NI*(85,7)
	78,5	77,3	*OII*(77,0, 76,2), *NII*(75,0, 77,9)
3,4	50,3	51,2	$N_2^+1N(1—3)$, *NI*, *OII*
1,9	41,8	41,7	*OII*(41,8)
1,3	4415,7	4415,8	*OII*(17,0, 14,9)
1,6	4568,8	4368,3	*OI*(68,3)
V.str.	4278,	4278,	$N_2^+1N(0—1)$
5,0	35,9	36,2	$N_2^+1N(1—2)$
1,4	4199,6	4199.5	$N_2^+1N(2—3)$
1,8	4058,3	4058,3	2*P*(0—3)
1,8	3997,3	3997,3	2*P*(1—4)
V.str.	3914,	3914	$N_2^+1N(0—0)$

The table IIIb contains the measured wavelength values of a great number of features which appear on the three spectrograms Nos. 3, 5 and 8 (Pl. I) and which can be detected on the photometer curves.

Taking into account the possible errors it appears that nearly all *the measured lines and bands can be identified with features which were*

Table III a
Wavelength (λ) and Intensity (I) in Infrared to λ = 6592.

λ	I	Interpretation
8850		$N_2$1P(1—0) (11—12)
38	21	$N_2$1P(1—0) (11—12)
8774	4	$N_2$1P (2—1)
11	10	$N_2$1P(2—1), NI (04, 11, 19)
8684	40	$N_2$1P(2—1), NI (81, 84, 86)
72	10	$N_2$1P(2—1)
56		$N_2$1P(2—1), NI(56),
27,5	21	NI(29)
8552,1		
39,5	10	$N_2$1P(3—2)
25		$N_2$1P(3—2)
8469	3	
47,4	20	OI(46,8, 46,4)
36	3	NII(39)
8352	8	N_2^+2N(3—2)
8300	5	N_2^+2N(3—2) $N_2$1P(4—3)
8218,1	6	NI(16,5 21,8), $N_2$1P(5—4), OI(22)
8187	4	NI(83,9)
53,7		
06,5	13	N_2^+2N(2—1)
8059	15	N_2^+2N(2—1), $N_2$1P(6—5)
7995,5	7	OI(95,1)
13,8	8	
7879,4	38	N_2^+2N(1—0), O_2^+1N(0—4)
54	11	$N_2$1P(7—6)
33,0	41	N_2^+2N(1—0)
20,0	5	
7774,0	31	OI(76, 74, 72)
48,1		$N_2$1P(2—0), N_2V.K(7—23)
35,3	15	$N_2$1P(2—0), N_2^+2N(6—4)
17	30	$N_2$1P(2—0) (8—7)
7697,8	15	N_2^+2N(6—4)
21,6	7	$N_2$1P(3—1)
7582,5	21	NI(87)1 N_2P(3—1)
00,6		N_2^+2N(5—3), $N_2$1P(4—2)
7486	13	OI(81), $N_2$1P(10—9) (4—2)
63,6	4	N_2^+2N(5—3), $N_2$1P(4—2)
7399,0		$N_2$1P(5—3), NI(97,5)
82,5	10	$N_2$1P(5—3)
70,5	11	$N_2$1P(5—3) NI(66)
60,0		$N_2$1P(11—10) NI(51,4)
45,6	10	$N_2$1P(11—10), NI(47,7), O_2^+ 1N(0—3)
41,7		$N_2$1P(11—10)
7284,5	8	$N_2$1P(6—4) N_2^+2N(4—2)
78,8		$N_2$1P(6—4)
71,4	10	$N_2$1P(6—4)
46,9	9	N_2^+2N(4—2)
32,4		$N_2$1P(12—11)
7098,8		$N_2$1P(12—11)

Table III a continued.

λ	I	Interpretation
7084,1	13	N_2^+2N(3—1)
68		$N_2$1P(8—6)
48,6	13	N_2^+2N(3—1)
6895,5	10	N_2^+2N(2—0) OII(95,3)
63,5		$N_2$1P(10—8)
58,3	14	N_2^+2N(2—0), $N_2$1P(3—0), O_2^+1N (0—2), NII(57,6)
34,1		N_2V.K.(3—19) O_2^+1N(0—2)
6787,4	3	$N_2$1P(4—1) (16—15)
80,8	13	$N_2$1P(4—1) (16—15), O_2^+1N(0—2)
48,5		$N_2$1P(4—1)
42,9		$N_2$1P(4—1), NI(41,3)
04,7		$N_2$1P(5—2), NI(06,2)
6693,5	5	$N_2$1P(5—2)
87,2	12	$N_2$1P(5—2)
74,5		$N_2$1P(12—10) (17—16), OII(78,2)
65,9		OII(66,9), NI(66,8)
55,2		NL(53,4, 56,6) OI(53,8), N_2^+2N(6—3)
49,0		NI(46,5)
30,0		NII(30,5)
21,7	3	$N_2$1P(6—3)' NI(22,5), N_2^+2N(6—3)
16,8	11	$N_2$1P(6—3)
08,0		$N_2$1P(6—3), NII(10,6)
6592,6		$N_2$1P(6—3)

previously measured in a similar way from spectrograms taken with the same spectrograph (16 and 19).

The intensities I (table IIIb) relative to that of the band N_2^+IN(1—3) (λ = 4651, I = 4,6) were measured photometrically from the moderately exposed features.

The last column gives for each feature the possible interpretations which have been found. The spectrograms Nos. 3, 5 and 8 only cover the spectral region from 6600 to 3880. For the sake of completeness and convenience we have mainly from paper 19 added to table IIIb the region from 6600 Å to the limit of our observations in the infra red. (λ = 8850. Table IIIa) and from earlier papers (cfr. 16) we have added the observed auroral ultra-violet features from 3880 to the limit of atmospherie transparency (Table IIIc.)

On account of the great number of lines and bands contained in the auroral luminescence it will often happen that a certain feature can be referred to lines or bands of different origin, and it may be difficult to tell to what extent each of

Table III b. Wavelength values measured from the Spectrograms No. 3, 5, 8 on pl. I.

Spectrogram No 3 λ	No 3 I	No 5 λ	No 5 I	No 8 λ	No 8 I	λ Previously observed	Interpretation
				6591,0	7,5	6592,6	1P(6—3)
						83,3	NII(83,4) $2p^2(^3P_2—^1D_2)$ (Forbidden)
						62,5	H_α
						54,5	NII(54,7), 1P(7—4)
						51,7	NII $2p^2$ $(^3P_1—^1D_2)$, forbidden 1P(7—4)
		6538,7	4,7	6541,4		40,8	NI(44,2), 1P(7—4)
		32,8		31,9			NII (33,0)
		22,1		23,6		27,7	NI(28,4) NII(22,3), 1P(7—4)
		11,5		11,9		12,1	NI(10,3)
		06,7				05,5	NI(06), NII(04,9)
		6498,8					NI(99,5)
		91,3					NI(91,3), NII(92,0)
		85,5					NI (84.9)
		78,2	3,0	6479,5		6480,2	NII(82), 1P(8—5), N_2^+2N(5—2), NIII(78,9)
		70,4	3,0				NI(71,0)
		67,3	5,5	68,6	5,7	66,8	NIII(66,9, 68,8)
		61,8 }		55,9			OI(53,6, 54,5), 1P(8—5)
		56,2 }	5,7				
		50,7 }					NIII (50,8)
				6443,1	7,2	6441,0	1P(8—5), N_2^+2N(5—2), 1P(8—5)
		6439,4	5,0			37,9	NI(37,3), N_2^+2N(5—2)
		34.				33,2	NI(28,0)
						6398,	NI(93,6), O_2^+1N(0—1), $N_2$1P(9—6)
		6391,5	5,4	6393,2	6,9	91,	OI$2p^4(^3P_0—^1D_2)$, O_2^+1N(0—1),1P(9—6)
		83,2	6,2	81,3		79,8	NI(78,0), O_2^+1N(0—1), 1P(9—6)
		63,8	49,0	63,8	str.	63,8	OI $2p^4(^3P_1—^1D_2)$, 1P(9—6)
		29,6				20,7	NI(21,7), 1P(10—7), S.R. (6—31)
						18,	1P(10—7)
		00,3	str.	6299,6	str.	6300,3	OI $2P^4(^3P_2—^1D_2)$, N_2^+2N(4—1)
		6276,0	3,3				NI(75,5)
		69,2	2,9	70,9	9,7	6272,4	NI(72,8), N_2^+2N(4—1), S.R. (2—28)
						65	OI(64,4, 66,9)
		46,6		40,0		43,8	NI(43,2)
		38,4		37,0		39,6	NI(37,5), 1P(11—8)
		23,4		19,8		22,5	NI(24), S.R. (5—30)
		6185,7	3,3	6182,1		6184,3	1P(12—9) (4—0)
		75,2		75,4		74,5	1P(12—9), S.R. (1—27), NII(73,4)
		(68,7)		(70,9)			1P(12—9) (4—0)
		61,0		65,5			1P(12—9) (4—0), N_2^+2N(8—4)
		57,1					1P(12—9) (4—0), OI(58, 57, 56)
		54,6		55,5	5,7	55,3	1P(4—0)
		34,0	8,0	37,2	6,7		N_2^+2N(8—4), NII(36,9)
		25,2		28,4	7,2	27,0	1P(5—1), V.K. (7—21), S.R. (4—29)
		14,3				19,0	S.R. (7—31)
		12,		09,2	6,9	09,5	1P(5—1), N_2^+2N(3—0), OI(06,3)
		00,6		6099,3			1P(5—1), O_2^+2N(1—14)?
		6092,9				6093,	1P(5—1)
		78				78	V.K. (3—18), S.R. (0—26), NI(75,7)
		70,3	3,8	69,1	5,1	71	1P(6—2)
		65,8				67,3	NI(69,0)
6063,5		62,6				62,0	1P(6—2), NI(61,9)
58,6		59,6		60,6		59,6	»
		53,8	3,2				»
		49,2					»
43,4		43,3	3,1	44,2		44,3	OI [(46,2, 46,5)], NI(44,8)

Table IIIb continued.

Spectrogram						λ	Interpretation
No 3		No 5		No 8		Previously observed	
λ	I	λ	I	λ	I		
		6039,8					O_2^+1N(0—0)
6025,2		24,7				6024,2	O_2^+1N(0—0), O_2 S.R. (3—28)
16,8							NI(17,7, 15,4), O_2^+1N(0—0)
		13,6	7,4	6013,5	5,6	11,2	N_21P(7—3), NI(08,4, 12,0), S.R. (6—30)
		06,9		04,8		02,0	O_2^+1N(0—0), N_2^+2N(7—3)
5996,6		5999,4	7,6				O_2^+1N(0—0), NI(5999,6)
90,7	2,8	90,5				5990,5	N_21P (7—3), O_2^+1N (0—0), OI(91,3)
		87,1					NI(87,5) »
(85,)		84,2					O_2^+1N(0—0) »
78,5		77,8	2,2	5975,1	4,7	75,8	O_2^+1N(1—1) (0—0), N_2^+2N(7—3)
75,1		74,2					O_2^+1N(1—1), NI(72,1)
		70,6				69,0	O_2^+1N(1—1), NI(66,4)
63,9		61,3					NI(62,1)
60,5				59,2		58,0	NI(58,8), NII(60,9), $1P$(8—4)
49,6	1,8	53,4	3,4	51,6	3,2	51,0	NI(51,1), NII(52,4), $1P$(8—4)
34,2	1,0	37,7		35,7		40,0	NII(40,3, 41,7), NI(41,9)
		30,2		33,0		32	NII(31,8), NI(31,2)
27,8		27,2		26,9		26,8	NII(27,8), NI(27,5) O_2^+1N(2—2)
07,7	1,0	07,6		03,5	2,4	03,3	N_21P(9—5), NI(05,07)
5896	1,9	5898,3		5895,4	3,1		NI (98,2)
92,3	2,9	92,3	10			5892,2	Na D_1 D_2, N_21P(9—5)
		87,1		88,2			$1P$(9—5)
		78,1				77,9	O_2^+1N (3—3)
75,1	1,2	75,2					
		70,9		70,9		69,0	
65,2	0,8	67,7				65,6	N_2^+1N (0—4), NI (63)
		59,0					NI(56,1)?
55,0	0,8	50,5		51,3		52,5	$1P$(10—6), NI(54)
45,2	0,7	43,2		45,4		42,0	$1P$(10—6), NI(41), O_2^+1N(4—4)
36,0	0,7	38,5	3,2	36,0			» S.R. (1—26)
30,0		33,5				30,9	» NI(34,8), N_2^+2N(6—2)
25,0		28,4		28,9	2,0		NI(29,6)
04,8	0,3	09,0		04,2		09,0	$1P$(11—7), NI(16), N_2^+2N(6—2)
		5799,8		00,7		01,0	$1P$(11—7), NI(03)
		5793,6				5790,0	NI(90,4, 93,5)
		87,0		5785,1		86,0	$1P$(11—7)
5779,5		77,4		76,1		80,	NI(81,7), V.K.(5—19)
		68,4		67,0		70,8	NI(68,6, 72,8)
		5757,8					NI(58,6)
		55,5		5752,4		5753,7	{NI(52,7), $1P$(12—8) N_2^+1N(1—5) {NII $2p^2(^1D_2—^1S_5)$
5750,7	0,7	48,5					NI(47,3), $1P$(12—8), OI(50,4)
46,6		45,2				45,0	{NI(47,3), NII(47,3), $1P$(12—8) {S.R. (0—25).
		38,9		38,6			NI(40, 35,6)
		31,5				31,0	NII(30,7), OI(31,1), N_21P(12—8)
		(28,4)					NI(28,8)
20,6		22,4		19,8		25,6	OI(20,6), N_21P(12—8), S.R. (6—29)
12,6		08,6				10,2	NI(10,7), NII(10,8), $1P$(13—9)
5698,3		5698,9		5697,6			$1P$(13—9)
90,1		91,5		92,4			»
86,9		87,0	2,0	84,8		5686,2	NII(86,2) N_2^+2N(5—1)
80,4	1,3	80,9	3,4	78,7	4,8	79,5	NII(79,6), (76), O_2^+2N(1—13)
67,3	0,7	74,9	1,7	66,3	1,9	66,2	NII(66,6), N_2^+2N(5—1),

Table IIIb continued.

Spectrogram						λ	Interpretation
No 3		No 5		No 8		Previously observed	
λ	I	λ	I	λ	I		
5616,4		5662,5	1,7	5666,3	1,9	66,2	NII(66,6), N_2^+2N (5—1)
		56,6				58,0	1P(14—10), N_2^+2N(2—6), S. R.(8—30)
30,8		29,8		29,0		30,0	O_2^+1N(1—0), 1P(5—0)
25,2	1,7	26,4		25,7			» »
		21,1		21,3		21,4	O_2^+1N(1—0), {1P(5—0), NI(23) (18), S.R. (2—26)
							» {V.K.(4—18)
16,3	1,8	16,0	5,6	18,7		16,0	» {1P(15—11), NI(16,5)
							» {S.R.(5—28)
06,6	1,9	06,3	6,3	10,5		12,7	» 1P(5—0), NI(11,3)
		01,8		01,1		02,0	» V.K. (0—15), NI(04,4) (00,5)
5597,4	2,3	5598.2				5595,	O_2^+1N(2—1), 1P(6—1) (15—11)
77,35str.		77,35		5577,35		77,35	OI($^1D_2$—$^1S_0$)
						66,5	O_2^+1N(3—2), 1P(16—12), NII(65,3)
61,1				58,1		58,5	1P(16—12), NI(60,4, 57,4)
55,4		55,5				54,0	1P(7—2), OI(54,9)
52,7		52,1		51,0		50,0	1P(7—2), NII(52,0), NI(51,4,) S,R.(7—29)
		44,4		43,0		43,0	1P(7—2), NII(43,5), N_2^+2N(4—0)
37,4		38,2		37,8		38,2	O_2^+1N(4—3)
		33,2				31,0	V.K.(7—20), NI(30,0), NII(30,3)
		22,5		22,8		21,0	O_2^+1N(5—4), NI(24), S.R.(4—27)
18,0		19,8				16,7	1P(8—3), NI(19,4)
		10,1		13,2		11,5	OI(12,7)
5499,4		00,7		5496,6		5496,5	{NI(96,6), NII(95,7), 1P(8—3)
							{O_2^+2N(0—12) ?
5493,4				5493,8		5492,0	OI(92,8)
		5489,4		89,0		87,5	OI(86,6), N_2^+1N(4—8)
75,9		72,3				77,0	NII(78,1), 1P(9—4)
				(64,5)		67,0	V.K. (3—17)
						61,7	NII(62,6), 1P(9—4)
						57,0	NII(54,3)
51,0				53,0		52,0	NII(52,1)
41,5						42,8	1P(10—5), O_2^+2N(0—12)
						37,3	OI(35,2, 35,8, 36,8), S.R. (0—24)
34,3		34,4				34,0	1P(10—5)
31,8				30,0			»
		27,6				26,0	S.R.(3—26)
20,2				22,4		21,8	1P(10—5) [N_2^+1N(5—9) ?]
						17,5	NI(19,3)
12,8		14,6				11,5	OI(10,8)
		07,4				05,3	1P(11—6)
				01,4		01,0	NI(01,2)
		5393,3				5392,0	NI(5392,7)
		87,6				90,5	1P(11—6)
						75,0	1P(12—7), V.K.(6—19), N_2^+1N(6—10)
		60,2		5364,4		68,5	1P(12—7), NI(71,0, 67,3)
5358,5				58,9	1,1	58,6	NI(56,8) (60,1)
53,6		55,7		53,9		(50,0)	NII(51,2)
						46	NI(44,2)
				41,4		42	NI(40,3), NII(40,2)
38,4				36,6		34,5	NI(34,3), N_2^+2N(7—2), 1P(13—8)
30,4				31,0		30,5	OI(29,0, 29,6, 30,7), NI(28,8)
23,5						19,0	1P(13—8), NII(21,0)
		16,8		15,0		15,0	NI(15,2), NII(13,4), NIII(14,5)
00,9		5299,2				01,0	N_2^+2N(7—2), 1P(14—9), NIII(97,9, 98,9)

Table IIIb continued.

Spectrogram						λ Previously observed	Interpretation
No 3		No 5		No 8			
λ	I	λ	I	λ	I		
5294,5				5296,3	1,1	5296,4	O_2^+1N(2—0), OI(99.0)
		91,3		91,5	1,0	92,0	O_2^+1N(2—0), NI(92,8), S.R.(7—28)
81,4	1,0	78,9		80,6	1,5	81,3	NI(81,2) O_2^+1N(2—0), 1P(14—9)
		74,1				75,0	O_2^+1N(3—1) (2—0), OI(75,1), 1P(15—10), S.R. (11—30)
69,1		69,4		71,1		72,0	1P(15—10), NII(72,6)
		60,1		64,8		64,0	1P(15—10), S.R. (9—29), NIII(60,9)
57,2	0,9	56,3	1,4	56,5	2,7	57,0	1P(15—10), O_2^+1N(4—2)
54,2		53,1		52,2		55,4	NOβ(3—18), O_2^+1N(4—2)
49,2	1,2	50,9				50,0	O_2^+1N(5—3), S.R. (4—26)
		5242,6				5242,5	O_2^+1N(6—4), S.R.(1—24), 1P(16—11)
5235,6				5327,9			1P(16—11)
32,4		33,1				34,0	O_2^+1N(7—5), V.K. (5—18)
27,9	1,7	28,6	2,9	28,7	4,8	27,9	N_2^+1N(0—3), NI(27,0)
17,1		17,8		(14,5)			1P(17—22)
09,6		09,0					»
01,0	1,4						»
5199,5		00,6	3,6	01,5	1,8	5199,3	NI2$p^3(^4S_{3/2}—^2D_{5/2\ 3/2})$, $3p^2S—5d$
97,6		5199,5		00,0			$^2P_{3/2\ 1/2}$(NII(99,5)
				5189,1		93,0	NI(87,1, 89,3, 91,7), N_2^+2N(6—1)
							NII(90,4)
80,6				81,1		80,	NI(79,6, 80,9, 82,5), NII(79,5, 80,3)
				79,3	1,0	77	NII(75,9), OII(76)
(75,2)		73,7				73,	NII(73,4)
69,3						67,5	NI(68,0), NII(68,2), N_2^+2N(6—1)
64,6		64,9		63,8		66,0	NI(65,8),) N_2^+2N(6—1)
58,9		59,9		57,6			S.R.(3—25 (8—28), OII(59,9)
57,0						53,0	NI(56), $N_2$1P(19—14,) S.R. (3—25)
50,4				51,2	1,5		S.R.(0—23) (10—29)
		47,4	1,0	49,3	1,7	48,1	N_2^+1N(1—4, NI(48,7)
42,5		36,5		38,9		40,0	NI(40,8)
30,8						32,0	OI(30,5), NI(30)
		20,7	1,1	19,8		19	
		15,3		16,9		14	
		11,7		10,2		08,5	
		06,1		03,9		05,0	NII(04,5)
5093,9				5092,8		5093,0	V'K. (4—17)
89,5				88,5			
86,4		5085,3		85,6			O_2^+2N(0—11)
				78,3		78,0	N_2^+1N(2—5), S.R.(11—29), G.K.(0—12)
72,9		75,4					NII(73,6), NI(75,9)
68,9		69,4		67,0		67,0	NI(68), S.R. (2—24)
59,3		59,4		58,5			NI(62, 55), V.K.(0—14) (59)
55,6		55,2		56,3		53,5	1P(11—5), NI(51,6, 54,7)
46,5	1,2			46,8	1,0	46,5	OI(47,7), 1P(11—5), S.R. (7—27)
45,1		43,8		45,2		43,0	NII(45,1)
33,2		33,4		33,3		32,0	V.K. (7—19), 1P(11—5), O_2^+2N(0—11)
5029,4		5026,7		5029,4		5029,0	1P(12—6)
						18,8	OI(18,8, 19,3, 20,1)
16,5		14,3		14,3		14.0	NII(12,0, 16,4), N_2^+1N(3—6)
10,2				09,2		10,7	NII(10.6, 11.2)
		08,2	2,4			(06,8)	OIII(06,9)?
04,6	1,7	04,6		05,4	2,2	04,7	NII(05,1)
03,4		02,7				02,7	NII(02,7)
01,3				01,7		01,4	NII(01,1)

Table IIIb continued.

Spectrogram						λ Previously observed	Interpretation
No 3 λ	I	No 5 λ	I	No 8 λ	I		
						4998,7	*NII*(97,2), N_2^+1*N*(4—1)
4995,5		4994,2				95,0	*NII*(94,4), S. R.(4—25)
87,5		84,4				90,0	*NII*(91,2, 87,4)
78,8				4980,0		81,0	*OI*(79,6)
						77,	S.R. (1—23), 2*P*(4—11)
74,0		73,6		74,4		73,3	2*P*(4—11)
67,0		65,4				67,7	*OI*(68,8) (67,9) 67,4)
60,9				61,2		61,5	V.K.(3—16)
		58,1		(56,2)		57,0	N_2^+1*N*(4—7)
53,8				52,5		55,0	*OII*(55,7)
41,9				43,2		42,0	*OII*(43, 41)
34,6		34,5		34,9		34,7	*NI*(35,0)
30,4		30,4		29,1		28,0	S.R. (10—28)
						23.0	*OII*(24,5), S.R. (8—27)
15,9		14,4		15,2		17,2	2*P*(1—7)
						15.0	*NI*(14,9)
						13,0	*NO*β(3—17)
						09,0	S.R. (5—29)
06,7		07,2		06,8		07,0	*OII*(06.8)
						05.0	S.R. (3—24)
4899,6		4898,8					V.K.(6—18), N_2^+2*N*(8—2)
97,4		96,4		4896,0		4896,0	*NII*(95,2), *NIII*(96,7)
				89,2		91,0	*OII*(90,0), *NO*β (3—17)
		86,3		86,5		86,0	*NI*(86,3), O_2 S.R. (0—22)
		83,7		82,8		82,9	*NI*(81,8), N_2^+2*N*(8—2), N_2^+1*N*(6—9), *NIII*(81,8)
				73,9		74,5	*OII*(72), *NIII*(73,6)
70,3		67,4		68,9		67,0	*NI*(68,9) *NIII*(67,2)
64,0		64,7		65,1		64,8	*OII*(64,9)
60,0		61,8				61,7	*H*β [*OII*(60,9), *NII*(60,4)]
							Weak
		4859,2					*H*β (Doppler band)
4857,6		56,6				4857,0	*OII*(56,8)
45,0		45,0				46,5	*NI*(47,4)
37,9		38,4		4837,9	0,5	38,0	*NI*(37,8)
		35,6				35,4	V.K. (2—15), S.R. (11—28)
		16,0				16,5	S.R. (2—23)
13,6				(14,8)		13,7	2*P*(2—8), S.R. (9—27)
		09,7		(11,7)		12,0	*NII*(10,3), *NO*β (2—16)
04,4		04,6					*NII*(03,3)
01,8		01,4				02,5	*OI*(01,8, 02,2, 03,0)
4798,		4797,				4798,7	
94,		95,3		4794,7		92,0	*NII*(93,7, *NO*β (2—16)
89,2						87,2	*NII*(88,1)
84,2				4781,8		82,0	*NII*(81,2)
						78.	*NII*(79,7)
74,9		72,9				72,0	*OII*(72,5, 72,9, 73,8)
71,3		69,5					V.K. (5—17) (71,3)
68,1		67,9				68,0	
64,4		63,9					S.R.(4—24) ?
53,9				54,5		54,2	*NI*(53,1), *OII*(52,7)
		51,8		50,6		51,5	*NI*(50,3), *OII*(51,3)
(26,7)		23,7		22,7	0,7	24,0	2*P*(3—9), S.R. (6—25)
		21,1				20,0	*NII*(18,4, 21,6), O_2^+2*N*(0—10)
4709,	str.	4709.	str.	4709.	str.	4709.0	N_2^+1*N*(0—2)

Table IIIb continued.

Spectrogram						λ Previously observed	Interpretation
No 3		No 5		No 8			
λ	I	λ	I	λ	I		
				4686,8		4686,	*NI*(85,7)
4678,3		4677,4	0,3	76,8		77,2	*OII*(77,0, 76,2), *NII*(77,9, 75,0) O_2^+2N(0—10)
70,5				71,1		71,5	*OI*(73,7, 72,8), *OII*(73,8), S.R. (3—23)
						68,	2*P*(0—5), *NI*(69,8)
62,1		61,8		62,3		61,5	*OII*(61,7), *NI*(60,0), N_2^+2N(6—0)
60,5		60,0		60,3			*NI*(60,0)
51,2	4,6	51,3	4,6	51,0	4,6	51,3	N_2^+1N(1—3), *NI*(51)' *OII*(50,9)
						50,2	*OII*(49,1), V.K. (4—16), N_2^+2N(6—0), 2*P*(4—10)
42,1	0,9			43,1		42,1	*OII*(41,8), *NII*(43,1), *NIII*(41,9)
37,7		39,7				38,7	*OII*(38,9), *NIII*(40,6)
33,8		33,2	0,6				S.R. (11—27), *NIII*(34,2)
30,9	0,4	31,7		31,3		31,4	*NII*(30,6)
21,8	0,15	23,1		22,9		22,0	*OII*(21,3), *NII*(21,4),
		15,3		14,4		14,0	*OII*(13,9), *NII*(13,7)
4609,6	0,3	4609,3		4610,3		4609,5	*OII*(10,1) (9,4), *NII*(09,4)
		06,6				08,0	*NII*(07,2), S.R. (7—25)
02,0		01,5				02,0	*NII*(01,5), *OII*(02,1)
00,2	0,4	4599,3	0,5	4599,9		00,4	N_2^+ IN(2—4)
4597,8	0;4	97,2		96,6		4596,7	*OII*(96,1)
92,0	0,4	93,0		91,5		91,2	*OII*(90,9), *NOβ* (3—16)
88,7		89,8		88,6		89,5	*OI*(89,0, 89,9)
		82,3		82,7		81,0	S.R. (2—22), *NOβ* (3—16)
73,0	0,3	75,0	0,8	73,0		73,4	2*P*(1—6), *NOβ*(3—16)
		69,5		70,6		70,0	*OIII*(69,5)
67,9				67,9		65,0	*NII*(64,8)
53,2		53,2		52,8		53,2	N_2^+1N(3—5), *NI*(53,4, 54,2)
51,2	0,26	51,2				52,0	*NII*(52.5)
50,0 ?		49,6	?				
45,0	0,4					47,0	N_2^+2N(9—2), *NIII*(46,3, 47,3)
		33,6				32,8	V.K.(3—15), *NIII*(34,6)
30,6				30,8		30,8	N_2^+2N(9—2), *NII*(30,4), *NIII*(30,8), *OIII*(29,7)
		23,9		23,9			*NIII*(23,6)
14,2		15,2		14,3		15,2	N_2^+1N(4—6) *NIII*(14,9)
09,2		10,5		10,7		10,5	S.R. (6—24), *NIII* (10,9)
		08.2				06,9	*NII*(07,6)
01,7		03,2		02,9			S.R. (1—21) (03,5)
4495,5		4497,4		4498,5		4498,7	*NI*(97,5, 99,1)' *NOβ* (2—15) (96,2)
						95,5	*NI*(94,7)
91,1	0,5	91,0	0,7	92,3	0,9	91,0	2*P*(2—7), NI(92,4, *OII*(91,2, 89,5)
87,9		88,5		88,0		88,3	*OII*(87,7, 88,2), *NII*(88,2)
84,6						84,6	*NI*(85,1), N_2^+1N(5—7)
		83,0				82,6	*OII*(82,9), *NOβ* (2—15), *OIII*(82,8)
74,7		76,5		75,0		76,3	*OII*(76,1, 77,9), *NII*(77,3), *OIII*(75,0)
		69,0		68,8		67,8	*OII*(67,8), N_2^+1N(6—8)
		66,0		66,1		66,0	*OII*(66,3)
65,6	0,2					65,5	*OII*(65,5), *NII*(65,5)
		57,7		57,8			*NII*(60,0), S.R. (3—22) (55,5), *OIII*(58,4)
51,7		51,6		51,9		51,4	*OII*(52,4)
		48,5	0,5			48,8	*NII*(47,0)
46,3		46,6		46,0		45,2	G.K. (0—10)
						42,0	*NII*(42,0), G.K.(0—10)
4440,2		4439,8		4439,0		4440,5	S.R. (11—26), *OIII*(40,1)
32,4	0,4	32,7		32,1		32,8	*NII*(31,8, 32,7, 33,5), G.K. (0—10)
						28,8	*NII*(28,0)
27,4	0,3	26,9		27,6		27,4	*NII*(27,2)

Table IIIb continued.

Spectrogram						λ	Interpretation
No 3		No 5		No 8		Previously observed	
λ	I	λ	I	λ	I		
		4424,0				24,0	V.K. (2—14) (24,0), *OIII*(24,3)
						23,2	S.R. (5—23)
		16,8		4416,7		16,7	*OII*(17,0), $N_2 2P$(3—8)
4414,4	0,8	15,8		15,5	0,6	15,0	*OII*(14,9)
11,8		10,8		11,7		11,5	S.R. (9—25) (11,3)
		06,3		06,1		05,7	*OII*(06,0), S.R. (7—24)
		03,4		02,3		02,7	$NO\beta$(1—14), $O_2^+ 2N$(0—9)
		4399,9				01,1	$NO\beta$(1—14) (01,5), $O_2^+ 2N$(0—9) (99,4) *i i*
		96,6		4396,8		4397,	*OII*(96,0)
		88,7		87,3			$NO\beta$(1—14) (86)
		80,0		81,5		81,3	V.K.(5—16) (80,7)
4379,0		78,5		78,7		79,0	*OII*(78,4), *NIII*(79,1), *OIII*(79,6)
77,2		77,2				77,4	*OII*(78,0)
68,3		68,3	1,0	68,3	0,9	68,3	*OI*(68,3) [*OII*(66,9, 69,3) ?]
58,1		58,0		57,6		58,3	*OII*(58,5, 57,3), *NI*(58,3)
51,2	0,3	50,6	0,3	50,0	0,3	51,5	*OII*(51,3)
						49.0	*OII*(49,4)
						48,	*OII*(47,4), *NIII*(48,4)
		46,7				46,6	*OII*(45,6) (44,3)
44,6	0,5	44,7	0,5	43,8	0,8	45,0	2*P*(0—4) (43,6)
		42,7				43,0	*OII*(43,4, 42,8)
						42,	*OII*(42,0)
40,3				39,8	0,7	41,	$H\gamma$ *Diffuce* (Doppler effect)
		38,5				39,	*OII*(40,3), *NIII*(39,5)
37,6		37,5				37,0	*OII*(36,9), *NI*(36,5)
34,7				(35,6)		34,5	*OII*(34,2), *OIII*(35,5)
		32,0	0,4			32,0	*OII*(31,8, 31,4)
27,6				29,2		29,4	*OII*(28,6, 27,8), *NIII*(28,2, 30,1, 30,4)
						26,3	*OII*(25,8) (27,5)
						23,1	*NI*(24,9), *NIII*(23,9)
20,5		20,7	0,3	21,9	0,7	21,2	*NI*(22,0), *NIII*(21,4)
18,7	0,3					19,4	*OII*(19,9)
		18,0	0,4	17,4	1,0	17,9	*OII*(17,7, 17,2), *NI*(17,7)
14,3		13,9		14,1		13,5	*OII*(13,4), *NI*(13,1)
		08,7				09,0	*OII*(09,0), $NO\beta$ (0—13)
4305,2				4305,6		4305,7	*NI*(05,5)
		4304,3		03,6		04,2	*OII*(03,8), $NO\beta$ (3—15)
4299,9		00,5					
93,4		4294,8		4296,3		4294,0	*OII*(94,7), *NIII*(94,8), S.R. (1—20)
92,5		92,0		92,3	0,5	92,0	*OII*(92,1), $NO\beta$ (0—13)
				87,2	0,3	88,4	*OII*(88,8), $NO\beta$ (3—15) *NIII*(88,2, 88,7)
						86,2	*OII*(85,6)
				83,4	0,3	84,8	*NI*(84,9), *NIII*(84,5)
78,0	str.	77.	str.	76,5	str.	78,0	$N_2^+ 1N$(0—1), V.K.(4—15), *OII*(76,6, 77,4)
41,4		42,		41,6		41,4	*NII*(41,8)
36,3	str.	36,0	4,2	36,3	4,6	36,1	$N_2^+ 1N$(1—2), *NII*(36,9, 37,0)
						31,0	*NI*(30,4), *OI*(33,3)
		29,0		28,8	0,8	29,0	*NI*(29,6)
						26,5	*NII*(27,8, S.R.(5—22)
		24,0				24,	*NI*(24,7)
				23,4 }	0,5	23,	*NI*(23,0), *OI*(22,8)
				21,5 }		21	*NI*(20,8)
				19,2		19	V.K. (0—12)
				17,7		17,5	*OI*(17,1)
		14,5		14,7	0,22	15,5	*NI*(15,9), $NO\beta$ (2—14) (15,2) *NIII*(15,7)

Table IIIb continued.

Spectrogram						λ Previously observed	Interpretation
No 3		No 5		No 8			
λ	I	λ	I	λ	I		
						14,0	*NI*(14,7), S.R. (0—19)
		4211,9				11,6	*NI*(13,0)
		07,3		4208,2	0,26	08,2	*NI*(09,1)
4206,2						06,1	*NI*(06,3)
				05,5	0,8	05,1	*NI*(05,7)
4199,7	1,1	4199,6	0,8	4199,2		4199,5	N_2^+1*N*(2—3), 2*P*(2—6), *NOβ*(2—14), *NIII*(00,9)
		96,6		96,5		95,8	*OII*(96,3, 96,7), *NIII*(95,7)
				93,3		93,5	*OII*(92,5), *NI*(93,5)
91,?		91,1					
89,0		89,2		89,6		89,8	*OII*(89,8)
						88,0	NI(87)
85,6				84,5	0,2	85,1	*OII*(85,5)
		80,0		79,9		80,5	*NI*(80,0), *NII*(79,7)
76,1		76,3		(75,2)		76,2	*NII*(76,2)
75,4		73,5				74,2	*NII*(73,5, 73,7)
72,3		71,0	0,27			71,3	*NII*(71,6), V.K. (3—14)
69,7		69,6		68,7	0,4	68,5	*OII*(69,3)
4167,9						4167,5	*NaI*(67,8)?
64,5				4165,4		65,7	*NI*(66,6)
						64,	*NI*(64,8), S.R. (3—20)
60,1						60,0	*NII*(60,8)
56,6				58,4		56,5	*OII*(56,5)
54,0						53,3	*OII*(53,3
				52,1		52,0	*NI*(51,5)
				48,1		48,9	*OII*(46,1)
45,0				44,9		45,5	*NI*(45,8), *NII*(45,8), V.K.(6—16) (45,7)
						42,7	*OII*(42,0, 42,1, 42,3), N_2^+1*N*(4—5)
						41,0	*OII*(40,7), 2*P*(3—7)
40,3				40,1	0,45	40,1	N_2^+1*N*(4—5)
38,9				38,4		38,8	
36,6				35,8	0,2	36,9	*NI*(37,6)
33,1						33,0	*OII*(32,8), *NII*(33,7)
30,9				30,4		30,0	*OII*(29,3), *NI*(29,2), [*NOβ* (1—13)]
		4124,8		24,7		24,7	*NII*(24,1), *OIII*(25,5)
				21,1		21,0	*OII*(21,5, 20,6, 20,3)
		19,1		17,0		18,3	*OII*(19,2)
14,9		15,7		13,8		14,5	*NI*(14,0), *OII*(13,8), *NOβ*(1—13), O_2^+2*N*(0—8) *i*
		12,6	0,7			12,0	*OII*(12,0)
						11,0	*OII*(10,8)
09,6		08,9		09,2		09,7	*OII*(10,2) *NI*(10,0), *NII*(10,0)
						06,5	*OII*(01,7, 06,0, 08,8)
				05,2		05,6	*OII*(05,0, 04,7)
02,2		02,8				03,0	*OII*(03,3), *NI*(02,2), *NIII*(03,6)
4099,5		4099,9		4099,2		00,0	2*P*(7—11), *NI*(99,9) (01,7)
		98,0		97,6		4097,6	*OII*(97,2, 97,3), *NIII*(97,3)
94,7				96,4		95,3	*OII*(94,2, 95,6, 96,2, 96,5), S.R. (1—19)
						94,0	2*P*(4—8), *OII*(94,2)
				93,0		92,8	*OII*(92,9)
				90,0		89,6	*OII*(89,3)
86,0				87,0	0,2	86,7	*OII*(87,1)
						85,5	*NII*(85,1)
						84,3	*OII*(84,7), (83,9)
				82,3		82,8	*NII*(82,9), O_2^+2*N*(0—8) *i*
				78,8		79,3	*OII*(78,9)
75,3	0,4	76,5		75,4	0,3	76,1	*OII*(75,9)

Table IIIb continued

Spectrogram No 3 λ	No 3 I	Spectrogram No 5 λ	No 5 I	Spectrogram No 8 λ	No 8 I	λ Previously observed	Interpretation
		4072,8	0,5	4073,0	0,4	73,0	*NII*(73,1), *OIII*(73,9)
4072,3	0,6					72,2	*OII*(72,2), V.K. (2—13)
70,8		70,2		70,0	0,4	70,8	*OII*(69,9, 69,6)
66,1						66,6	
				65,2		64,7	S.R. (3—20)
		59,4				61,	*OII*(61,0, 60,6)
58,4	2,7	58,4	1,7	58,5	1,6	58,5	2*P*(0—3)
						57,0	*NII*(57,0)
		54,9		54,7	0,17	53,6	*OII*(54,1), (54,6)
52,2		53,7		53,4		52,6	
51,0				51,4	0,17	51,7	
		48,1		48,1		48,1	*OII*(48,2)
46,9						47,0	*OII*(46,2)
						45,0	*OII*(45,0), *NII*(44,8), S.R. (5—21)
43,7				42,5		43,2	*NII*(43,5)
41,3		41,0	0,29	41,6	0,23	41,1	*NII*(41,3), *OII*(41,3), *NO*β(0—12)
37,3				35,9		36,6	*NI*(37,4)
34,8						34,9	*OII*(35,1), *NII*(35,1)
31,9						33,1	*OII*(33,2), *NI* (33,6)
		(28,4)		29,4		29,5	*NO*β (0—12)
26,5				25,9		26,2	*OII*(26,4), *NII*(26,1)
				22,6		23,7	*OII*(24,0)
13,1				11,5		10,9	*NI*(11,0)
09,0						08,7	
05,2						05,8	*NIII*(03,6)
		3999,2	1,4	01,0		01,0	*NI*(01,0, 01,7)
3996,9	2,9	97,8	1,7	3997,3	1,6	3997,3	2*P*(1—4), *NIII*(98,7)
						95,0	*NI*(94,9), *NII*(95,0)
				93,1	0,37	92,4 }	
91,7						91,5 }	
89,3		89,8		89,0	0,23	89,1 }	
				86,6		87,5	S.R. (2—19)
85,1				85,0		85,5	*OII*(85,5)
				83,2		82,5	*OII*(82,7)
						81,	
				78,9		79,0	
3976,7						3977,9	V.K. (1—12)
73,2				3973,6		73,4	*OII*(73,2)
						68,5	*NI*(70,0)
						61,	*NO*β (2—13), *OIII*(61,6)
56,7				55,4		55,	*OI*(54,7, 54,6), *NII*(55,9),
						54,	*OI*(53,1, 53,0), *OII*(54,4)
49,4				48,8		49,0	*NO*β (2—13)
						47,2	V.K. (4—14), *OI*(47,6, 47,5 47,3)
45,2				43,3		45,	*OII*(45,0)
42,3	0,8			42,6		42,	2*P*(2—5), *NII*(42,8)
41,6						41,5	
38,6	0,75						V.K. (7—16) (39,0), *NIII*(38,5)
30,7						30,5	?
19,3				19,8		18,5	*OII*(19,3), *NII*(19,0)
14,	str.	14,	str.	14,	str.	14,	N_2^+1*N*(0—0), S.R. (1—18)
3888,3		3887,1				3887,8	V.K. (0—11), S.R. (3—19)
85.0				3885,1		85,	N_2^+1*N*(1—1)
						83,	*OII*(82,4) (83,2)
						80,5	*NO*β (1—12)

Table III c. Auroral Features in the Ultra violet.

λ	I	Interpretation
3873,8	1,0	*OII* (75,8, 74,1, 72,4), S.R. (5—20)
3857,5		N_2^+1N(2—2), $2P$(4—7)O_2^+2N(0—7)
		V.K. (3—13), *OII*(57,2)
3821,8		N_2^+1N(4—4), *OII*(21,6)
3805,3	4,9	$2P$(0—2), *OII*(03,1)
3771,6	1,0	V.K. (2—12)
3755,2	4,2	$2P$(1—3), V.K. (5—14)
3728,4	1,0	*OII*(29,2, 28,9, 27,3). Forbidden
3711,3	2,4	$2P$(2—4), *OII*(12,7)
3686	1,6	V.K. (1—11)
3671		$2P$(3—5), V.K. (4—13) (7—15)
3603	1,0	V.K. (0—10) O_2^+2N(0—6)i
3583	1,6	N_2^+1N(1—0), V.K. (3—12)
3578	9,8	$2P$(0—1), V.K. (6—14)
3563,5	1,6	N_2^+1N(2—1)

Table III c (continued)

λ	I	Interpretation
3536,3	4,9	$2P$(1—2), N_2^+ $1N$ (4—3)
3503,5	2,2	$2P$(2—3), V.K. (2—11)
3484	1,0	$2P$(7—8)
3467,5	3,0	$2P$(3—4), *NI*(66)
3429	2,0	V.K. (1—10)
3371,3	9,0	$2P$(0—0), *OII*(71,9)
3339,3	1,2	$2P$(1—1), V.K. (3—11)
3285,3	1,8	$2P$(3—3), *OII*(87,6)
3202,7	2,2	V.K.(1—9)
3192,4		V.K. (4—11)
3168,7		$2P$(9—7)
3159,3	5,8	$2P$(1—0)
3135,7	3,6	$2P$(2—1), V.K. (0—8), *OII*(34,8)
3114		$2P$(3—2), *OII*(13,9)

the nearly coinciding bands or lines contribute to the particular auroral feature.

As long as we have no instrument which combines a great light-power with a much higher dispersion than that of the «V» spectrograph, we have to take our refuge in other procedures, and we may call attention to the following:

a. With a well-corrected instrument atomic lines can be distinguished from bands by their greater sharpness. By diminishing the slit opening, the apparent intensity of lines relative to that of bands will increase.

b. The great variability of the spectral composition of the auroral luminescence may help us to obtain spectrograms, where certain lines or bands are enhanced, while others are weaker or absent. Thus in some spectrograms, parts within the region of long waves may be dominated by bands of the first positive group of N_2. They may mask a number of weak features, which, however, may be detected and identified on other spectrograms where the $N_2 1P$ bands are weak or practically absent.

c. If the spectral composition of the light emitted from a definite atom or molecule in a neutral or ionised state could be regarded as invariant and if some of the lines or bands from the same origin could be proved to appear, this would involve that also the rest of the spectral lines belonging to the emitting particle would appear with the intensity distribution characteristic of the invariant spectrum.

With considerations of this kind, however, due account must be taken of the fact that the intensity distribution of features belonging to a certain kind of emitting particles may greatly depend on the excitation process and the physical conditions under which the luminescence has been excited.

Still considerations of this kind may be extremely useful because there will as a rule be at any rate groups of lines or bands for which the intensity distribution may be fairly invariant.

The application of this procedure of interpretation of spectral features will call for an intimate study of the spectral intensity distribution corresponding to various types of excitation.

§ 4. Groups of Auroral Features.

As a step towards the application of these procedures, we have from our wavelength tables divided the features into groups in such a way that those of a certain group are emitted from the same sort of particles.

Those members of a group for which the wavelength is not shared by features of any other group or for which the identification in some way is established, will be marked in a suitable way.

The term symbols for the transition of each feature will be indicated and may give us information about the possible appearance of those lines which correspond to features also shared by members of other groups.

Apart from the hydrogen lines and the yellow sodium doublet ,the identification of which is easily settled, we have in the case of the auroral luminescence to deal with the three gruops of atomic oxygen OI, OII and OIII and of the other three from atomic nitrogen NI, NII and NIII.

In the case of molecular spectra the bands belonging to the same system form a group, and we have to deal with the following band systems (band groups):

N_2

Vegard-Kaplan (V. K.): A $^3\Sigma_u^+ - X\ ^1\Sigma_g^+$

1st pos. group (1. P) B $^3\Pi_g - A\ ^3\Sigma_u^+$

2nd pos. group (2. P) C $^3\Pi_u - B\ ^3\Pi_g$

N_2^+

1st negative group (N_2^+ 1N): B' $^2\Sigma_u^+ - X'^2\Sigma_g^+$

Meinel bands (N_2^+ 2N): A' $^2\Pi - X'\ ^2\Sigma_g^+$

O_2

Schuman-Runge Bands (S.R): B $^3\Sigma_u^- - X\ ^3\Sigma_g^-$

Atmospherie absorption Bands: A $^1\Sigma_g^+ - X^3\Sigma_g^-$

O_2^+

1st negative group (O_2^+1N): b $^4\Sigma_g^- - a^4\Pi_u$

Second negative group (O_2^+ 2N): $A^2\ \Pi_u - X^2\Pi_g$

NOβ- Bands B $^2\Pi - X\ ^2\Pi_{3/2\ 5/2}$

§ 5. The Line Groups.

The lines possibly belonging to the groups OI OII and OIII are given in tables IVa, IVb and IVc respectively. Those of the groups NI, NII and NIII in tables Va, Vb and Vc.

Those lines for which the position on the spectrogram is not shared by features of another group, are indicated by a star (*).

The first column gives wavelength values. The second the symbols of the atomic transition and the third contains the energy of the upper state in electron-volts (e. V.).

Table IV a.
Term combination and Excitation Potential of Auroral *OI* Lines.

λ		Termcombination	e. V. (Upper level)
*8446,8		$3s\ ^3S_1 - 3p\ ^3P_1$	10,99
*8446,4		$3s\ ^3S_1 - 3p\ ^3P_{0,2}$	10,99
*7995,1		$3p\ ^3P_2 - 3s'\ ^3D_3$	12,54
*7775,5		$3s\ ^5S_2 - 3p\ ^5P_1$	10,74
*7774,2		$3s\ ^5S_2 - 3p\ ^5P_2$	10,74
*7772,0		$3s\ ^5S_2 - 3p\ ^5P_3$	10,74
7480,7		$3s''\ ^3P_0 - 3p''\ ^3D_1$	15,78
6653,8		$3s''\ ^1P_1 - 3p''\ ^1S_0$	16,23
6456,0	=	$3p\ ^5P_3 - 5s\ ^5S_2$	12,66
6454,5		$3p\ ^5P_2 - 5s\ ^5S_2$	12,66
6553,6		$3p\ ^5P_1 - 5s\ ^5S_2$	12,66
*6363,8		$2p^4\ (^3P_1 - {}^1D_2)$	1,967
*6300,3		$2p^4\ (^3P_2 - {}^1D_2)$	1,967
*6266,9		$3p'\ ^3F_4 - 4d'\ ^3F_4$	16,07
*6264,6		$3p'\ ^3F_3 - 4d'\ ^1G_4$	16,07
6158,2	=	$3p\ ^5P_3 - 4d\ ^5D_4$	12,75
6156,8		$3p\ ^5P_2 - 4d\ ^5D_{3,2}$	12,75
6156,0		$3p\ ^5P_1 - 4d\ ^5D_{2,1,0}$	12,75
6106,3		$3p'\ ^3D_2 - 4d'\ ^3F_4$	16,07
6046,5		$3p\ ^3P_{2,0} - 6s\ ^3S_1$	13,04
6046,2		$3p\ ^3P_1 - 6s\ ^3S_1$	13,04
5995,3		$3p'\ ^3D_{3,2} - 4d'\ ^3P_2$	16,11
5993,2		$3p'\ ^3D_1 - 4d'\ ^3P_1$	16,11
5991,9		$3p'\ ^3D_2 - 4d'\ ^3P_1$	16,11
5991,3		$3p'\ ^3D_1 - 4d'\ ^3P_0$	16,11
5958,6		$3p\ ^3P_{2,0} - 5d\ ^3D$	13,07
5958,5		$3p\ ^3P_1 - 5d\ ^3D$	13,07
5750,4		$6p\ ^3P - 3d'\ ^3P_2$	15,28
5731,1		$6p\ ^3P - 3d'\ ^3P_1$	15,29
*5577,35		$2p^4\ (^1D_2 - {}^1S_0)$	4,19
5554,9		$3p\ ^3P_2 - 7s\ ^3S_1$	13,22
5512.7		$3p\ ^3P_2 - 6d\ ^3D$	13,23
*5492,8		$3p'\ ^1F_3 - 5d'\ ^1G_4$	16,39
5486,6		$3p'\ ^1F_3 - 5d'\ ^3G_4$	16,39
5436,8	=	$3p\ ^5P_3 - 6s\ ^5S_2$	13,03
5435,8	=	$3p\ ^5P_2 - 6s\ ^5S_2$	13,02
5435,2	=	$3p\ ^5P_1 - 6s\ ^5S_1$	13,02

Table IV a (cont).
Term combination and Excitation Potential of Auroral *OI* Lines.

λ		Termcombination	e. V. (Upper level)
*5410,8		$3p'\ ^3F_3 - 5d'\ ^1G_4$	16,39
		$^3F_4 - {}^3F_4$	16,39
5330,7	=	$3p\ ^5P_3 - 5d\ ^5D_4(_3)$	13,06
5329,6	=	$3p\ ^5P_2 - 5d\ ^5D_{3,2}(_1)$	13,06
5329,0	=	$3p\ ^5P_1 - 5d\ ^5D_{2,1,0}$	13,06
5299,0		$3p\ ^3P_2 - 8s\ ^3S_1$	13,32
5275,1		$3p\ ^3P_2 - 7d\ ^3D$	13,34
5130,5		$3p\ ^3P_2 - 8d\ ^3D$	13,40
5047,7		$3p\ ^3P_2 - 10s\ ^3S_1$	13,44
5020,1	=	$3p\ ^5P_3 - 7s\ ^5S_2$	13,21
*5019,3	=	$3p\ ^5P_2 - 7s\ ^5S_2$	13,21
5018,8	=	$3p\ ^5P_1 - 7s\ ^5S_2$	13,21
*4979,6		$3p\ ^3P_2 - 11s\ ^3S_1$	13,47
4968,8	=	$3p\ ^5P_3 - 6d\ ^5D_4(_3)$	13,23
*4967,9	=	$3p\ ^5P_2 - 6d\ ^5D_{3,2}(_1)$	13,23
4967,4	=	$3p\ ^5P_1 - 6d\ ^5D_{2,1,0}$	13,23
4803,0	=	$3p\ ^5P_3 - 8s\ ^5S_2$	13,32
4802,2	=	$3p\ ^5P_2 - 8s\ ^5S_2$	13,32
4801,8	=	$3p\ ^5P_1 - 8s\ ^5S_2$	13,32
4773,8	=	$3p\ ^5P_3 - 7d\ ^5D_4(_3)$	13,33
*4772,9	=	$3p\ ^5P_2 - 7d\ ^5D_{3,2}(_1$	13,33
4772,5	=	$3p\ ^5P_1 - 7d\ ^5D_{2,1,0}$	13,33
4673,7	=	$3p\ ^5P_3 - 9s\ ^5S_2$	13,40
4672,8	=	$3p\ ^5P_{2,1} - 9s\ ^5S_2$	13,40
*4589,9		$3p\ ^5P_3 - 10s\ ^5S_2$	13,44
4589,0		$3p\ ^5P_{2,1} - 10s\ ^5S_2$	13,44
*4368,3	=	$3s\ ^3S_1 - 4p\ ^3P$	12,36
4233,3		$4p\ ^3P - 3d'\ ^3P_2$	15,28
4222,8		$4p\ ^3P - 3d'\ ^3P_1$	15,29
*4217,1		$4p\ ^3P - 3d'\ ^3P_0$	15,29
3954,7		$3p\ ^3P_2 - 3s''\ ^3P_2$	14,12
3954,6		$3p\ ^3P_1 - 3s''\ ^3P_2$	14,12
3953,1		$3p\ ^3P_{2,0} - 3s''\ ^3P_1$	14,12
3953,0		$3p\ ^3P_1 - 3s''\ ^3P_1$	14,12
3947,6		$3s\ ^5S_2 - 4p\ ^5P_1$	12,28
*3947,5		$3s\ ^5S_2 - 4p\ ^5P_2$	12,28
3947,3		$3s\ ^5S_2 - 4p\ ^5P_3$	12,28

Table IV b.

Term combination and Excitation Potential of Auroral *OII*-lines

λ		Term combination	e. V. (Upper level)
6666,9		$3d\ ^2P_{3/2} - 4p\ ^2P_{1/2}$	30,79
*4955,7		$3p\ ^2P_{3/2} - 3d\ ^2D_{3/2}$	29,06
*4943,0		$3p\ ^2P_{3/2} - 3d\ ^2D_{5/2}$	29,06
*4941,0		$3p\ ^2P_{1/2} - 3d\ ^2D_{3/2}$	29,06
*4924,5		$3p\ ^4S_{3/2} - 3d\ ^4P_{5/2}$	28,81
*4906,8		$3p\ ^4S_{3/2} - 3d\ ^4P_{3/2}$	28,82
4890,9		$3p\ ^4S_{3/2} - 3d\ ^4P_{1/2}$	28,83
*4871,5		$3p'\ ^2P_{3/2} - 3d'\ ^2D_{5/2}$	31,37
*4864,9		$3p\ ^4S_{3/2} - 3d\ ^4D_{1/2}$	28,85
(4860,9)	=	$3p'\ ^2P_{1/2} - 3d'\ ^2D_{3/2}$	31,37
*4856,8	=	$3p\ ^4S_{3/2} - 3d\ ^4D_{3/2}$	28,85
*4856,4		$3p\ ^4S_{3/2} - 3d\ ^4D_{5/2}$	28,85
4752,7	=	$3p\ ^2D_{5/2} - 3d\ ^4D_{5/2}$	28,85
4751,3	=	$3p\ ^2D_{5/2} - 3d\ ^4D_{7/2}$	28,85
4677,0	=	$3d\ ^2D_{5/2} - 4f\ ^2G_{7/2}$	31,71
4673,8		$3s\ ^4P_{3/2} - 3p\ ^4D_{1/2}$	25,63
4661,7	=	$3s\ ^4P_{3/2} - 3p\ ^4D_{3/2}$	25,63
4650,9	=	$3s\ ^4P_{1/2} - 3p\ ^4D_{1/2}$	25,63
4649,1	=	$3s\ ^4P_{5/2} - 3p\ ^4D_{7/2}$	25,66
4641,8	=	$3s\ ^4P_{3/2} - 3p\ ^4D_{5/2}$	25,64
*4638,9	=	$3s\ ^4P_{1/2} - 3p\ ^4D_{3/2}$	25,63
4621,3		$3d\ ^2D_{5/2} - 4f\ ^4F_{5/2}$	31,74
4613,7		$3d\ ^2D_{5/2} - 4f\ ^4F_{7/2}$	31,75
(4613,1)		$3d\ ^2D_{5/2} - 4f\ ^2F_{5/2}$	31,75
4610,1	=	$3d\ ^2D_{3/2} - 4f\ ^4F_{5/2}$	31,74
4602,1	=	$3d\ ^2D_{3/2} - 4f\ ^2F_{5/2}$	31,75
*4596,1	=	$3s'\ ^2D_{3/2} - 3p'\ ^2F_{5/2}$	28,35
4590,9	=	$3s'\ ^2D_{5/2} - 3p'\ ^2F_{7/2}$	28,35
4491,2	=	$3d\ ^2P_{3/2} - 4f\ ^2D_{5/2}$	31,69
4489,5	=	$3d\ ^3P_{1/2} - 4f\ ^2D_{3/2}$	31,71
4488,2	=	$3d'\ ^2P_{3/2} - 4f'\ ^2D_{5/2}$	34,22
4487,7	=	$3d'\ ^2P_{1/2} - 4f'\ ^2D_{3/2}$	34,22
4482,9		$3d\ ^2D_{5/2} - 4f\ ^4D_{5/2}$	31,71
4477,9	=	$3d\ ^2P_{3/2} - 4f\ ^4D_{5/2}$	31,71
4476,1	=	$3d\ ^2P_{1/2} - 4f\ ^4D_{3/2}$	31,72
*4469,4	=	$3s\ ^6S_{5/2} - 3p\ ^6P_{3/2}$	33,19
*4467,8	=	$3s\ ^6S_{5/2} - 3p\ ^6P_{5/2}$	33,19
*4466,3	=	$3d\ ^2P_{3/2} - 4f\ ^4D_{3/2}$	31,72
4465,5	=	$3s\ ^6S_{5/2} - 3p\ ^6P_{7/2}$	33,19
*4452,4	=	$3s\ ^2P_{3/2} - 3p\ ^2D_{3/2}$	26,22
4417,0	=	$3s\ ^2P_{1/2} - 3p\ ^2D_{3/2}$	26,22
*4414,9	=	$3s\ ^2P_{3/2} - 3p\ ^2D_{5/2}$	26,24
*4406,0		$3p\ ^2D_{5/2} - 3d\ ^2D_{3/2}$	29,06
4396,0		$3p\ ^2D_{5/2} - 3d\ ^2D_{5/2}$	29,06
4378,4	=	$3d'\ ^2D_{5/2} - 4f'\ ^2F_{7/2}$	34,20
*4378,0	=	$3d'\ ^2D_{3/2} - 4f'\ ^2F_{5/2}$	34,20
4369,3	=	$3p\ ^2D_{3/2} - 3d\ ^2D_{3/2}$	29,06
4366,9	=	$3s\ ^4P_{5/2} - 3p\ ^4P_{3/2}$	25,83
4358,5		$3d\ ^4D_{7/2} - 4f\ ^4D_{7/2}$	31,69
4357,3		$3d\ ^4D_{5/2} - 4f\ ^4F_{7/2}$	31,69
*4351,3	=	$3s\ ^2D_{5/2} - 3p'\ ^2D_{5/2}$	28,50
*4349,4	=	$3s\ ^4P_{5/2} - 3p\ ^4P_{5/2}$	25,84
*4347,4	=	$3s'\ ^2D_{3/2} - 3p'\ ^2D_{3/2}$	28,50

Table IV b (cont.)

Term combination and Excitation Potential of Auroral *OII*-lines

λ		Term combination	e. V. (Upper level)
4345,6		$3s\ ^4P_{3/2} - 3p\ ^4P_{1/2}$	25,83
*4344,3	=	$3d\ ^4D_{5/2} - 4f\ ^4G_{7/2}$	31,70
4343,4	=	$3d'\ ^2D_{5/2} - 4f'\ ^2D_{5/2}$	34,22
*4342,8	=	$3d'\ ^2D_{3/2} - 4f'\ ^2D_{3/2}$	34,22
4342,0	=	$3d\ ^2F_{7/2} - 4f\ ^2G_{9/2}$	31,73
4340,3	=	$3d\ ^2F_{5/2} - 4f\ ^2G_{7/2}$	31,71
4336,9		$3s\ ^4P_{3/2} - 3p\ ^4P_{3/2}$	25,83
*4334,2	=	$3d\ ^4D_{5/2\ 3/2} - 4f\ ^4D_{5/2}$	31,71
4331,8		$3p'\ ^2D_{3/2} - 3d'\ ^2D_{3/2}$	31,37
*4331,4		$3p'\ ^2D_{3/2} - 3d'\ ^2D_{5/2}$	31,37
4328,6	=	$3p'\ ^2P_{3/2} - 3d'\ ^2S_{1/2}$	31,69
*4327,8	=	$3p'\ ^2D_{5/2} - 3d'\ ^2D_{3/2}$	31,37
4327,5	=	$3p'\ ^2D_{5/2} - 3d'\ D_{5/2}$	31,37
*4325,8	=	$3s\ ^4P_{1/2} - 3p\ ^4P_{1/2}$	25,83
*4319,9	=	$3p'\ ^2P_{1/2} - 3d'\ ^2S_{1/2}$	31,69
4317,7	=	$3d\ ^4P_{3/2} - 4f\ ^2D_{5/2}$	31,69
*4317,2	=	$3s\ ^4P_{1/2} - 3p\ ^4P_{3/2}$	25,83
4313,4		$3d\ ^2F_{7/2} - 4f\ ^4F_{9/2}$	31,75
4309,0		$3d\ ^4D_{1/2} - 4f\ ^4D_{1/2}$	31,72
4303,8	=	$3d\ ^4P_{5/2} - 4f\ ^4D_{7/2}$	31,69
4294,7	=	$3d\ ^4P_{3/2} - 4f\ ^4D_{5/2,3/2}$	31,72
4292,1	=	$3d\ ^2F_{5/2} - 4f\ ^4F_{5/2}$	31,74
4288,8	=	$3d\ ^4P_{1/2} - 4f\ ^4D_{1/2}$	31,72
4285,6	=	$3d\ ^2F_{5/2} - 4f\ ^4F_{7/2}$	31,75
4196,7		$3p'\ ^2D_{3/2} - 3d'\ ^2P_{1/2}$	31,46
4196,3		$3p'\ ^2D_{3/2} - 3d'\ ^2P_{3/2}$	31,46
4192,5	=	$3p'\ ^2D_{5/2} - 3d'\ ^2P_{3/2}$	31,46
*4192,5	=	$3p'\ ^2D_{5/2} - 3d'\ ^2P_{3/2}$	31,46
4189,8	=	$3p'\ ^2F_{7/2} - 3d'\ ^2G_{9/2}$	31,31
*4185,5	=	$3p'\ ^2F_{5/2} - 3d'\ ^2G_{7/2}$	31,31
*4169,3		$3p\ ^4P_{5/2} - 3d\ ^4P_{5/2}$	28,81
*4156,5	=	$3p\ ^4P_{5/2} - 3d\ ^4P_{3/2}$	28,82
*4153,3	=	$3p\ ^4P_{3/2} - 3d\ ^4P_{5/2}$	28,81
4142,3		$3p\ ^6P_{3/2} - 3d\ ^6D_{5/2}$	36,18
4142,1		$3p\ ^6P_{3/2} - 3d\ ^6D_{3/2}$	36,18
4142,0		$3p\ ^6P_{3/2} - 3d\ ^6D_{1/2}$	36,18
4140,7		$3p\ ^4P_{3/2} - 3d\ ^4P_{3/2}$	28,82
4132,8		$3p\ ^4P_{1/2} - 3d\ ^4P_{3/2}$	28,82
4129,3		$3p\ ^4P_{3/2} - 3d\ ^4P_{1/2}$	28,83
4121,5		$3p\ ^4P_{1/2} - 3d\ ^4P_{1/2}$	28,83
4120,6	=	$3p\ ^4P_{5/2} - 3d\ ^4D_{3/2}$	28,85
*4120,3	=	$3p\ ^4P_{5/2} - 3d\ ^4D_{5/2}$	28,85
4119,2	=	$3p\ ^4P_{5/2} - 3d\ ^4D_{7/2}$	28,85
4113,8		$3p'\ ^2F_{7/2} - 3d'\ ^2D_{5/2}$	31,37
*4112,0		$3p\ ^4P_{5/2} - 3d\ ^2F_{5/2}$	28,86
4110,8		$3p\ ^4P_{3/2} - 3d\ ^4D_{1/2}$	28,85
*4110,2		$3p'\ ^2F_{5/2} - 3d'\ ^2D_{3/2}$	31,37
4108,8		$3d\ ^4F_{7/2} - 4f\ ^4G_{7/2}$	31,70
*4107,1		$3d\ ^4F_{5/2} - 4f\ ^4D_{7/2}$	31,69
4106,0		$3p\ ^4D_{7/2} - 3d\ ^4F_{5/2}$	28,68
4105,0		$3p\ ^4P_{3/2} - 3d\ ^4D_{3/2}$	28,85
*4104,7		$3p\ ^4P_{3/2} - 3d\ ^4D_{5/2}$	28,85
4103,3		$3p\ ^4P_{1/2} - 3d\ ^4D_{1/2}$	28,85

Table IV b (cont.)

Term combination and Excitation Potential of Auroral *OII*-Lines

λ		Term combination	e. V. (Upper level)
4097,3	=	$3p\ ^4P_{1/2} — 3d\ ^4D_{3/2}$	28,85
4097,2	=	$3d\ ^4F_{7/2} — 4f\ ^4G_{9/2}$	31,71
4096,5	=	$3p\ ^4P_{3/2} — 3d\ ^2F_{5/2}$	28,86
4096,2	=	$3d\ ^4F_{5/2} — 4f\ ^4G_{5/2}$	31,70
4095,6	=	$3d\ ^4F_{5/2} — 4f\ ^4G_{7/2}$	31,70
4094,2		$3p\ ^4D_{5/2} — 3d\ ^4F_{3/2}$	28,67
*4092,9	=	$3p\ ^4D_{7/2} — 3d\ ^4F_{7/2}$	28,67
*4089,3	=	$3d\ ^4F_{9/2} — 4f\ ^4G_{11/2}$	31,73
*4087,1	=	$3d\ ^4F_{3/2} — 4f\ ^4G_{5/2}$	31,70
*4084,7	=	$3p\ ^4P_{5/2} — 3d\ ^2F_{7/2}$	28,88
*4083,9	=	$3d\ ^4F_{5/2} — 4f\ ^2G_{7/2}$	31,71
*4078,9	=	$3p\ ^4D_{3/2} — 3d\ ^4F_{3/2}$	28,67
*4075,9	=	$3p\ ^4D_{7/2} — 3d\ ^4F_{9/2}$	28,70
4072,2	=	$3p\ ^4D_{5/2} — 3d\ ^4F_{7/2}$	28,69
*4069,9	=	$3p\ ^4D_{3/2} — 3d\ ^4F_{5/2}$	28,68
*4069,6	=	$3p\ ^4D_{1/2} — 3d\ ^4F_{3/2}$	28,67
*4061,0	=	$3d'\ ^2F_{5/2} — 4f'\ ^2G_{7/2}$	34,19
*4060,6	=	$3d'\ ^2F_{7/2} — 4f'\ ^2G_{9/2}$	34,19
*4054,6		$3d'\ ^2F_{5/2} — 4f'\ ^2F_{5/2}$	34,20
*4054,1		$3d'\ ^2F_{7/2} — 4f'\ ^2F_{7/2}$	34,20
*4048,2		$3d\ ^4F_{7/2} — 4f\ ^4F_{7/2}$	31,75
*4046,2		$3d\ ^4F_{7/2} — 4f\ ^4F_{9/2}$	31,75
4045,0		$3d\ ^4F_{7/2} — 4f\ ^2F_{7/2}$	31,75
4041,3		$3d\ ^4F_{5/2} — 4f\ ^4F_{5/2}$	31,74
4035,1		$3d\ ^4F_{5/2} — 4f\ ^2F_{5/2}$	31,75
4033,2		$3d\ ^4F_{3/2} — 4f\ ^4F_{3/2}$	31,74
4026,4		$3d\ ^4F_{3/2} — 4f\ ^2F_{5/2}$	31,75

Table IV b (cont.)

Term combination and Excitatioo Potential of Auroral *OII*-Lines

λ		Term combination	e. v. (Upper level)
*4024,0		$3d'\ ^2F — 4f'\ ^2D$	34,22
*3985,5		$3p\ ^4P_{1/2} — 3d\ ^2P_{3/2}$	28,93
*3982,7		$3s\ ^2P_{3/2} — 3p\ ^2P_{1/2}$	26,55
*3973,2	=	$3s\ ^2P_{3/2} — 3p\ ^2P_{3/2}$	26,55
3954,4	=	$3s\ ^2P_{1/2} — 3p\ ^2P_{1/2}$	26,55
*3945,0	=	$3s\ ^2P_{1/2} — 3p\ ^2P_{3/2}$	26,55
3919,3		$3s'\ ^2D_{3/2} — 3p'\ ^2P_{1/2}$	28,82
3883,2		$(3p\ ^4D_{3/2} — 3d\ ^4P_{3/2})$	28,82
		$(3p\ ^4D_{7/2} — 3d\ ^4D_{5/2})$	28,85
3882,4		$3p\ ^4D_{7/2} — 3d\ ^4D_{7/2}$	28,85
3875,8		$3p\ ^4D_{7/2} — 3d\ ^2F_{5/2}$	28,88
3874,1		$3p\ ^4D_{1/2} — 3d\ ^4P_{3/2}$	28,82
3872,4		$3p\ ^4D_{3/2} — 3d\ ^4P_{1/2}$	28,83
3857, 2		$3p\ ^4D_{5/2} — 3d\ ^2F_{5/2}$	28,86
3821,6		$3p\ ^2P_{1/2} — 4s\ ^2P_{1/2}$	29,79
3803,1		$3p\ ^2P_{3/2} — 4s\ ^2P_{3/2}$	29,81
3729,2		$3p'\ ^2P_{1/2} — 4s'\ ^2D_{3/2}$	32,14
3728,9		$2p^3(^4S_{3/2} — ^2D_{5/2})$	3,23
3727,3		$3s\ ^4P_{5/2} — 3p\ ^4S_{3/2}$	26,38
3712,7		$3s\ ^4P_{1/2} — 3p\ ^4S$	26,38
3371,9		$3d\ ^4F_{9/2} — 5p\ ^4D_{7/2}$	32,37
3287,6		$3p\ ^4P_{5/2} — 4s\ ^4P_{5/2}$	29,61
3134,8		$3p\ ^4D_{7/2} — 4s\ ^4P_{5/2}$	29,61
3113,9		$3p\ ^4D_{3/2} — 4s\ ^4P_{5/2}$	29,61

Table IV c

Some *OIII*-lines possibly present in the Auroral spectrum.

λ	Term combination	e. V. (Upper level)
4569,5	$3p'\ ^1D_2 — 3d'\ ^1F_3$	52,84
4534,0		
4529,7	$3p\ ^5S_2 — 3d\ ^5D_3$	49,35
4482,8		
4475,0	$3p'\ ^1D_2 — 3d'\ ^1D_2$	52,84
4458,4		
4440,1		
4424,3		
4379,6		
4125,5		
4073,9	$3s\ ^3P_1 — 3p'\ ^3D_2$	46,44
3961,6	$3s\ ^1P_1 — 3p\ ^1D_2$	38,00
3757,2		
3754,7		
3728,7	$3p\ ^3D_3 — 3d\ ^3F_4$	49,78

Table V a

Auroral NI-lines

λ	Term combination	e. V.
8719	$3s\ ^4P_{5/2} — 3p\ ^4D_{5/2}$	11,75
8711	$3s\ ^4P_{3/2} — 3p\ ^4D_{3/2}$	11,75
8704	$3s\ ^4P_{1/2} — 3p\ ^4D_{1/2}$	11,75
8686	$3s\ ^4P_{1/2} — 3p\ ^4D_{3/2}$	11,75
8684	$3s\ ^4P_{3/2} — 3p\ ^4D_{5/2}$	11,75
8681	$3s\ ^4P_{5/2} — 3p\ ^4D_{7/2}$	11,76
8629	$3s\ ^2P_{3/2} — 3p\ ^2P_{3/2}$	12,12
8221,8	$3s\ ^4P_{3/2} — 3p\ ^4P_{1/2}$	11,83
8216,5	$3s\ ^4P_{5/2} — 3p\ ^4P_{5/2}$	11,84
* 8183,9	$3s\ ^4P_{3/2} — 3p\ ^4P_{5/2}$	11,84
7587	$3p\ ^4S_{3/2} — 5s\ ^4P_{5/2}$	13,63
7366	$3p\ ^4S_{3/2} — 4p\ ^4P_{1/2}$	13,26
7351,4	$3p\ ^4S_{3/2} — 4p\ ^4P_{3/2}$	13,26
7347,7	$3p\ ^2D_{5/2} — 4d\ ^2D_{5/2}$	13,69
6741,3	$3p\ ^4P_{3/2} — 4d\ ^4P_{1/2}$	13,68
6706,2	$3p\ ^4P_{3/2} — 4d\ ^4P_{5/2}$	13,68
6666,8	$3p\ ^2P_{3/2} — 5d\ ^2P_{3/2}$	13,98
6656,6	$3p\ ^4D_{3/2} — 5s\ ^4P_{1/2}$	13,61
6653,4	$3p\ ^4D_{5/2} — 5s\ ^4P_{3/2}$	13,61
* 6646,5	$3p\ ^4D_{1/2} — 5s\ ^4P_{1/2}$	13,61
6622,5	$3p\ ^4D_{5/2} — 5s\ ^4P_{5/2}$	13,63
6544,2	$3p\ ^4D_{5/2} — 5s\ ^2P_{3/2}$	13,65
6528,4	$3p\ ^4D_{3/2} — 5s\ ^2P_{3/2}$	13,65
* 6510,3	$3p\ ^4D_{5/2} — 4d\ ^4F_{3/2}$	13,66
6506	$3p\ ^4D_{7/2} — 4d\ ^4F_{7/2}$	13,67
* 6499,5	$3p\ ^4D_{5/2} — 4d\ ^4F_{5/2}$	13,66
6491,3	$3p\ ^4D_{3/2} — 4d\ ^4F_{3/2}$	13,66
6484,9	$3p\ ^4D_{5/2} — 4d\ ^4F_{7/2}$	13,67
6471,0	$3p\ ^4D_{3/2} — 4d\ ^2P_{1/2}$	13,67
6437,3	$3p\ ^4D_{3/2} — 4d\ ^4P_{1/2}$	13,68
* 6428,0	$3p\ ^4D_{1/2} — 4d\ ^4P_{1/2}$	13,68
6417,1	$3p\ ^4D_{1/2} — 4d\ ^4P_{3/2}$	13,68
6393,6	$3p\ ^4D_{5/2} — 4d\ ^2D_{5/2}$	13,69
6378,0	$3p\ ^4D_{3/2} — 4d\ ^2D_{5/2}$	13,69
6321,7	$3p\ ^4S_{3/2} — 6s\ ^4P_{1/2}$	13,95
* 6275,5	$3p\ ^4S_{3/2} — 6s\ ^4P_{5/2}$	
6272,8	$3p\ ^2D_{5/2} — 5d\ ^2P_{3/2}$	13,98
* 6243,2	$3p\ ^2D_{3/2} — 5d\ ^2P_{3/2}$	13,98
6237,5	$3p\ ^2D_{3/2} — 5d\ ^2P_{1/2}$	13,98
6224	$3p\ ^4S_{3/2} — 5d\ ^2P_{1/2}$	13,98
6075,7	$3p\ ^2P_{3,2} — 6d\ ^4P_{3/2}$	14,16
6069,0	$3p\ ^2P_{3/2} — 6d\ ^4P_{5/2}$	14,16
6061,9	$3p\ ^2P_{1/2} — 6d\ ^4P_{3/2}$	12,97
	$2p^4\ ^4P_{1/2\ 3/2} — 3d\ ^4F_{3/2\ 5/2}$	12,98
6044,8	$2p\ ^4P_{5/2} — 3d\ ^4F_{5/2}$	12,98
6012,0	Not classified	
6008,4	$3p\ ^3S_{1/2} — 4d\ ^2P_{3/2}$	13,66
5999,6	$3p\ ^2S_{1/2} — 4d\ ^2P_{1/2}$	13,67
* 5987,5	Not classified	
5972,7	» »	
* 5962,1	» »	
5958,8	» »	
5951,1	$(3p^4)^4P_{3/2} — 3p'\ ^2P_{1/2}$	13,94
5941,9	$(3p^4)^4P_{3/2} — 3p'\ ^2P_{3/2}$	13,92

Table Va (continued)

Auroral NI-lines

λ	Term combination	e. V.
5931,2	Not classified	
5927,5	» »	
5905,1	» »	
5898,2	» »	
5863	» »	
5854	$3p\ ^4P_{5/2} — 6s\ ^4P_{3,2}$	13,96
5841	$3p\ ^4P_{3/2} — 6\ ^4P_{3,2}$	13,96
5834,8	$3p\ ^4P_{1/2} — 6s\ ^4P_{3/2}$	13,96
5839,6	$3p\ ^4P_{5/2} — 6s\ ^4P_{5/2}$	13,97
5829,6		
5816	$3p\ ^4P_{3/2} — 6s\ ^4P_{5/2}$	13,97
5803	$3p\ ^4P_{5/2} — 5d\ ^4F_{5/2}$	13,98
* 5790,4	$3p\ ^4P_{5/2} — 5d\ ^4F_{7/2}$	13,98
5781,7	$3p\ ^4P_{5/2} — 5d\ ^4D_{5/2}$	13,99
* 5772,8	$3p\ ^4S_{3/2} — 7s\ ^4P_{3/2}$	14,14
* 5768,6	$3p\ ^4P_{3/2} — 5d\ ^4D_{5/2}$	13,99
5764,5	$3p\ ^4P_{5/2} — 5d\ ^4P_{3/2}$	13,99
* 5758,6		
5752,7	$3p\ ^4P_{5/2} — 5d\ ^4P_{5/2}$	14,00
5747,3	$3p\ ^4S_{3/2} — 7s\ ^4P_{5/2}$	14,15
* 5728,3	$3p\ ^4S_{3/2} — 6d\ ^4D_{3/2}$	14,15
5710,7	$3p\ ^4S_{3/2} — 6d\ ^4P_{3/2}$	14,16
5623	$3p\ ^4D_{5/2} — 6s\ ^4P_{3/2}$	13,96
5618	$3p\ ^4D_{1/2} — 6s\ ^4P_{1/2}$	13,95
5616,5	$3p\ ^4D_{7/2} — 6s\ ^4P_{5/2}$	13,97
5611,3	$3p\ ^4D_{3/2} — 6s\ ^4P_{3/2}$	13,96
5604,4	$3p\ ^4D_{1/2} — 6s\ ^4P_{3/2}$	13,96
5600,5	$3p\ ^4D_{5/2} — 6s\ ^4P_{5/2}$	13,97
5530,0	$3p\ ^4D_{3/2\ 5/2} — 5d\ ^4P_{3/2\ 5/2}$	13,99
		14,00
5524	$3p\ ^4D_{1/2} — 5d\ ^4P_{3/2}$	13,99
5519,4	$3p\ ^4D_{3/2} — 5d\ ^4P_{5/2}$	14,00
5496,6	Not classified	
* 5419,3	» »	
* 5401,2	» »	
* 5392,7	$3p\ ^4P_{5/2\ 1/2} — 7s\ ^4P_{3/2\ 1/2}$	14,14
		14,13
5371,0	$3p\ ^4P_{5/2} — 7s\ ^4P_{5/2}$	14,15
5367,3	$(2p^4)^4P_{3/2} — 4p\ ^4D_{3/2}$	13,24
* 5360,1	$3p\ ^4P_{3/2} — 7s\ ^4P_{5/2}$	14,15
* 5356,8	$(2p^4)^4P_{3/2} — 4p\ ^4D_{5/2}$	13,24
* 5344,2	$(2p^4)^4P_{5/2} — 4p\ ^4D_{5/2}$	13,24
5340,3	$3p\ ^4P_{5/2} — 6d\ ^4P_{3/2}$	14,16
5334,3	$3p\ ^4P_{5/2} — 6d\ ^4P_{5/2}$	14,16
5328,8	$(2p^4)^4P_{5/2} — 4p\ ^4D_{7/2}$	13,25
5315,2	$(2p^4)^4P_{1/2} — 4p\ ^4P_{1/2}$	13,26
5292,8	$(2p^4)^4P_{52\ 3/2} — 4p\ ^4P_{3/2\ 5/2}$	13,26
		13,27
5281,2	$(2p^4)^4P_{5/2} — 4p\ ^4P_{5/2}$	13,27
	$2p^3(^4S_{3/2} — {}^2D_{5/2\ 3/2})$	2,38
5199,5	$3p\ ^2S — 5d\ ^2P$	13,98
5189,3	$3p\ ^4D_{7/2} — 7s\ ^4P_{5/2}$	14,15
5182,5	Not classified	
5180,9	» »	

Table Va (continued)

Auroral NI-lines

λ	Term combination	e. V.
5179,6	$3p\ ^4D_{7/2} — 6d\ ^4D_{5/2}$	14,15
5168,0	Not classified	
5165,8	$3p\ ^4D_{5/2} — 6d\ ^4D_{5/2}$	14,15
5156	$3p\ ^4D_{3/2} — 6d\ ^4D_{5/2}$	14,15
* *5140,8*	$3p\ ^4D_{5/2} — 6d\ ^4P_{5/2}$	14,15
5130	$3p\ ^4D_{1/2} — 6d\ ^4P_{1/2}$	14,16
5068	Not classified	
5054,7	» »	
5051,6	» »	
* *4935,0*	$3s\ ^2P_{3/2} — 4p\ ^2S_{1/2}$	13,20
4914,9	$3s\ ^2P_{1/2} — 4p\ ^2S_{1/2}$	13,20
4886,3	Not classified	
4881,8	» »	
* 4868,9	» »	
* 4847,4	» »	
* *4837,8*	» »	
4753,1	» »	
4750,3	» »	
* 4685,7	» »	
4669,8	» »	
4660,0	» »	
4651,0	» »	
4554,2	» »	
4553,4	» »	
4499,1	» »	
4497,5	» »	
* 4494,7	» »	
4485,1	» »	
4358,3	» »	
4336,5	» »	
* 4324,9	» »	
* *4322,0*	» »	
4317,7	» »	
4313,1	» »	

Table Va (continued)

Auroral NI-lines

λ		Term combination	e. V.
* *4305,5*		Not classified	
* 4284,9		» »	
4230,4		$3s\ ^4P_{5/2} — 4p\ ^4P_{3/2}$	13,26
* 4229,6		Not classified	
* *4224,7*	=	$3s\ ^4P_{2/1} — 4p\ ^4P_{1/2}$	13,26
4223,0		$3s\ ^4P_{5/2} — 4p\ ^4P_{5/2}$	13,27
* 4220,8		Not classified	
4215,9	=	$3s\ ^4P_{1/2} — 4p\ ^4P_{3/2}$	13,26
4214,7	=	$3s\ ^4P_{3/2} — 4p\ ^4P_{5/2}$	13,27
* 4213,0		Not classified	
* *4209,1*	=	» »	
* 4206,3		» »	
* *4205,7*		» »	
* 4187		» »	
4180,0		» »	
* *4166,6*	=	» »	
* 4164,8		» »	
* *4151,5*	=	$3s\ ^4P_{5/2} — 4p\ ^4S_{3/2}$	13,32
4145,8	=	Not classified	
* *4137,6*		$3s\ ^4P_{1/2} — 4p\ ^4S_{3/2}$	13,32
4129,2		Not classified	
4114,0		$3s\ ^2P_{3/2} — 3p'\ ^2D_{3/2}$	13,70
4110,0		$3s\ ^2P_{3/2} — 3p'\ ^2D_{5/2}$	13,70
4102,2		Not classified	
4099,9	=	$3s\ ^2P_{1/2} — 3'\ ^2D_{3/2}$	13,70
4037,4		Not classified	
4033,6		» »	
* *4011,0*		» »	
* 4001,7		» »	
* 4001,0		» »	
3994,9		» »	
* 3970,0		» »	
3957,0		» »	
3466		$2p^3(^4S_{3/2} — ^2P_{1/2\ 3/2})$	3,57

Table V b Auroral *NII*-lines.

λ	Term combination	e. V.
8439,0	$3p\ ^1S_0 — 3d\ ^1P_1$	23,57
6857,6	$3p\ ^5S_2 — 3d\ ^5P_1$	30,34
*6630,5	$3p\ ^1D_2 — 4p\ ^1P_1$	25,06
6610,6	$3p\ ^1D_2 — 3d\ ^1F_3$	23,47
*6583,4	$2p^2\ (^3P_2 — ^1D_2)$	1,898
6554,7	$3d\ ^3D_2 — 4p\ ^3D_1$	25,13
*6533,0	$3d\ ^3D_2 — 4p\ ^3D_2$	25,13
6522,3	$3d\ ^3D_1 — 4p\ ^3D_2$	25,13
6504,9	$3d\ ^3D_3 — 4p\ ^3D_3$	25,15
6492,0	$3d\ ^3D_2 — 4p\ ^3D_3$	25,15
6482,0	$3s\ ^1P — 3p\ ^1P_1$	20,40
6173,4	$3d\ ^3F_3 — 4p\ ^3D_2$	25,13
6136,9	$3d\ ^3F_3 — 4p\ ^3D_3$	25,15
5952,4	$3p\ ^3P_2 — 3d\ ^3D_2$	23,24
{5941,7	$3p\ ^3P_2 — 3d\ ^3D_3$	23,24
{5940,3	$3p\ ^3P_1 — 3d\ ^3D_1$	23,23
5931,8	$3p\ ^3P_1 — 3d\ ^3D_2$	23,24
5925,8	$3p\ ^3P_0 — 3d\ ^3D_1$	23,23
5767,4	$3s\ ^1P_1 — 3p\ ^3D_1$	20,64
5755,0	$2p^2\ (^1D_2 — ^1S_0)$	4,052
5747,3	$3s\ ^1P_1 — 3p\ ^3D_2$	20,65
5730,7	$3s\ ^3P_2 — 3p\ ^3D_1$	20,64
5710,8	$3s\ ^3P_2 — 3p\ ^3D_2$	20,65
5686,2	$3s\ ^3P_1 — 3p\ ^3D_1$	20,64
5679,6	$3s\ ^3P_2 — 3p\ ^3D_3$	20,66
5666,6	$3s\ ^3P_1 — 3p\ ^3D_2$	20,65
5565,3	$3s\ ^5P_3 — 3p\ ^5D_2$	27,77
5552,0	$3s\ ^5P^3 — 3p\ ^5D_3$	27,78
5543,5	$3s\ ^5P_2 — 3p\ ^5D_2$	27,77
5530,3	$3s\ ^5P_2 — 3p\ ^5D_3$	27,78
5495,7	$3p\ ^3P_2 — 3d\ ^3P_2$	23,41
5478,1	$3p\ ^3P_1 — 3d\ ^3P_2$	23,41
5462,5	$3p\ ^3P_1 — 3d\ ^3P_1$	23,42
*5454,3	$3p\ ^3P_1 — 3d\ ^3P_0$	23,42
*5452,1	$3p\ ^3P_0 — 3d\ ^3P_1$	23,42
*5351,2	$3p\ ^5P_3 — 3d\ ^5P_3$	30,34
5340,2	$3p\ ^5P_3 — 3d\ ^5P_2$	30,34
5321,0	$3p\ ^5P_{1,2} — 3d\ ^5P_{2,1}$	30,34 30,34
5313,4	$3p\ ^5P_1 — 3d\ ^5P_1$	30,34
5199,5	$3p\ ^5D_4 — 3d\ ^5F_5$	30,18
5190,4	$3p\ ^5D_4 — 3d\ ^5F_4$	30,17
{5180,3	$3p\ ^5D_2 — 3d\ ^5F_2$	30,17
{5179,5	$3p\ ^5D_4 — 3d\ ^5F_5$	30,18
5175,9	$3p\ ^5D_3 — 3d\ ^5F_4$	30,17
5173,4	$3p\ ^5D_2 — 3d\ ^5F_3$	30,17
5168,2	$3p\ ^5P_1 — 3d\ ^5D_2$	30,41
*5104,5	$3p\ ^1S_0 — 4s\ ^1P_1$	24,53
*5045,1	$3s\ ^3P_2 — 3p\ ^3S_1$	20,93
5016,4	$3p\ ^3D_2 — 3d\ ^3F_2$	23,12
5012,0	$3s\ ^5P_3 — 3p\ ^5P_3$	28,02
*{5011,2	$3s\ ^5P_2 — 3p\ ^5P_1$	28,01
*{5010,6	$3s\ ^3P_1 — 3p\ ^3S_1$	20,93
*5005,1	$3p\ ^3D_3 — 3d\ ^3F_4$	23,14
*5002,7	$3s\ ^3P_0 — 3p\ ^3S_1$	20,93
*{5001,5	$3p\ ^3D_2 — 3d\ ^3F_3$	23,13
*{5001,1	$3p\ ^3D_1 — 3d\ ^3F_2$	23,12
4997,2	$3s\ ^5P_1 — 3p\ ^5P_1$	28,01
*4994,4	$3s\ ^5P_2 — 3p\ ^5P_3$	28,02

Table V b (cont.) Auroral *NII*-lines.

λ	Term combination	e. V.
*{4991,2	$3s\ ^5P_1 — 3p\ ^5P_2$	28,02
*{4987,4	$3p\ ^3S_1 — 3d\ ^3P_0$	23,42
4895,2	$(2p^3)^1D_2 — 3p\ ^1P_1$	20,40
4860,4	$3p\ ^5D_4 — 3d\ ^5P_3$	30,34
4810,3	$3p\ ^3D_3 — 3d\ ^3D_2$	23,24
4803,3	$3p\ ^3D_3 — 3d\ ^3D_3$	23,24
4793,7	$3p\ ^3D_2 — 3d\ ^3D_1$	23,23
*4788,1	$3p\ ^3D_2 — 3d\ ^3D_2$	23,24
*4781,2	$3p\ ^3D_2 — 3d\ ^3D_3$	23,24
*4779,7	$3p\ ^3D_1 — 3d\ ^3D_1$	23,24
4721,6	$3p\ ^5D_4 — 3d\ ^5D_3$	30,41
4718,4	$3p\ ^5D_4 — 3d\ ^5D_4$	30,41
4677,9	$3d\ ^1P_1 — 4f\ ^1D_2$	26,02
4675,0	$3s\ ^1P_1 — 3p\ ^3P_0$	21,14
4643,1	$3s\ ^3P_2 — 3p\ ^3P_1$	21,15
4621,4	$3s\ ^3P_1 — 3p\ ^3P_0$	21,14
4613,7	$3s\ ^3P_1 — 3p\ ^3P_1$	21,15
4609,4	$3d\ ^1F_3 — 4f\ ^1F_3$	26,16
4607,2	$3s\ ^3P_0 — 3p\ ^3P_1$	21,15
4601,5	$3s\ ^3P_1 — 3p\ ^3P_2$	21,15
*4564,8	$3p\ ^1P_1 — 3d\ ^3F_2$	23,12
*4552,5	$3d\ ^1F_3 — 4f\ ^3G_4$	26,19
4530,4	$3d\ ^1F_3 — 4f\ ^1G_4$	26,20
*4507,6	$3p\ ^3D_3 — 3d\ ^3P_2$	23,41
4488,2	$3p\ ^3D_2 — 3d\ ^3P_2$	23,41
4477,3	$3p\ ^3D_2 — 3d\ ^3P_1$	23,42
4465,5	$3p\ ^3D_1 — 3d\ ^3P_1$	23,42
*4447,0	$3p\ ^1P_1 — 3d\ ^1D_2$	23,19
4442,0	$3d\ ^3P_1 — 4f\ ^3D_2$	26,21
{4433,5	$3d\ ^3P_0 — 4f\ ^3D_1$	26,21
{4432,7	$3d\ ^3P_2 — 4f\ ^3D_3$	26,21
{4431,8	$3d\ ^3P_2 — 4f\ ^3D_2$	26,21
*4428,0	$3d\ ^3P_1 — 4f\ ^3D_1$	26,21
*4427,2	$3d\ ^3P_1 — 4f\ ^1D_2$	26,22
4375	$3p\ ^1P_1 — 3d\ ^3D_2$	23,24
{4237,0	$3d\ ^3D_2 — 4f\ ^3F_3$	26,16
{4236,9	$3d\ ^3D_1 — 4f\ ^3F_2$	26,16
4227,8	$3p\ ^1D_2 — 4s\ ^1P_1$	24,53
4179,7	$3d\ ^3D_3 — 4f\ ^3D_3$	26,21
4176,2	$3d\ ^1D_2 — 4f\ ^1F_3$	26,16
*{4173,7	$3d\ ^3D_2 — 4f\ ^3D_3$	26,21
*{4173,5	$3d\ ^3D_2 — 4f\ ^3D_2$	26,21
4171,6	$3d\ ^1D_2 — 4f\ ^3F_3$	26,16
*4160,8	$3d\ ^3D_2 — 4f\ ^{3,1}D_{1,2}$	26,21 26,22
4133,7	$3s\ ^5P_2 — 3p\ ^5S_2$	28,54
*4124,1	$3s\ ^5P_1 — 3p\ ^5S_2$	28,54
4110,0	$3d\ ^1D_2 — 4f\ ^3D_2$	26,21
4082,9	$3d\ ^3F_3 — 4f\ ^3F_3$	26,16
*4073,1	$3d\ ^3F_2 — 4f\ ^3F_3$	26,16
*4057,0	$3d\ ^3F_4 — 4f\ ^3G_4$	26,19
4044,8	$3d\ ^3F_3 — 4f\ ^3G_3$	26,19
*4043,5	$3d\ ^3F_3 — 4f\ ^3G_4$	26,19
4041,3	$3d\ ^3F_4 — 4f\ ^3G_5$	26,20
4035,1	$3d\ ^3F_2 — 4f\ ^3G_3$	26,19
4026,1	$3d\ ^3F_3 — 4f\ ^1G_4$	26,20
3995,0	$3s\ ^1P_1 — 3p\ ^1D_2$	21,59
3955,9	$3s\ ^3P_1 — 3p\ ^1D_2$	21,59
3919,0	$3p\ ^1P_1 — 3d\ ^1P_1$	23,57

Table V c.

Auroral *NIII*-lines. Possibly present in Aurora.

λ	Term combination	e. V.
6487,6	$3p\ ^4P_{5/2} - 3d\ ^4D_{3/2}$	41,25
6478,9	$3p\ ^4P_{5/2} - 3d\ ^4D_{5/2}$	41,26
6468,8	$3p\ ^4P_{3/2} - 3d\ ^4D_{1/2}$	41,25
6466,9	$3p\ ^4P_{5/2} - 3d\ ^4D_{7/2}$	41,26
* 6450,8	$3p\ ^4P_{1/2} - 3d\ ^4D_{1/2}$	41,25
5314,5	$3p\ ^4P_{5/2} - 3d\ ^4P_{5/2}$	41,67
5298,9	$3p\ ^4P_{5/2} - 3d\ ^4P_{3/2}$	41,68
5297,9	$3p\ ^4P_{3/2} - 3d\ ^4P_{5/2}$	41,68
5272,6	$3p\ ^4P_{3/2} - 3d\ ^4P_{1/2}$	41,69
5260,9	$3p\ ^4P_{1/2} - 3d\ ^4P_{1/2}$	41,69
4896,7	$3p\ ^4D_{7/2} - 3d\ ^4F_{5/2}$	40,94
4881,8	$3p\ ^4D_{5/2} - 3d\ ^4F_{3/2}$	40,93
4873,6	$3p\ ^4D_{5/2} - 3d\ ^4F_{5/2}$	40,94
4867,2	$3p\ ^4D_{7/2} - 3d\ ^4F_{9/2}$ $3p\ ^4D_{3/2} - 3d\ ^4F_{3/2}$	40,95 40,93
4641,9	$3p\ ^2P_{3/2} - 3d\ ^2D_{3/2}$	33,13
4640,6	$3p\ ^2P_{3/2} - 3d\ ^2D_{5/2}$	33,13
4634,2	$3p\ ^2P_{1/2} - 3d\ ^2D_{3/2}$	33,13
4547,3	$3s\ ^4P_{5/2} - 3p\ ^4D_{3/2}$	38,39
4546,3	$3p\ ^4S_{3/2} - 3d\ ^4P_{5/2}$	41,68
4534,6	$3p\ ^4P_{5/2} - 3d\ ^4D_{5/2}$	41,26
4530,8	$3p\ ^4P_{3/2} - 3d\ ^4D_{1/2}$	41,25
* 4523,6	$3p\ ^4P_{3/2} - 3d\ ^4D_{3/2}$	41,25
4514,9	$3p\ ^4P_{5/2} - 3d\ ^4D_{7/2}$	41,26
4510,9	$3p\ ^4P_{3/2} - 3d\ ^4D_{5/2}$ $3p\ ^4P_{1/2} - 3d\ ^4D_{3/2}$	41,26 41,25
4379,1	$4f\ ^2F_{5/2,7/2} - 5g\ ^2G_{7/2,9/2}$	42,53
4353,6	$3p\ ^4D_{7/2} - 3d\ ^4D_{5/2}$	41,26
4348,4	$3p\ ^4D_{7/2} - 3d\ ^4D_{7/2}$	41,26
4339,5	$3p\ ^4D_{5/2} - 3d\ ^4D_{3/2}$	41,25
4335,5	$3p\ ^4D_{5/2} - 3d\ ^4D_{5/2}$	41,26
4330,4	$3p\ ^4D_{3/2} - 3d\ ^4D_{1/2}$	41,25
4330,1	$3p\ ^4D_{5/2} - 3d\ ^4D_{7/2}$	41,26
4328,2	$3p\ ^4D_{3/2} - 3d\ ^4D_{3/2}$	41,25
4323,9	$3p\ ^4D_{3/2} - 3d\ ^4D_{5/2}$ $3p\ ^4D_{1/2} - 3d\ ^4D_{1/2}$	41,26 41,25
4321,4	$3p\ ^4D_{1/2} - 3d\ ^4D_{3/2}$	41,25
4294,8	Not classified	
4288,7	« «	
4288,2	« «	
4284,5	« «	
4200,0	$4p\ ^2P_{3/2} - 5s\ ^2S_{1/2}$	41,37
4195,7	$4p\ ^2P_{1/2} - 5s\ ^2S_{1/2}$	41,37
4103,4	$3s\ ^2S_{1/2} - 3p\ ^2P_{1/2}$	30,45
4097,3	$3s\ ^2S_{1/2} - 3p\ ^2P_{3/2}$	30,46
4003,6	Not classified	
3998,7	« «	
3938,5	« «	
3934,4	« «	
3771,4	$3p\ ^4D_{5/2} - 3d\ ^4P_{3/2}$	41,25
3771,1	$3s\ ^4P_{5/2} - 3p\ ^4S_{3/2}$	38,95
3754,6	$3s\ ^4P_{3/2} - 3p\ ^4S_{3/2}$	38,95
3374,1	$3s\ ^4P_{5/2} - 3p\ ^4P_{3/2}$	39,34
3367,4	$3s\ ^4P_{5/2} - 3p\ ^4P_{5/2}$	39,34

§ 6. Remarks on the Excitation of Auroral Atomic Lines.

In dealing with the composition of the auroral spectrum and its variability we have, as stated in previous papers, to take into account that the auroral luminescence is excited by solar ray bundles composed of electrons mixed with positive ions. For this reason we have compared the auroral spectra with spectra obtained when oxygen and nitrogen are bombarded with cathode rays (electrons) and canal rays (positive ions). (Cfr. paper (24) p. 58 and Pl. II, a, b, c, d and e), paper (25), p. 3, pt. I, paper (26) p. 162, pt. 5, paper (27) and (28) Since the discovery of the hydrogen showers in the upper atmosphere (1939) and the doppler displacement of H_β in 1940—41, we know that the auroral luminescence is produced by electric ray bundles composed of electrons electrostatically neutralized by positive ions, mainly protons.

The relative proton flux increases with the proton-velocity, which is very variable, and may be responsible for many of the variability effects (cfr. 27, 29, 30, 31) to be dealt with in connection with the spectrograms taken with the «F»-spectrograph.

The type of spectra, obtained when the principal components of the atmosphere (oxygen and nitrogen) are exited by canal rays and by electron rays, are illustrated by the spectrograms reproduced on Pl. II. They were taken at Würzburg 1912. Some of them were given in paper 24 pl. II fig. 2.

The spectrograms (a) and (b) on pl. II of this paper were obtained from the negative glow and the canal rays in pure oxygen. We notice the $O_2^+ IN$-bands are strong and the lines comparatively weak in the negative glow, where the luminescence is mainly produced by swift electron rays. In the canal ray spectrum, however, the bands are hardly visible, although numerous strongly exposed lines appear.

The difference between the canal ray spectrogram (c) and those of negative glow (d) is even more pronounced in the case of nitrogen, where the neg. glow spectra are dominated by the (N_2^+ *IN*)bands and some faint band heads of the strongest $N_2 2P$ bands. In the canal rays spectrum the lines dominate relative to the bands.

Spectrum (e) from the positive column corresponds to excitation by very slow electrons with the result that the relative intensity of the ($N_2 1P$) and ($N_2 2P$)-bands increases. The intensity variations of the nitrogen bands with velocity of the exciting electrons (the excitation functions) have been dealt with in great detail in previous investigations (32, 33).

The relative increase in intensity of the positive N_2-bands with decreasing electron energy is clearly illustrated in paper 33 fig. 5. This explains the fact that the intensity of the ($N_2 1P$)-bands in aurora increases with decreasing height, and that low aurorae appear red near the bottom edge (red aurorae of type B).

In the application of the spectrograms on Pl. II to auroral phenomena, we must take into account that the discharge tubes contain gas in the molecular state, while in the auroral region oxygen and nitrogen are dissociated and even ionoized to a degree which varies with altitude.

Anyhow, we must expect that electron excitation will give a spectral type essentially different from that produced by the protons, and that variation of the relative proton flux will produce variations in the spectral intensity distribution of the auroral luminescence. These effects will be dealt with later.

The bands which appear in the spectrum from the negative glow in N_2 and O_2 are well identified in the auroral luminescence.

The line spectra produced by canal rays, however, may help us by the interpretation of the lines, which, within the limit of error, coincide with features on the auroral spectrograms.

The results of the wavelength measurements Pl. IIb and IIc are given in table VI (a, b). For the sake of orientation the wavelength of some of the stronger lines are given on Pl. II.

Table VI a
Lines excited in Oxygen by Canal rays.
From spectrogram Pl. II b.

λ	Interpr.	λ	Interpr.
6456	OI	4343	OII
6158	»	39	»
5436	»	34	»
5331	»	27	»
5019	»	20	»
4968	»	18	»
4861	OII	05	»
02	OI	4295	»
4773	»	92	»
52	OII	88	»
05 }	MAS- »	85	»
00 }	KED »	80	
4676	»	77	
62	»	[1]55	
50	»	4190	OII
42	»	86	»
09	»	83	»
03	»	55	»
4597	»	19	»
91	»	4098	»
4491	»	92	»
79	»	89	»
71	»	87	»
53	»	84	»
17	»	75	»
15	»	72	»
4379	»	70	»
68	OI	61	»
51	OII	3972	»
49	»	60	»
47	»	45	»

[1] Masked by strong Neg. Nitrogen bands in Aurora.

Table VI b
Lines excited in Nitrogen by Canal rays.
From spectrogram Pl. II c.

λ	Interpr.	λ	Interpr.
5005	NII	4242	NII
4709	N_2^+1N(0—2)	37	»
4678	NII	28	»
70	NI	24	NI
60	NI	16	»
51	N_2^+1N(1—3)	[1]08	»
43	NII	00	$N_2 2P$(2—6)
31	NII	4180	NII
[1]26	NI	77	»
21	NII	72	»
14	»	67	NI
07	»	52	»
01	»	46	»
4572	$N_2 2P$(1—6)	46	NII
52	NI, NII	41	$N_2 2P$(3—7)
30	NII	10	NI
24	NIII	00	»
15	»	4082	NII
4488	NII	73	»
65	»	59	$N_2 2P$(0—3)
47	»	44	NII
42	»	42	»
33	»	36	»
27	»	26	»
4379	NIII	3998	$N_2 2P$(1—4)
44	NI	95	NII
4278	N_2^+1N(0—1)	3914	N_2^+1N(0–0)

[1] Masked by strong Neg. Nitrogen bands in Aurora.

It appears that all the *O*-lines with the exception of a few marked with a (1) on table VI, which are masked by strong nitrogen bands, appear in our tables IV (a, b, c) containing the *OI*, *OII* and *OIII* lines, which nearly coincide with auroral spectral features.

Also the canal ray — nitrogen lines on spectrogram Pl. IIc correspond to features observed on the auroral spectrograms taken by means of the «V» spectrograph.

On the tables IV and V the canal ray lines from table VI are marked (=).

It is to be remembered that the O-canal ray spectrogram only covers the spectral region (6500—3900 Å) and that the *N*-spectrum only the region (5000—3900 Å).

Now there should be good reason to assume that the auroral atomic lines which in tables IV and V are marked with a star, and for which no other reasonable interpretation is found really appear in the auroral luminescence. Further we have reason to believe, that also the *O*- and *N*-lines of the canal ray spectrograms may be present in the auroral luminescence.

§ 7. Verification of Atomic Line Interpretation.

On the different auroral spectrograms, for which the exposure has been sufficient to show a number of weak features, the atomic lines may be marked by their great sharpness, even when they nearly coincide with orher features. Their line character may also be more clearly marked on the photometer curves. For each spectrogram of this type a number of lines can be correctly interpreted in this way.

On account of the variable composition of the auroral luminescence and variation of experimental conditions (eg. sort of plate, slit aperture). lines which are not clearly indicated on one spectrogram may be distinctly seen on others.

From this way of reasoning we have for a number of our best spectrograms taken out the lines for which a fairly reliable interpretation can be given. At present we have for this purpose selected the following spectrograms:

a. Spectrogram taken at Oslo Feb. 23—24 1950 reproduced in paper (16) fig. 2 and (19) Pl. I No. 4.
b. Spectrogram from Tromsø April 3—5 1951. Paper (19). Pl. I No. 3.
c. Spectrogram Pl. I Nos. 3 and 5 of this paper.
d. For region in yellow and red we have used the spectrograms paper (19). Pl. I Nos. 1a and 2 and spectrograms Nos. 1 and 2 Pl. I of this paper.
e. For the infra-red region the two spectrograms paper 19 Pl. II have been used.

Reduced reproductions of photometer curves from the two auroral spectrograms mentioned under point a) and b), one from Oslo (1950) and one from Tromsø (1951) are shown in fig. 1a and 1b.

Fig. 2 gives photometer curves for the long-wave part (5577—6900) of the «*V*»-spectrograms, Nos. 1 and 2 on pl. I in the present paper.

Photometer curve corresponding to spectrogram Pl. II No. 2 paper 19, covering the interval from 6300 to 8900 in the infrared is reproduced on fig. 3.

The interpretation of the most conspicuous auroral features are indicated in connection with the photometer curves.

The auroral atomic *O*- and *N*-lines, which are identified in the way here described, are indicated in tables IV and V by special printing types. If a feature corresponds to atomic lines in two groups, both lines are indicated by the special types.

In tables IV and V the lines marked either with * or = or printed in a special type should most probably appear in the auroral luminescence. Table VII gives the number (*N*) of atomic oxygen and nitrogen-lines in various states of ionisation which are marked in this way and also the number (*n*) of those which are not marked.

Table VII
Number of Oxygen and Nitrogen Lines possibly present in Aurorae.

	OI	OII	OIII	NI	NII	NIII
N	59	128	8	106	81	24
n	14	28	5	65	35	19
N+n	73	156	13	171	116	43

As will be seen from tables II and III and from table 2 of paper (19) most of the lines (including those indicated by (n) have been meas-

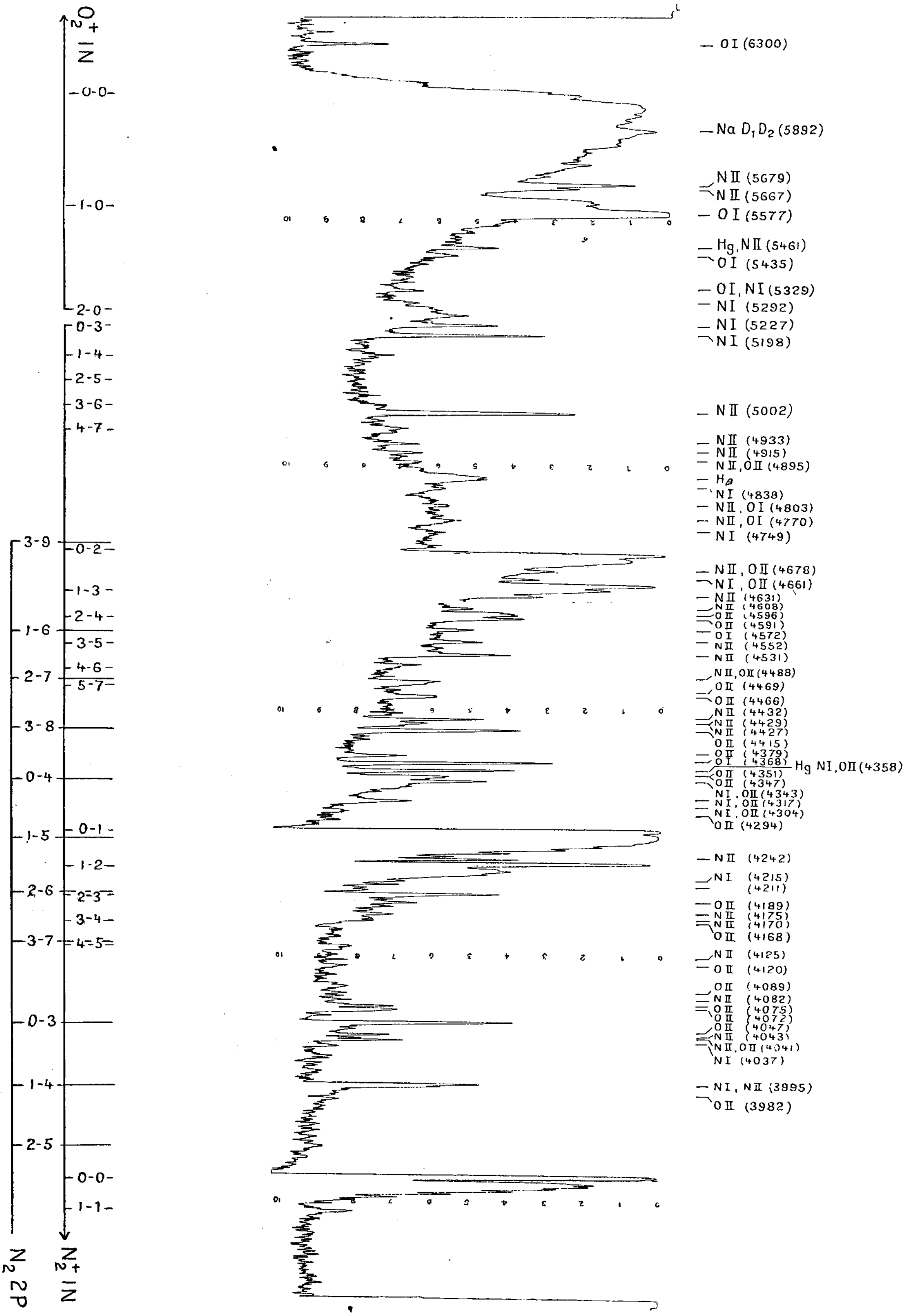
O_2^+ 1N
N_2^+ 1N
N_2 2P
OI (6300)
Na $D_1 D_2$ (5892)
NII (5679)
NII (5667)
OI (5577)
Hg, NII (5461)
OI (5435)
OI, NI (5329)
NI (5292)
NI (5227)
NI (5198)
NII (5002)
NII (4933)
NII (4915)
NII, OII (4895)
H_β
NI (4838)
NII, OI (4803)
NII, OI (4770)
NI (4749)
NII, OII (4678)
NI, OII (4661)
Hg NI, OII (4358)
NII (4242)
NI (4215)
OII (3982)
NI, NII (3995)
NI (4037)

Fig. 1a

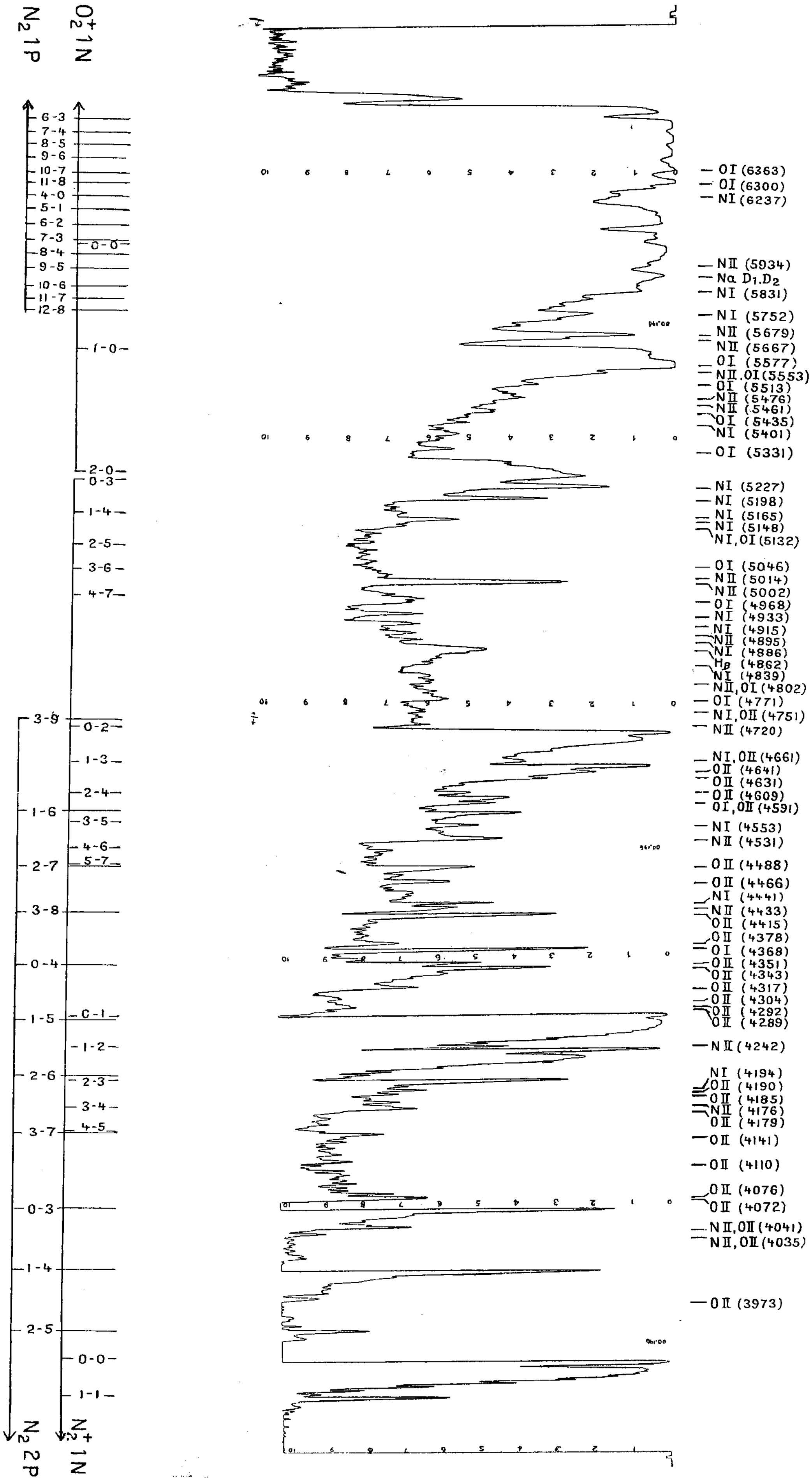

O_2^+ 1N
N_2 1P
N_2^+ 1N
N_2 2P
OI (6363)
OI (6300)
NI (6237)
NII (5934)
Na D1.D2
NI (5831)
NI (5752)
NII (5679)
NII (5667)
OI (5577)
NII.OI (5553)
OI (5513)
NII (5476)
NII (5461)
OI (5435)
NI (5401)
OI (5331)
NI (5227)
NI (5198)
NI (5165)
NI (5148)
NI, OI (5132)
OI (5046)
NII (5014)
NII (5002)
OI (4968)
NI (4933)
NI (4915)
NII (4895)
NI (4886)
Hβ (4862)
NI (4839)
NII, OI (4802)
OI (4771)
NI, OII (4751)
NII (4720)
NI, OII (4661)
OII (4641)
OII (4631)
OII (4609)
OI, OII (4591)
NI (4553)
NII (4531)
OII (4488)
OII (4466)
NI (4441)
NII (4433)
OII (4415)
OII (4378)
OI (4368)
OII (4351)
OII (4343)
OII (4317)
OII (4304)
OII (4292)
OII (4289)
NII (4242)
NI (4194)
OII (4190)
OII (4185)
NII (4176)
OII (4179)
OII (4141)
OII (4110)
OII (4076)
OII (4072)
NII, OII (4041)
NII, OII (4035)
OII (3973)

Fig. 1.b

ured from a number of spectrograms taken with the «*V*»-spectrograph during the winters 1949/50, 1950/51, 1951/52 and 1952/53, and, therefore we believe that also most of the lines in the group indicated by (*n*) appear in the auroral luminescence.

§ 8. Auroral Lines Observed by other Scientists.

During the last few years a number of atomic lines from *O* and *N* have been obtained, measured and identified by a number of scientists particularly in Canada and in USA. In this connection we may refer to a report by Petrie and Small No 41) and papers by Meinel (e.g. Nos. 35 and 36) where it is stated that a number of auroral atomic lines have been obtained on auroral spectrograms. As far as their observations go, the auroral linefeatures they obtain are in good agreement with the results previously found by us both as regards wave-length values and interpretation.

The number of atomic *O*- and *N*-lines observed by Petrie and Small (P & S) and by Meinel are given in table VIII.

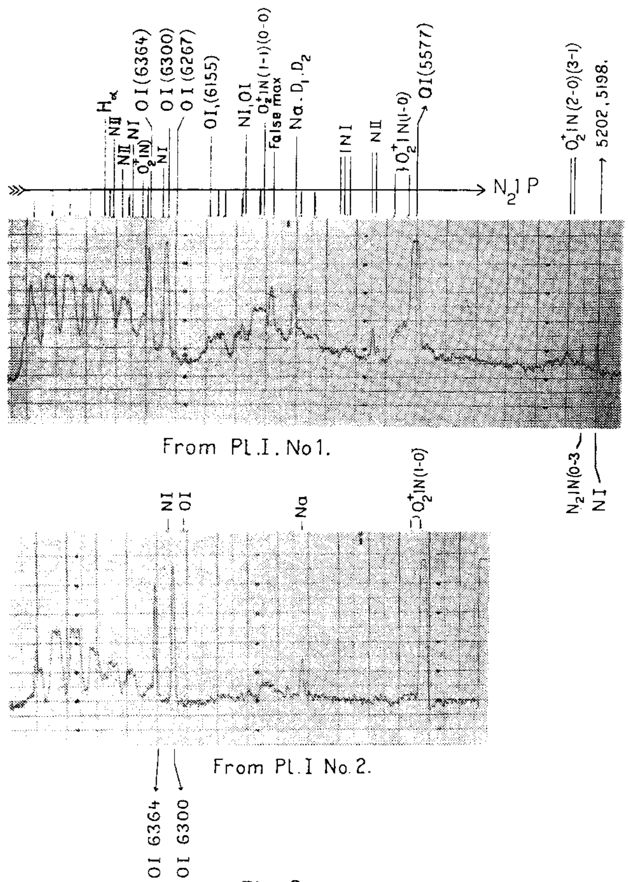

Fig. 2

Fig. 3

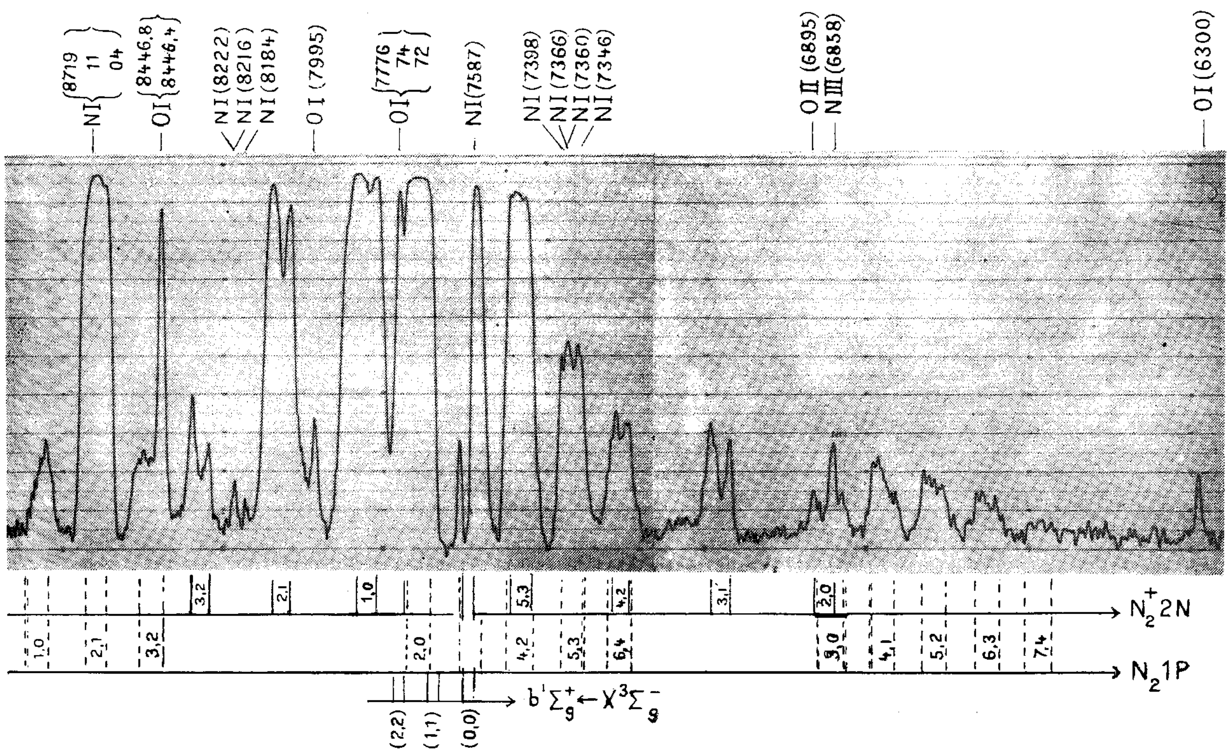

Table VIII
Number of measured Lines

	OI	OII	NI	NII
P & S........	10	15	13	19
Meinel	12	1	8	0

All the lines observed by Petrie and Small have been observed by us and interpreted in the same way with the exception of the *NI*-line $\lambda = 8242$, which has not been detected on our spectrograms. A feature at $\lambda = 5026$ has been observed by us, but identified as 1P(12—6) and not as a NII line.

The lines observed by Meinel have also been observed on our spectrograms (16, 19), with the exception of the *OI* line 3693 and the *NI* line 8243.

Chamberlain and Oliver (50) have published wavelength tables with interpretations, founded on previous investigations on the auroral spectrum. As far as the tables go they agree well with our earlier and present results.

Barbier and Williams (49) have published results of auroral spectrograms in the short wave region (5000—3100) by means of a spectrograph with dispersion 150 Å/mm at $\lambda = 3200$ and 630 Å/mm at $\lambda = 5000$. On account of the small dispersion the accuracy is small. Most of the lines and bands, however, are situated near known auroral features. In the region towards the ultra violet end are listed a number of features which were never observed on our spectrograms covering the ultra-violet region, and their presence in the auroral luminescence needs further investigation and confirmation.

A comparison between auroral spectrograms taken at Tromsø and at Oslo have shown that the forbidden lines of *OI* and *NI* are greatly enhanced towards lower latitudes, when compared e.g. with the intensities of the bands N_2^+IN (65, 66, 19). The very marked enhancement of the forbidden doublet *NI* ($^4S_{3/2}$—$^2D_{3/2, 5/2}$) has been verified in a very striking way by spectrograms taken by J. Dufay and collaborators in southern France (46, 47).

The forbidden lines from the metastable ground states are found in the auroral luminescence for *OI*, *NI* and *NII*, and in the case of *OII*, at any rate, the doublet 3728, 3725, appears. The two lines 7335, 7321 fall in an infra-red region not yet sufficiently well explored. The variability of the forbidden *OII* and *NII* lines has not yet been studied.

§ 9. Problems in Auroral Spectral Analysis.

As already mentioned the correctness of our interpretations can be verified by utilising the fact that the band systems as a rule show a typical intensity distribution and that a group of lines with a common upper level of transitions have a definite intensity distribution determined by intrinsic atomic probabilities. But apart from this the spectral composition of the auroral luminescence is subject to great variations.

It must first of all be remembered that we are not dealing with a thermic radiation, which for a known composition and state of matter is essentially a function of temperature (55).

Primarily the auroral luminescence is due to solar electric rays composed of electrons and positive ions (e.g. protons), but the effect of these vary with the composition of the solar ray bundles, and with the distribution of velocity of each type of electric rays. The excitation potential and the excitation functions vary with the type of ray-corpuscle and with the particle to be excited (cfr. paper (61) and (62).

Further we know that the gases in the auroral region exist in several modifications and that the absolute and relative concentration of these varies greatly with altitude, latitude and with time.

Finally we must take into account secondary processes such as secondary electron rays and collisions of the second kind.

In dealing with the spectral composition of the auroral luminescence, we must therefore first of all rely on and start from observed facts.

Results of numerous investigations on the theory of intensity distributions of lines and bands within the auroral spectrum have been published in recent years (cfr. 55, 63 and 64). It would, however, lay outside the plan of this paper to enter further into this vast field.

§ 10. Band Systems Present in the Auroral Luminescence.

In § 4 ten band systems, which may probably appear in the aurorae, were given. The 3 N_2 systems and the N_2^+IN system have been known to be present in the auroral spectrum for about 20 years. The 1st negative group O_2^+IN of oxygen was for the first time clearly shown on an auroral spectrogram taken Feb. 23. 1950 with the «V» spectrograph (15, 16). The second negative system N_2^+2N was found by Meinel (23) to appear in the infrared region of the auroral spectrum.

On the «V» spectrogram from Feb. 1950 we also found that a number of auroral features coincide with vibrational bands of the Schuman-Runge (S.R) system of O_2 and with NO_β-bands.

From the «V» spectrograms dealt with in this paper some features were found to coincide with bands of the O_2^+2N system. Recently Chamberlain, Fan and Meinel (24) found that bands of the forbidden atmospheric system $O_2(A^1\Sigma - X^3\Sigma)$ are found in the infra-red part of the auroral emission spectrum. The same emission phenomenon is also clearly seen on the infra-red spectrograms obtained at Tromsø in January 1951 (paper 19 pl. II and III). The combined emission and absorption phenomenon is illustrated in fig. 3 on the photometer curve from the infra-red part of the spectrogram 2a pl. II paper 19.

The bands of the systems N_22P and N_2^+1N which up to the present have been found to coincide with auroral features on our spectrograms are given in the tables IX and X. As the intensity-distribution of the bands within a system may vary considerably, the relative intensities given must be considered as a kind of mean values for the Auroral Observatory at Tromsø.

The bands of the system N_21P, V.K., N_2^+2N, O_2 *S.R.*, O_2^+1N and NO_β, which coincide with auroral features are represented by diagrams figs. 4. 5, 6, 7, 8, 9, giving the quant numbers (n', n") of the vibrational transitions. The bands, for which we have found no other interpretation, are indicated by circles round the points of the diagrams. As each of these systems has a number of bands which fulfil this condition, we have reason to believe that not only the systems N_21P, V.K., N_2^+2N and O_2^+1N, but also the systems O_2 S.R. and NO_β appear in the auroral luminescence.

Some of the bands of the system O_2^+2N coincide with weak auroral features, most of which belong to a vibrational series (o-n), where $n = 8, 9, 10, 11, 12$. The band (o-11) ($\lambda = 5086$) represents the only interpretation as yet found for this auroral feature. This fact and the regularity of the vibrational transitions support the assumption that bands of the O_2^+2N-system are present in the auroral spectrum.

Table IX. Wavelength and Relative Intensity of Auroral N_22P bands.

n' \ n''	0	1	2	3	4	5	6	7	8	9
0	3771 9,0	3578 9,8	3805 4,9	4059 2,5	4343 2,0	4668 0,2	4977			
1	3159 5,8	3339 1,2	3536 4,9	3755 4,2	3998 2,9	(4269) 0	4573 0,3	4916 0,2		
2		3136 3,6	(3309) 0	3503 2,2	3711 2,4	3942 1,6	4200 1,5	4491 (1,0)	4814 0,1	
3			3114 W	3285 1,8	3467[x] 3,0	3671	(3894) 0	4141 1,4	4417 0,7	4724 0,2
4								3857	4094 0,9	4358 0,8	(4650)

[x] Coincides with the forbidden *NI* line 3466 Å

Table X. Wavelength and Relative Intensity of N_2^+1N-Bands in the Auroral Luminescence.

n' \ n''	0	1	2	3	4	5	6	7	8	9	10
0	3914 47	4278 24	4709 7,8	5228 1,2	5866 W						
1	3583 1,6	3884 2	4236 6	4652 4,6	5149 0,3	5753 W					
2		3563 1,6	3858 W	4199 2	4601 3,4	5078 W	5658 W				
3			3550 W	(3836)ˣ W	4174 1	4553 2	5014 W	5566 W			
4				3536 W	3822 W	4142 1	4516 1	4962 W	5488 W		
5								4489 0,1	4915 W		
6									4467 0,1	4880 W	
7										4465 0,1	
8											4468 0,1

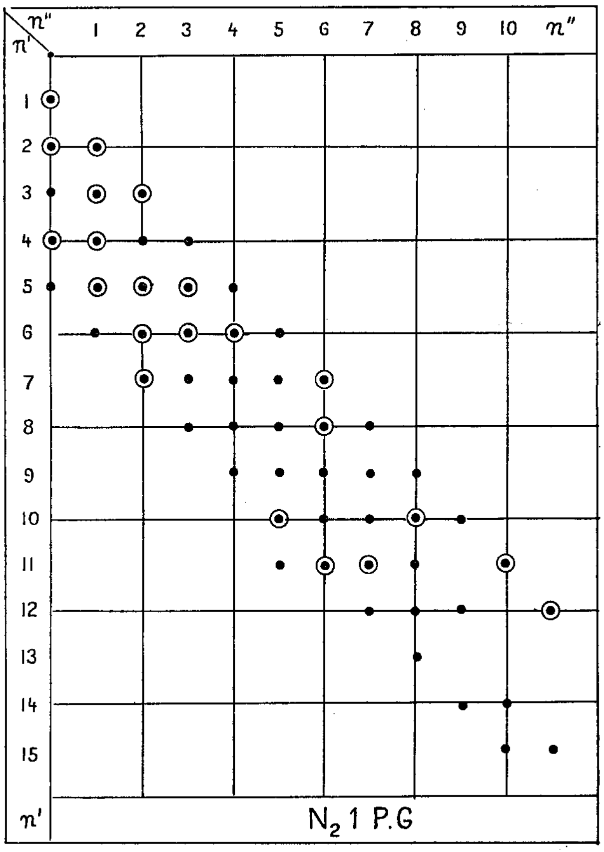

Fig. 4.

Fig. 5.

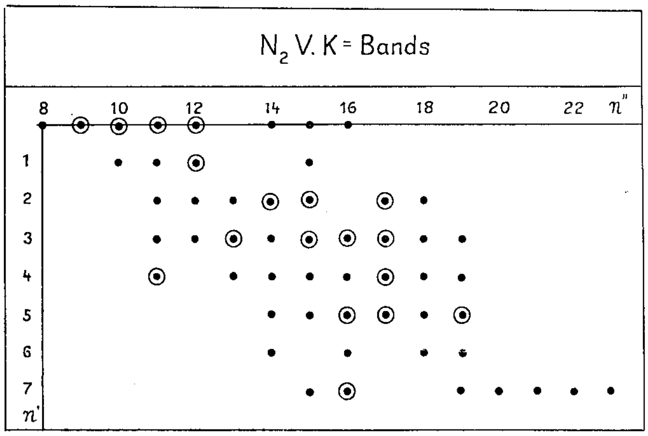

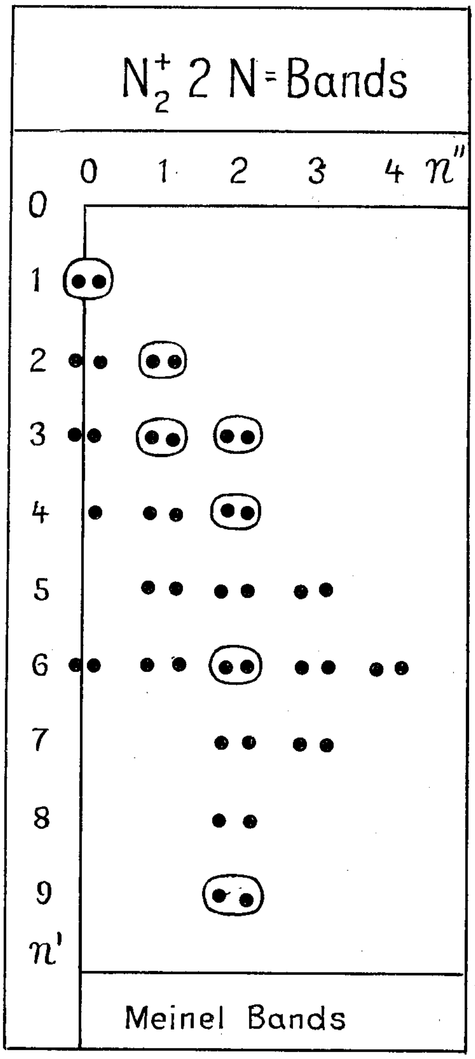

Fig. 6.

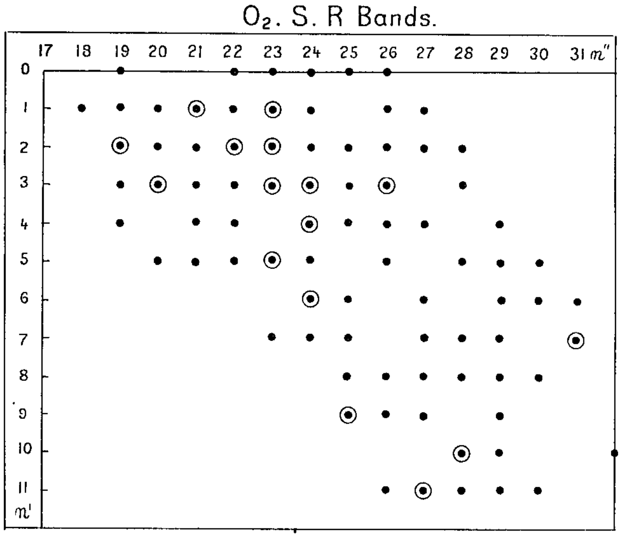

Fig. 7.

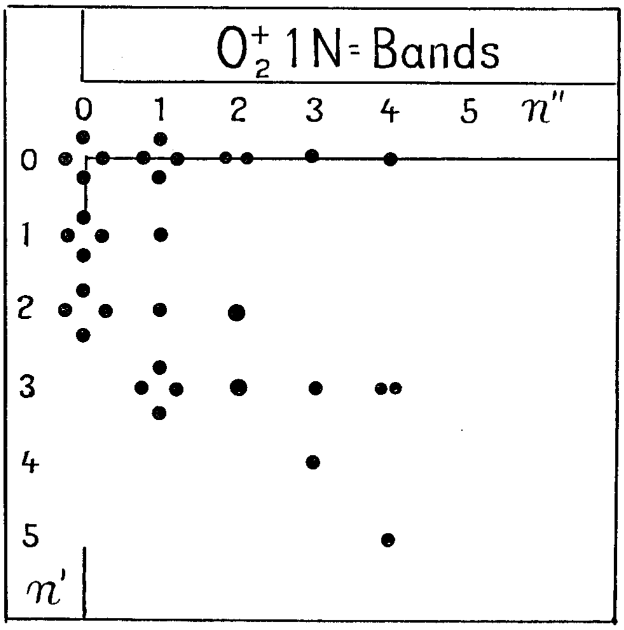

Fig. 8.

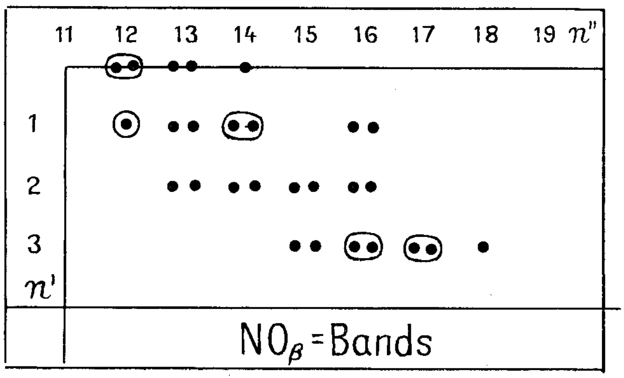

Fig. 9.

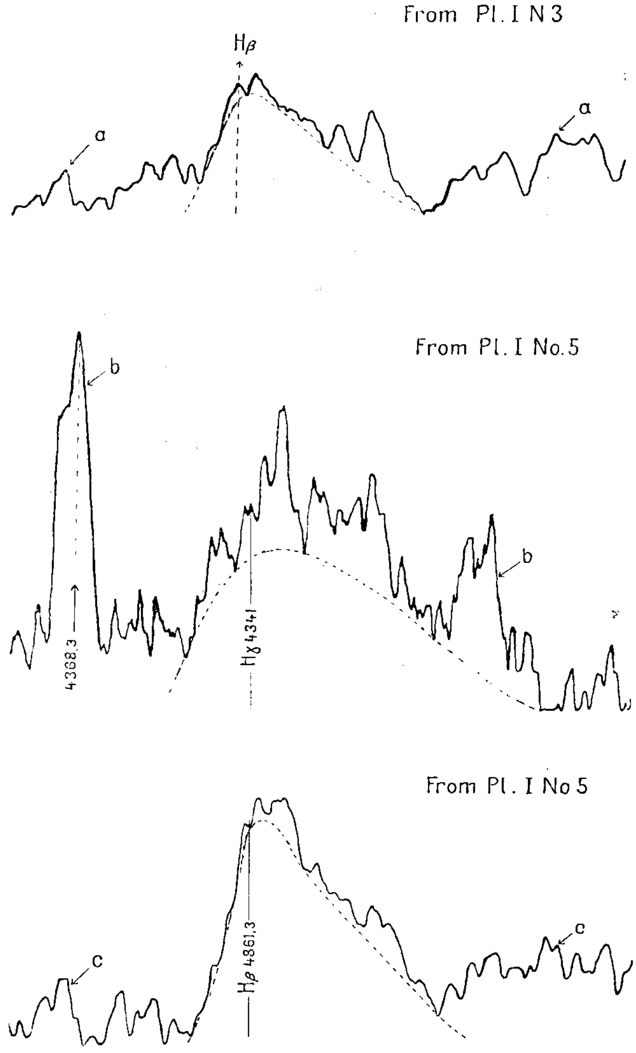

Fig. 10.

§ 11. Doppler Displacement and Proton Velocities.

When the spectrograms *Nos.* 1, 2, 4 and 5 on plate I were taken, the spectrograph («*V*») was directed towards magnetic zenith during the exposure, but only No. 5 was sufficiently exposed to show H_β and H_γ-lines distinctly and with great Doppler displacement towards shorter waves.

On the other hand, the spectrogram pl. I, No. 3 showed the H_β-line with Doppler displacement, although the spectrograph was not always directed towards magnetic zenith, but it will, by somewhat long exposures, be directed towards aurorae near the zenith.

A photometer curve of the H_β-line on spectrogram No. 3 and of H_β and H_γ for spectrogram No. 5 are shown on fig. 10. The dotted smoothed curves on these diagrams are given in a greater scale on fig. 11.

The maximum proton velocity $(V_p)^-$ derived from the maximum displacement towards shorter waves and the maximum velocity in the opposite direction $(V_p)^+$ are given in the table XI.

Table XI
Observed Proton Velocities

Date of spectrogram	$(V_p)^-$ cm/sec	$(V_p)^+$ cm/sec	Remarks
28.11 1940-16.1.41	$1.36.10^8$	$1.23.10^8$	From Tromsø H_β
14.10-20.10.1941.	1.97 -	1.17 -	From Tromsø H_β
23.2.1950	1.75 -	1.05 -	From Oslo H_β
17.1.-9.2.1951	2.22 -	0.68 -	From Tromsø H_β
28.1-6.3.1952	2.78 -	0.53 -	From Tromsø H_β
25.9.-18.12.1952	2.30 -	0.67 -	From Tromsø H_γ
25.9.-18.12.1952	2.37 -	0.67 -	From Tromsø H_β

In this table the earlier results regarding Doppler displacements which were obtained at Tromsø and Oslo from 1941 to 1951, are included.

§ 12. Temperature Measurements from «V» Spectrograms.

On each of the 8 spectrograms of pl. I at least one of the negative nitrogen bands 4278 and 3914 gives suitable photographic density for temperature measurements.

By the exposure of the three spectrograms pl. I No. 1, 4, and 5 the spectrograph was directed towards magnetic zenith, and an image of the radiation point and of the tops of the auroral streamers nearest to it, is thrown on the slit. This means that the N_2^+1N bands on these spectrograms correspond to the high altitude near the tops of auroral ray-streamers. Consequently the band-temperatures derived from these spectrograms should correspond to a mean altitude, which will depend on the type of aurorae, but which is considerably greater than the height of say 100—120 km where the auroral streamers usually are most intense. If the corona is formed by very long auroral rays, the spectrogram may correspond to several hundred km. The spectrograms from the radiation point of a corona may therefore give good facilities for measuring ionospheric temperatures up to altitudes of several hundred km.

The photometer curves of 4 of the bands are

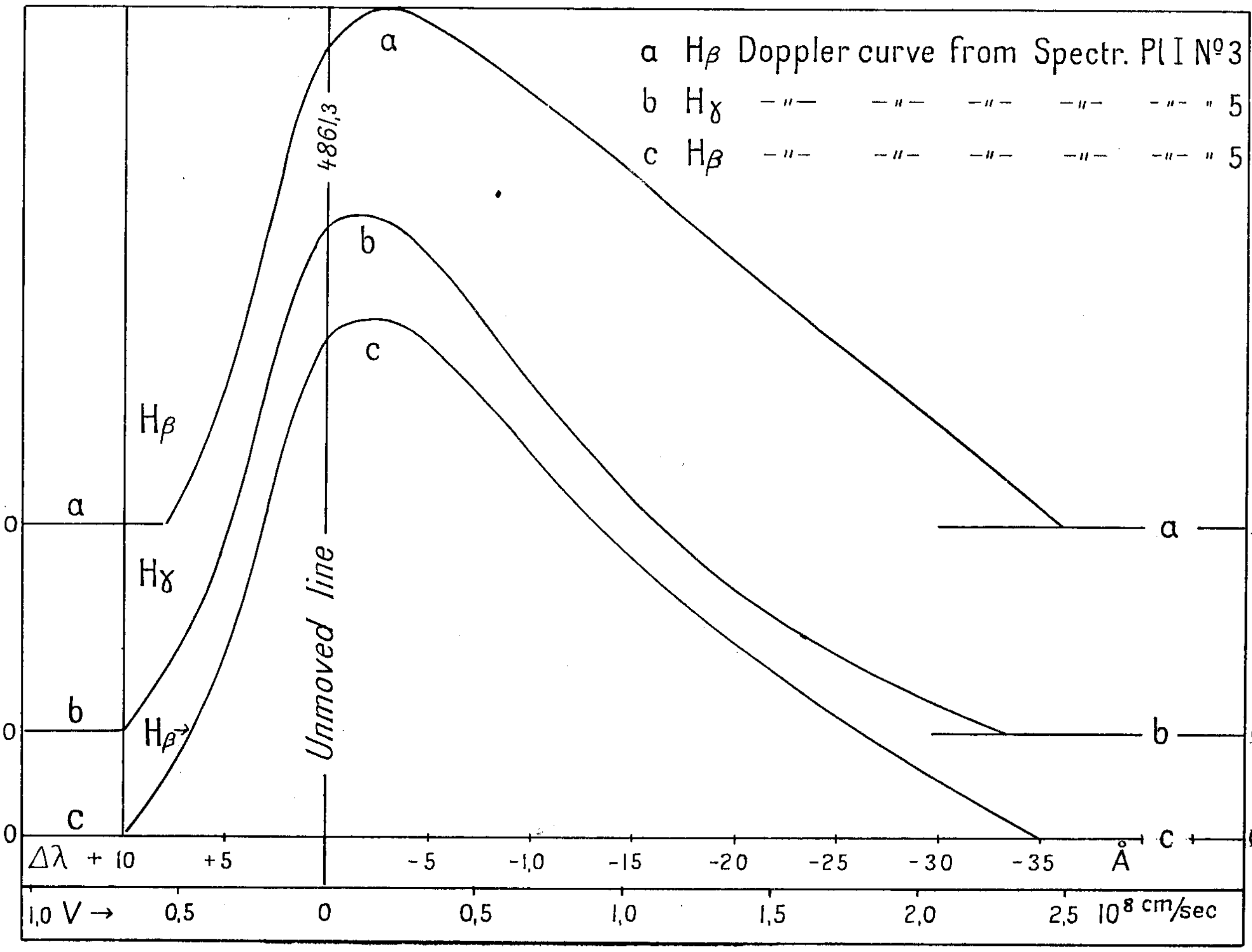

Fig. 11.

Table XII
Temperatures derived from «V» Spectrograms

Pl. I	Date of exposure	Band	T_m	$T_\varkappa$	T_{mean}	Remarks
			K^0	K^0	K^0	
No. 1	10.11.51—15.1.52	4278	235	246	240	Towards mag. Z
2	27.1.52	4278	231	239	235	Towards mag. equator
3	28.1—6.3.1952	3914	243	237	240	Various forms
4	18.3—25.3.52	4278	202	215	209	Towards magn. Z.
4	»	3914	240	207	224	»
5	25.9.—18.12.52	3914	190	210	200	»
		4278	195	248	221	»
6	8—9.1.53	4278	215	216	215,5	A. tow. N.
7	13—24.1.53	4278	172	175	173,5	A & D.
8	28—29.1.53	3914	221	236	228,5	A. & D. near Z.
	Mean Kelvin⁰		214,4	222,9	218,7	
	Mean Centigrad		— 58,6°	— 50,1°	— 54,3°	
	Mean from rad. point		— 60,6°	— 47,8°	— 54,2°	

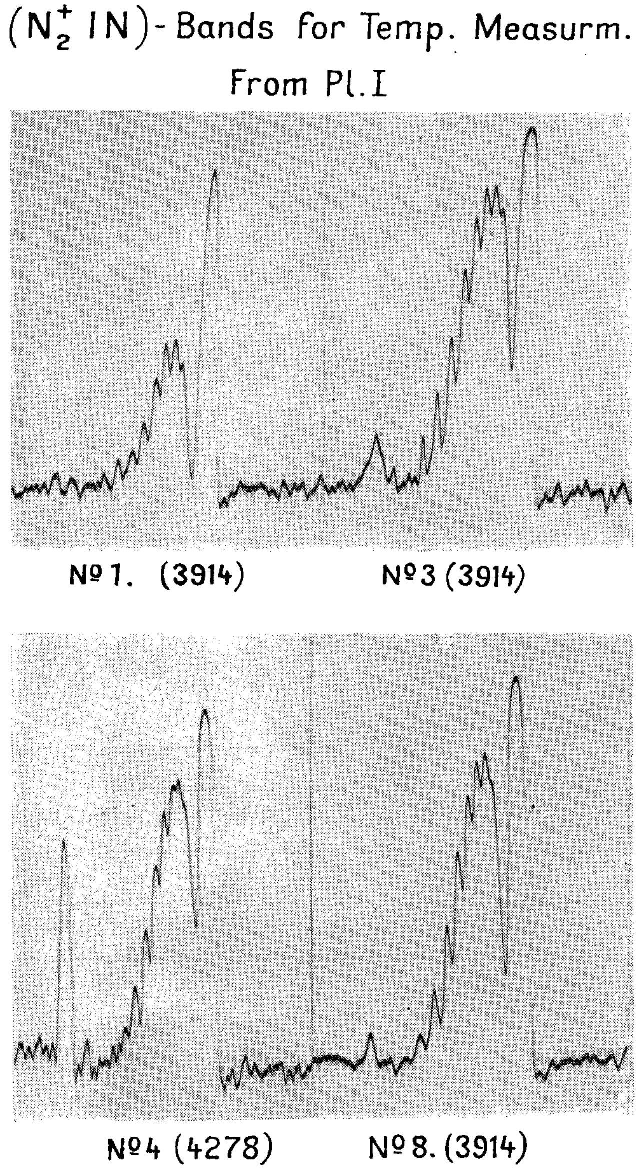

Fig. 12.

reproduced on fig. 12. The individual rotational lines are seen to be separated which involve reliable results.

The method of determining the temperature from band spectra has been described in detail in previous papers (5, 56, 57 and 58) and its correctness verified by direct experiments (44, 45), and as regards the procedure of temperature determination by means of rotational bands, we may refer to these papers.

The temperature has been determined from 10 bands and the results are given in table XII.

As usual the temperature has been determined in two different ways: T_m is the temperature derived from the rotational quant number K_m corresponding to maximum intensity of the rotational R-branch by means of the equation:

$$T_m = 2{,}96\, K_m\, (2K_m + 1) \qquad (1)$$

$T_\varkappa$ is derived from the relation:

$$\left.\begin{aligned} \log_{10}(I_K/K) &= -\varkappa\,(K+1)\,K \\ \text{where}\quad \varkappa &= \frac{h^2 \log_{10} \varepsilon}{8\,\pi_1^2\, j\, k\, T_\varkappa} \quad \text{or} \\ T_\varkappa &= \frac{1.286}{\varkappa} \end{aligned}\right\} \qquad (2)$$

In table XIV the values of T_m, $T_\varkappa$ and $T_{mean} = \dfrac{T_m + T_\varkappa}{2}$ are given.

The first two lines at the bottom give the mean values in Kelvin degrees and centigrades. The mean values from the top of rays, near the radiation point, are given in the bottom line of the table and are seen to be nearly equal to the total mean values.

Thus neither these determinations nor the previous ones indicate any increase of temperature with increase of altitude.

The extraordinary high temperature, which Petrie (42) derives from one of his auroral spectrograms, has been dealt with in previous papers (59, 60) and found to be explained by the fact that the rotational energy of the nitrogen molecules is increased by exictation with positive ions (protons), and that the relative number of protons in the solar ray bundles increase with altitude and towards lower latitudes. In paper (60) p. 98 the following explanation is given:

«This unusual intensity distribution is no doubt to be explained in the same way as that of the spectrogram taken by Størmer. The Petrie spectrogram is probably taken from aurora at a great altitude and low latitude which give great probability for intensive proton influx. The auroral luminescence is mainly produced by proton excitation which is shown to increase the rotational energy (5) and to give a much too high «Ionospheric temperature.»

Thus spectrograms of Petrie do not at all interfere with or violate the correctness of the measurements of the ionospheric temperature undertaken by us at Tromsø.»

SECTION B

VARIABILITY EFFECTS AND THE «F» SPECTROGRAMS

§ 13. Introductory Remarks.

During the last 32 years much work has been devoted to the study of the variations in the auroral spectrum, and the results have been dealt with in a number of papers (2, 5, 6, 67, 68, 65, 66, 9, 18, 30, 31, 32, 60 and 28).

The variability effects may be divided into the following groups:

a. Variations with latitude.
b. — - altitude.
c. — - solar activity.
d. — due to effect of sunlight.
e. — with auroral type (type effects).
f. — due to changes in the composition of the bundles of electric solar rays which produce the aurorae.

a. *Latitude effects.*

The forbidden *OI* lines (5577, 6300, 6364) and the forbidden *NI* doublet (5201, 5198) and the hydrogen lines and perhaps the $N_2V.K.$ bands are enhanced towards lower latitudes. The frequency of red aurorae of type A. increases with increasing distance from the magnetic axix point.

b. *Altitude effects.*

The intensity of the red doublet and the *H*-lines compared with that of the green line (5577) and the bands N_2^+1N increases towards greater altitude. As a rule the intensity of the bands of N_2^+1N relative to that of the green line increases upwards. The bands of N_21P are greatly enhanced towards lower altitudes and may give the auroral bands a red lower border (Red aurorae of type B.).

c. *Changes with solar activity.*

The average relative intensity of the red *OI* doublet (6300, 6364) and the frequency of red aurorae of type A increases with solar activity (25 p. 58, 59). If the great enhancement of the *OI* doublet is due to proton excitation, also the auroral hydrogen lines should be enhanced with increased solar activity.

Certain facts indicate that the red aurorae of type B are most frequent in periods of sun-spot minimum (25, p. 58, 59).

d. *Sunlight effects.*

The forbidden red *OI* doublet is found to be enhanced, when the aurorae are exposed to sunlight (69, 70).

e. *Regarding type effects.*

We refer to paper 68. It is possible that the type effects may be at any rate partly due to differences in altitudes and in the light distribution along the streamers.

f. *Variations in spectral intensity distribution due to changes in the composition of the solar ray bundles*, have now become a matter of the greatetst importance, since the discovery of the doppler effect of auroral hydrogen lines (10, 12, 13, 14) had shown that the solar electric ray bundles contain protons which enter into the atmosphere with velocities of the order of several thousand km/sec.

During recent years particular interest has been devoted to the study of the influence of the solar proton radiation on the auroral luminescence and its variations (12, 14, 17, 18, 22, 30, 31, 32).

§ 14. The Properties of the Solar Ray Bundles.

As pointed out in the introduction and as shown in previous papers (cf. paper 1, 3, 5, 6, 14, 17, 18 22) the solar bundles are composed of electron rays, electrostatically neutralized by positive ions (mainly protons), and the mutual electro-magnetic attraction between the current filaments produces an automatic focussing effect, which helps to give the bundle a fairly limited and definite cross-section. If the bundle consists of electrons and protons, we have

$$\left.\begin{aligned} \nu_e &= e\, n_e\, V_e \\ \nu_p &= e\, n_p\, V_p \end{aligned}\right\} \qquad (3a)$$

ν_e and ν_r are electron and proton flux, (n) is the number of particles in unit volume and V velocity. The condition of electrostatic neutralisation gives:

$$n_e = n_p = n$$

And this leads to the following simple, but fundamental equations:

$$\frac{\nu_p}{\nu_e} = \frac{V_p}{V_e} \qquad (3b)$$

The current density (i) and the deviating force (K) acting on unit volume of the solar bundle are expressed by the formulae:

$$i = \text{en}\,(V_e - V_p) \qquad (4)$$

$$K = \text{en}\,(V_e - V_p)\, F \sin\varphi = i\, F \sin\varphi \qquad (5)$$

If we take spectrograms with long exposure by turning the spectrograph in any direction, where aurorae appear, the intensity of the hydrogen lines relative to one of the stronger features of the auroral spectrum, will give a kind of average value of the relative proton flux, which is measured by the velocity ratio (V_p/V_e).

Now we know that very often, especially near the auroral zone, the relative intensity of the strongest H-lines, H_α and H_β, may for long periods of time be too small to be observed, even on heavily exposed spectrograms. At other times, and especially at lower latitudes, the intensity of the H_α or H_β lines may be comparable with the stronger bands of the groups N_2^+1N or N_21P.

The absence of H-lines mean that $V_p \ll V_e$ and that the auroral luminescence is mainly produced by the electron rays. This also involves that a solar bundle, where all rays consist of protons like that proposed by Bennett and Hilburt (43), is incapable of explaining fundamental auroral phenomena and facts.

Increase of relative intensity of the H-lines means increase of relative proton flux ν_p/ν_e and increase of the part of the luminescence, which is excited by protons.

The spectrum produced by protons differ in many ways from that produced by electrons and this means that change of relative proton flux will produce variations in the spectral composition of the auroral luminescence.

By coordinating typical variations in the intensity distribution with the intensity of the hydrogen lines, we may be able to detect typical differences between the results of proton- and electron-excitation, which may lead to a physical explanation of the observed variations.

Some results along these lines have already been obtained and published (17, 18, 22, 32, 60). They will be more fully described in connection with the treatment of the «F» spectrograms.

The constitution of the solar ray bundles here given leads to two variability effects of the auroral H-lines which can be tested experimentally and give an important verification of the correctness of my auroral theory.

As the electron velocity (V_e) is greater than V_p, the equations (4) and (5) show that the magnetic field produced by the bundle, the automatic focussing effect and the deviating force (K) is dominated by the electron flux.

On the other hand the protons will dominate the magnetic stiffness (inertia) of the bundle provided $V_p > \frac{V_e}{1800}$ (cf. 14, 18, 22).

To reach down to 100 km, which corresponds to the bottom edge of an ordinary aurorae, the electrons must have a velocity of about $6 \,.\, 10^9$ cm/sec., and in that case the magnetic stiffness would be dominated by the protons if $V_p > 2 \,.\, 10^6$. This means that the magnetic stiffness due to the protons may be more than a hundred times as great as that of the electrons for an ordinary aurora.

§ 15. The Latitude Effect of Proton Influx.

According to the theory of Størmer, the magnetic latitude of an aurora decreases with increasing magnetic stiffness (or inertia) of the ray bundle, or with increasing velocity of the protons. As the relative proton flux is proportional to the relative velocity V_p/V_e, it will on an average increase with decreasing magnetic latitude.

When we remember that the intensity of the $N_2^+ 1N$-bands in aurora mainly result from electron excitation, the intensity of the H-lines e.g. relative to the band 4709 of the $N_2^+ 1N$-system should increase towards lower magnetic latitudes.

It must be remembered that even at the same locality the relative intensity of a hydrogen line is subject to great variations, so the variations with latitude must be a statistical effect.

A comparison between the relative H_β —intensity $\left(I \frac{H\beta}{4709}\right)$ measured on auroral spectrograms taken at Oslo and the intensities measured at Tromsø showed that the average relative H_β -intensity was about 6 times greater at Oslo than at Tromsø. These results were given in the papers (18 and 31).

In order to obtain, as far as possible, comparable spectrograms at the two stations, we have during recent winter-seasons taken spectrograms at Oslo and Tromsø on the same sort of plate with practically identical spectrographs, which were adjusted in the same way.

In order to have a good chance of obtaining the H_β-line with measurable intensity, we had to use long exposures. This had also the advantage that the H_β-features represented the average intensity during the time interval of the exposure. The observational work was carried out in collaboration with G. Kvifte. The results, which will be found in paper (32), were in good agreement with those previously published, and they showed that the average relative H_β-intensity at Oslo was about 6 times greater than at Tromsø.

The latitude effect of the relative proton flux is so great that it can be studied from a single station where there is a chance of obtaining sufficiently exposed spectrograms from the northern and from the southern sky.

Tromsø gives a good chance of obtaining comparable spectrograms from N and S, and from apparently the same auroral type. During the few last winter seasons a considerable number of pairs of (S and N) spectrograms have been taken and unless the auroral type in the two directions are essentially different, the spectrograms never fail to show a very prononuced latitude effect. A latitude effect obtained in this way was shown in a note to Nature (30). Here spectrogram No. 1, taken towards S, showed the H_α-line, while spectrogram (No 3) from the N-direction shows no trace of H_α.

These results have also been confirmed by numerous spectrograms taken at Tromsø during the two last winters.

§ 16. The Altitude Effect of Proton Flux.

When the solar ray bundle enters into the atmosphere, the electron and the proton beam can be electro-statically neutralized by atmospheric ions, so the electron and proton rays are absorbed independently of each other, and the height at which the protons and electrons stop, can be determined from the laws governing the absorption of each of these types of ray.

The absorption, range and distribution of luminosity along the auroral streamers have been the subjects of many previous investigations, and reference may be made to a paper published in The Phil. Mag. 1921 (71) and to paper (14). In tables III and IV of the last of these papers the height at which electrons or protons stop for a given velocity or energy, are given. To reach down to 100 km electrons would require an energy of about 10^4 el. Volts, while protons would need an energy about 20 times greater. Still the electron velocity would be about 10 times greater than that of the electrons. A proton energy of 10^4 e. V. would make the protons stop at an altitude of about 130 km.

In most cases (at any rate near the auroral zone) the proton flux and the relative proton velocity V_p/V_e is small, and under such conditions the protons will stop at an altitude (h_p) which is greater than the height (h_e) where the the electrons stop.

The greatest proton velocity derived from Doppler displacements is of the order of 2—3. 10^8 cm/sec, which corresponds to 4-5.10^4 el. Volts and a stopping height h_p, of about 113—115 km. For most aurorae the predominant part of the auroral luminescence is emitted below this height. As the aurorae may come down below 80 km, there will be an interval of 30—35 km where the luminosity is exited by electrons.

In order to emit the H-lines the protons must pick up an electron. When the protons enter the atmosphere the neutralisation process sets in, and the H-line emission gradually increases to a maximum just above the stopping height. As the proton rays may be somewhat heterogeneous, and on account of the influence of the magnetic field on the ray-orbits, the maximum of luminosity produced by the protons as well as by the electrons will not be sharp (cfr. paper 71).

When the hydrogen (or proton) precipitation has been going on for a long interval of time, hydrogen may accumulate in the atmosphere, and this would have the effect that the electron rays below h_p would excite the H-lines, without noticeable doppler effect. The concentration of hydrogen will probably be small and the sharp H-lines produced below h_p will be very weak.

Thus the constitution of the solar bundles here given leads to the consequence that the H-line-emission and the luminescence produced by the protons should be found above an altitude h_p considerably greater than the height (H_e) of the bottom edge. The height h_p increases with the decrease of proton velocity.

In order to verify this consequence of my auroral theory, we may proceed in the following two ways.

If auroral arcs, bands, draperies or groups of rays are situated at some distance from zenith, it is possible to compare spectrograms taken near the bottom edge with others taken from near the top of the streamers, and if these are fairly long as in ray-groups and draperies, we may get pairs of spectrograms corresponding to height differences of 50 km or much more in the case of very long rays.

In the second procedure we direct the spectrograph towards magnetic zenith and form a picture on the slit of the radiation point and its nearest surroundings. If an auroral corona is formed by fairly long streamers the tops of these will seem to meet near the radiation point ,and in this way we find that a great part of the light entering the slit is emitted near the top of the rays and streamers. In this way we have already been able to show that such an altitude effect of the H-lines exists (cfr. paper 30, 60, 22).

As the spectral composition of the auroral luminescence produced by protons differs essentially from that excited by electrons, it is evident that the variation of the spectral intensity distribution with altitude depends on the magnitude of the proton flux which is indicated by that of the relative intensity of H-lines.

In the study of the variation effects it is of fundamental importance to take into account the influence of changes in the proton flux.

§ 17. Auroral Spectrograms Taken with the «F» Spectrograph.

The dispersion and light power of the «*F*»-spectrograph were given in § 1. The somewhat successful spectrograms which were obtained during the two winters 1951/52 and 52/53 are reproduced on Pl. III (A and B) and Pl. IV. The type of photographic plate, the date, the effective time of exposure and remarks regarding the operation of the spectrograph and auroral types for each spectrogram are to be found in the explanations to the plates at the end of this paper.

The density of spectral features seen in relation to the exposure time gives an idea of the light power of the instrument and of the great variations of the intensity of the various auroral displays. In the case of very strong aurorae strongly exposed spectrograms were obtained in a few minutes. (We may e.g., refer to the spectrograms Pl. III A No. 4, 5, 6, 9, 11 (exposure 3 min.) and the spectrograms on Pl. IV, No. 4, 7, 23, 24). In the case of the heavily exposed spectrograms 9, 10, 11 and 12 pl. IV the exposure lasted from 1 to 7 hours.

We have tried three sorts of plates Kodak 103a (C, E, F). The two plates C and E may perhaps be the most sensitive in the green region, but have the disadvantage that the sensitivity-range towards long waves is too short to give a satisfactory sensitiveness for H_α.

As we know from previous intensity measurements, H_α is much stronger than H_β and H_γ, and if the plate is highly sensitive to H_α, this line is the best indicator for the presence of small effects of hydrogen (or protons).

If we want to study hydrogen effects, we should use a plate for which the high sensitiveness in red reaches beyond the H_α line. The 103a-*F* plate fulfils this condition. The use of H_α as hydrogen indicator, however, meets with the difficulty that H_α falls in between a sequence of bands belonging to the $N_2 1P$-system, and these bands are often very strong, but as their intensity distribution seems to keep fairly constant and has been measured, even a weak H_α-effect will disturb the normal intensity distribution, and we may, by photometric methods, be able to find an approximate value of the relative H_α-intensity. The intensity distribution of the red sequence of $N_2 1P$ bands is given in table XIII.

Table XIII
Intensity distribution of red sequence of $N_2 IP$ bands.

	Transition	Intensity
6 840	3 — 0	100
6 750	4 — 1	108
6 700	5 — 2	106
6 612	6 — 3	97
6 562	$H\alpha$	
6 540	7 — 4	85
6 455	8 — 5	68
6 380	9 — 6	50

§ 18. Presence and Absence of H-lines.

Out of the 41 spectrograms on plates III and IV only 8 show H-lines (or proton effect) although many of the spectrograms which show no trace of H-lines are very heavily exposed. *In these cases the relative proton flux* $^{v_p}/v_e$ *has been very small, and the auroral luminescence is mainly effected by the electron rays of the solar bundle.*

The predominant influence of the electron rays on the excitation of the auroral luminescence is also evident from the great intensity of the red $N_2 1P$ bands which are particularly well shown on the spectrograms taken on 103a-F plates. These facts and many other properties of the auroral spectra cannot be explained by the *proton* bundle proposed by Bennett and Hulbert.

§ 19. Latitude and Altitude Effects of H-lines.

The 4 spectrograms (Pl. III B) which were taken in rapid succession on the same plate near 23^h00^m on December 3. 1951, call for great interest and have already been dealt with in a note to Nature (30). Spectrogram 1 taken near the horizon towards S shows the H_α-line, while it is absent on spectrogram 3 taken towards N. As the two spectrograms appear to be nearly identical in all other respects, the appearance of H_α on No. 1 must be due to latitude effect. The presence of H_α on the spectrograms 2 and 4 which corresponds to the higher part of auroral rays must be regarded as an altitude effect.

The altitude effect is shown very clearly by comparing the spectrograms Pl. IV No. 15 and 16. On the first one, which corresponds to the upper part of a drapery, H_α appears very distinctly in between the red $N_2 1P$-bands, while the second, taken on the same 103a-F plate from the lower part of an aurora, shows no trace of H_α.

The two spectrograms Pl. IV, No. 10 and 11, showing H_β, were taken 25—27. Oct. 1952 with long exposure from various auroral forms in whatever direction they appeared. Some of the light may therefore come from high altitudes and from aurorae on the southern sky.

The spectrogram Pl. IV No. 12 was taken 8.11. towards N and NW from the strongest part of A and D, and in this case the appearance of H_β must be due to an extraordinary strong proton flux at that time.

§ 20. Spectrograms of Pulsating Aurorae.

The Pl. IV contains two spectrograms (*Nos.* 5 and 26) taken on 103a—C plates from pulsating. aurorae. Both of them show the same somewhat unusual features. Compared with the green line (5577) the red OI-doublet and the $N_2^+ 1N$ bands are enhanced, while the red bands of the $N_2 1P$-system are very weak. No H-lines appear and the luminescence is mainly due to electron excitation. All these typical features are explained by assuming that the height of the pulsating aurorae (at any rate in the present cases) is greater than that we ordinarily find for the usual arcs, bands and draperies.

§ 21. The Spectrum of Red Aurorae of Type (A).

The spectrogram Pl. IV No. 13, taken on 103a-C plate from red aurorae of type (A) is extremely interesting.

It is well known that the red colour of this type is caused by the enhancement of the forbidden red OI-doublet, but in addition to the strong red OI-lines the spectrogram shows the following unusual features:

H_α and H_β appear with a relative intensity, which is of a higher order of magnitude than we are used to observe at Tromsø and which is clearly illustrated by the other auroral spectrograms reproduced in this paper.

Table XIV
Intensity distribution.

	Interpretation	Intensity	Remark
6561	$H\alpha$	39	
6364	$OI(^3P_1—^1D_2)$	600	
6300	$OI(^3P_2—^1D_2)$	1800	over exposed
5892	$Na\ D_1D_2$	55	
5577	$OI\ (^1D_2—^1S_0)$	> 2000	over exposed
4862	$H\beta$	5.1	
4709	$N_2^+ 1N(0—2)$	7.6	
4278	» (0—1)	24.4	
3914	» (0—0)	38.4	

The relative intensities of some of the features of spectrogram No. 13 are given in table XIV, from which we see that the H_β line is nearly as strong as the negative nitrogen band 4709 and H_α very much stronger. The intensity of this N_2^+1N band is put equal to 7,6, which is the value we usually found from ordinary aurorae, when the intensity of the green line is put equal to 100. In the present case, however, the intensity of the green line is too great to be measured, although the negative bands are weak.

The photographic density of the red OI line 6364 is very great, but just small enough for a photometric estimate of its intensity, which we found to be about 600 relative to the values of the negative N_2^+-bands. This would make the intensity of the red line (6300) equal to about 1800, and, as seen from the spectrograms, the intensity of the green line (5577) is considerably greater than that of (6300), and it must have a value of some thousands in our scale.

These intensity relations may perhaps be better understood by saying that relative to the intensity of the green line the intensities of the N_2^+1N and N_21P-bands are more than 20 times smaller than they are usually found. This is also evident when we compare the spectrogram No. 13 with others on the Pl. IV, taken on the same sort of photographic plates and with about the same density of exposure of the green line (Cf. eg. Nos. 5, 7, 20, 22, 23, 24, 26).

It is also of interest to notice the unusually great relative intensity of the yellow sodium line. As the exposure took place late at night in January, the Na-line cannot be enhanced by twilight.

As shown by the present spectrograms as well as by the results previously published (18, 22, 32, 60) the relative H-line intensity (or relative proton flux) at Tromsø is ordinarily very small and the typical red aurorae of type (A) very rare. The rare occurrence of a red aurora of type (A) is now accompanied by the rare occurrence of a great relative proton flux, and as the type of spectrogram 13 is essentially different from that produced by electrons, we are forced to assume that the unusual intensity distribution shown by the spectrogram from red aurorae of type (A) is caused by the great relative proton flux. This means that an unusually great part of the luminescence is exited by protons.

This conclusion is further strongly supported by the unusually small relative intensity of the nitrogen bands and by the fact that the intensity of the forbidden red OI doublet as well as that of the relative proton flux increases upwards and towards lower latitudes.

The fact that the intensity of the N_2^+1N bands relative to that of the forbidden OI lines (5577, 6300, 6364) decreases towards lower latitudes (65, 66), is a consequence of the latitude effect of the proton flux.

This explanation of the formation of the red aurorae of the (A) type is also very interesting from a physical point of view. It means that by proton excitation of oxygen there is a greater probability for bringing the O-atom directly to the $^1D_2$-state.

§ 22. Correlation between the Intensity Variations of the Forbidden NI-lines and that of the Proton Flux.

The forbidden transitions between the metastable groundstates $^4S_{3/2}$, $^2D_{5/2, 3/2}$ and $^2P_{1/2, 3/2}$ give the following NI-lines which are observed in the auroral spectrum:

1. Transitions ($^4S_{3/2}$ — $^2D_{5/2, 3/2}$) give the green doublet (5202, 5197) appearing on our spectrograms as a somewhat broad line with a wavelength 5199.
2. Transition ($^4S_{3/2}$—$^2P_{1/2, 3/2}$)give the line 3466,

which however, falls near to the band $N_2 2P$ (3—4) (λ = 3467,5).

3. Transitions ($^2D_{3/2, 5/2}$ — $^2P_{1/2, 3/2}$) give lines in infra-red not observed in the auroral spectrum.

The green doublet, which is the only forbidden *NI*-line for which we have as yet been able to study intensity variations, falls in the neighbourhood of the bands $N_2^+ 1N$(0—3) (λ=5228) and $O_2^+ 1N$ (7—5) (λ = 5234).

It will be convenient to express the relative intensity of the green *NI*-doublet by the ratio: I_{5199}/I_{5228}, which we write $I\left(\frac{5199}{5228}\right)$

Previous comparisons between the relative intensity $I\left(\frac{5199}{5228}\right)$ at Tromsø and Oslo have shown a great increase towards lower latitudes (19 p. 15).

Some of the «*F*» spectrograms reproduced on Pl. IV show the line 5199 and the band head (5228) with very suitable exposure for intensity measurements.

These spectrograms also show very distinctly the lines 5679 and 5002, which according to table Vb should have about the same excitation potential of 21 volts.

On the photometer curve fig. 13 these two lines, the forbidden green *NI*-line and the $N_2^+ 1N$ (0—3) band are indicated. The measured relative intensities are given in table XV.

Table XV.
Latitude Effect of *NI*(5199).

Plate IV No.	$I\left(\frac{5199}{5228}\right)$	$I\left(\frac{5679}{5002}\right)$
6	0,42	2,1
10	0,94	2,2
11	0,30	1,9
12	0,54	2,1
Mean «*F*» Tromsø	0,55	2,075
From Oslo	2,05	1,95

The values in the last column show that the relative intensity $I\left(\frac{5679}{5002}\right)$ of the two *NII*-lines is the same on all the 4 «*F*»-spectrograms at Tromsø and the difference between the values for Tromsø and Oslo is not greater than the possible error.

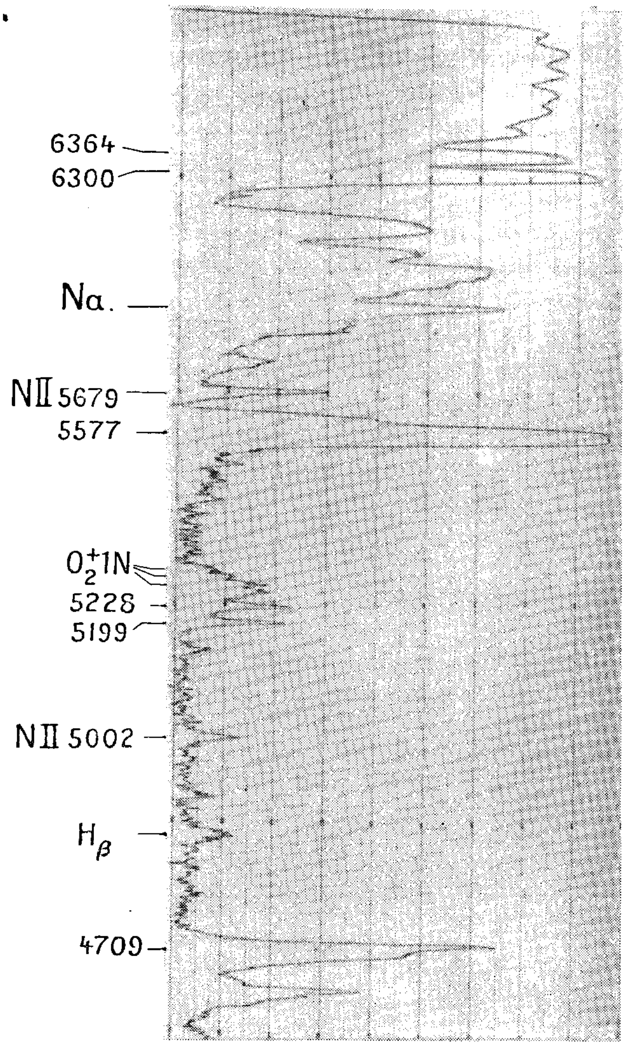

Fig. 13.

On the other hand, the relative intensity of the forbidden *NI*-line on the four Tromsø spectrograms varies considerably from a maximum of 0,94 to the smallest value 0,3. But the mean value at Tromsø 0,55 is very much smaller than the value found at Oslo (2.05). Thus the intensity for the forbidden green *NI*-doublet, like that of the forbidden *OI*-lines, increases rapidly towards lower latitudes. Spectrograms obtained by Dufay et al. (46, 47) from southern Europe show a quite strong forbidden *NI*-line (5199) while no trace of the bands $N_2 1N$(0—3) or $O_2^+ 1N$(7—5) is to be seen.

The rate at which the relative intensity of the forbidden *NI* doublet (5199) increases towards lower latitudes is of about the same order of magnitude as the latitude effect of the red *OI* doublet and that of the proton flux. The forbidden green *NI*-doublet as well as the *OI* doublet are due to transitions from the lowest metastable state ^2D. *This similarity with the red OI-doublet and the strong correlation between the latitude effect, suggest that a predominant fraction of the forbidden NI-line emission is due to proton excitation. This means that the probability for transfer of a neutral N-atom to the metastable ^2D-sate, is very much greater for protons than for electrons.*

A more direct connection between the intensity of the *NI*-doublet (5199) and that of the *H*-lines is shown by the «*V*»-spectrograms on Pl. I, Nos. 1, 3 and 5. They were taken towards magnetic zenith, and show a fairly great relative *H*-line intensity, while No. 8 shows no trace of *H*-lines. The measured relative intensity $I\left(\frac{5199}{5228}\right)$ from the four spectrograms is given in table XVI.

Table XVI.
Correlation between $I\left(\frac{5199}{5228}\right)$ and Proton Flux.

Pl. I No.	Photogr. Pl.	$I\left(\frac{5199}{5228}\right)$	Remarks
1	103a—F	1,00	Tow. mag. Z, $H\alpha$ effect
3	103a—T	0,83	Tow. mag. Z, $H\beta$ effect
5	103a—C	1,54	Tow. mag. Z, $H\beta$ and $H\gamma$ effect
8	103a—C	0,42	No trace of H-lines

The means relative intensity of the three lines showing proton flux is nearly three times greater than that of the spectrogram No. 8, for which the relative proton flux, in spite of high exposure, is too small to be observed.

The possible intensity variations of the forbidden *OII* and *NII* lines have not yet been investigated but from a physical point of view it seems likely, that, under the conditions present in the auroral region, also the probability for transfer of *O*-and *N*-ions to the metastable ground states is greater for a proton than for an electron of the solar bundle.

The spectrogram earlier referred to, which was taken by Petrie (42) and which gave an unusually high apparent band temperature, also showed an extraordinary great intensity of the Vegard-Kaplan bands. We found that the abnormal temperature was caused by a great proton flux. Therefore the unusually great intensity of the V.K. bands indicates that a proton has a greater chance than an electron for transferring the N_2-molecule from the ground state $X^1\Sigma$ to the metastable $A^3\Sigma$—state.

§ 23. Determination of the Ionospheric Temperature by means of N_2^+ IN-bands Taken with the «F» Spectrograph.

Auroral spectrograms obtained in March 1923 (1, 2) showed that the intensity of the N_2^+1N-bands relative to that of the green auroral line increased with altitude, and that these bands formed a predominant part of the auroral luminescence up to the tops of the longest auroral stremers reaching altitudes of 600—800 km.

This result showed that in the auroral region the density of matter decreased upwards much more slowly than could be accounted for by the ordinary barometric height formula, when we assumed that the temperature kept below a few hundred degrees Kelvin.

From the intensity distribution of the rotational bands of the *R*-branch of one of the strongest N_2^+1N-bands (eg. 3914 or 4278) it was found, by experiments and from theoretical considerations, that the temperature in the region corresponding to the spectrograms was far below 0^0C. This led to the development of a theory of the ionosphere based on the photo-electric action of a solar radiation of the type of soft X-rays.

Although the correctness of this theory has been confirmed in a great many ways, it may still be a matter of interest to measure the rotational band temperatures at the greatest possible heights by taking auroral spectrograms from the tops of the highest observable auroral ray bundles or streamers.

For our present purpose no great accuracy of the temperature measurements is needed. If the slow fall of density upwards (or the rapid increase of the «scale height») should be accounted for by temperature variations, the temperature had to increase rapidly, and at altitudes of say 200—300 km reach values of thousands of degrees Kelvin.

In order to obtain spectrograms with suitable

Table XVII.

Ionospheric Temperature determined from »F« spectrograms.

Plate no.		Date	Band	T_m	$T_\varkappa$	Type of Aurora
Pl. III, No.	3	8—12,51	3914		197° K	Strongest part of A, B and R.
»	4	»	»		193° K	Red Lower border of B and D. h = ca. 45°
»	5	»	»		183° K	Strong redidsh yellow A low tow. W
»	6	9—12, 51	»		208° K	Ray structure vivid.
»	9	13—1, 52	4278		247° K	Ray structure, change of colour.
»	10	»	»		233° K	Reddish A in rapid motion
»	11	»	3914		201° K	Reddish and Green, rapid motion.
Pl. IV, No.	1	27/1—20/2.52	»	224° K	240° K	Upper part of Rays.
»	2	15.3—21.3.52	»	224° K	253° K	Lower part of Rays.
»	6	2—10, 52	»		155° K	Reddish A in N-NE,h = 15—45°.
»	7	3—10, 52	»		199° K	D. with ray structure red low. border.
»	10	25.10—26.10.52	»	246° K	237° K	Various Aur. weak H.
»	13	14—11. 52	»	182° K	198° K	Red Au. type A, tow. W.
»	14	14—1. 53	4278		268° K	A. near Zenith.
Not copied		»	3914	176° K	201° K	A. near Zenith.
»	17	24—1. 53	4278	193° K	270° K	A and D various direction.
»		»	3914	202° K	216° K	A and D various direction.
Pl. IV, No.	18	26—1. 53	»		202° K	B and D mostly.
»	19	28—1, 53	»		224° K	Top of B and R with ray structure.
»	20	29—1, 53	»	163° K	164° K	A. tow. N h = ca. 30°.
»	21	»	»	189° K	208° K	Bottom of A and R tow. W.
»	22	»	»	163° K	179° K	Top of Aurora.
»	23	30—1, 53	»	151° K	153° K	Bottom of A tow. W and NW.

photographic density of the strongest N_2^+1N-bands it is essential to use a spectrograph which combine the highest possible light power with a fairly good dispersion and sharpness of lines.

The «*F*» spectrograph fulfils these requirements in a satisfactory way.

In order to obtain some experience with regard to the accuracy with which the ionosperic temperature can be measured with this instrument, measurements have been carried out by means of the band 4278 or 3914 from the spectrograms on plate III A and IV. For the measurements we have used the method which is well known from previous papers (56, 57, 58). The results are collected in Table XVII.

The bands used by the determinations are listed in the third column. The next two columns contain the temperatures T_m and $T_\varkappa$. In the last column we have briefly indicated the auroral type and manner of operation.

On account of the small dispersion, the position of the intensity maximum of the R-branch is not always well defined, and we should therefore recommend relying mainly on the $T_\varkappa$-values.

Taking into account the smaller dispersion, the values found do not show great variations, and they give no indication of increasing temperature with increasing altitude.

The temperatures found from the «*F*» spectrograms and given in table XVII agree well with those found from the «*V*» spectrograms as seen in Table XII and from the mean values in Table XVIII.

Table XVIII

Comparison of Temperatures from «*V*» and «*F*» Spectrograms.

Spectrograph	T_m	$T_\varkappa$
«*V*»	214° K	223° K
«*F*»	192° K	220° K

The results show that the «*F*» spectrograph may be used with advantage by trying the possibility of a very great increase of temperature with altitude.

Acknowledgments.

I wish to express my thanks to Director E. Tønsberg, Mr. S. Berger and Mr. S. Larsen of the Auroral Observatory, Tromsø, for most valuable help in connection with the observational work and to Mr. A. Kyrkjeeide and Mr. O. Skjeggestad for their very able assistance at Oslo in connection with the treatment of the auroral spectrograms. I am also greatly indebted to «Norges Almenvitenskapelige Forskningsråd» for the financial support of my auroral investigations.

Physical Institute, Oslo University.

LIST OF PAPERS

1. L. Vegard: Ann. d. Phys. IV, 50, p. 583, 1916.
2. L. Vegard: Det Norske Vid.-Akad. Oslo. Skr. I. No. 8, 9, 10, 1923; Phil. Mag. 46, p. 193, 1923.
3. L. Vegard: Results of Observations from the Solar Eclipse in Norway, June 29, 1927, and the Constitution of the Solar Corona and Sunspots. Det Norske Vid.-Akad. Oslo. Skr. I. No. 2, 1928.
4. L. Vegard: Die Corona der Erde und Sonne und ihre Beziehungen zu kosmischen Erscheinungen. Gerlands Beiträge z. Geoph. 32, p. 288, 1931.
5. L. Vegard: Geof. Publ. (G.P.), Oslo, Vol. IX, No. 11, 1932.
6. L. Vegard: Phys. of the Earth. Ed. by J. A. Fleming. Vol. VIII, p. 573, 1938. (Written in 1933.)
7. L. Vegard: Ergebnisse d. exakt. Nat. wiss. Vol. XVII, p. 229, 1938.
8. L. Vegard: Coronal Phenomena and their Relation to Solar and Terrestrial Processes. G. P. Vol. XVI, No. 1, 1944.
9. L. Vegard: Hydrogen Showers in the Auroral Region. Nature 144, p. 1089, 1939.
10. L. Vegard and E. Tønsberg: G. P. Vol. XIII, No. 5, 1941. G. P. Vol. XVI, No. 2, 1944.
11. L. Vegard: Proc. of the Meeting at Brussels of the Mixed Commis. on Ionosphere, July 1948, p. 111.
12. L. Vegard: Phys. Soc. Gassiof Committee. Report p. 82, 1948.
13. L. Vegard: Trans. of the Oslo Meeting of IUGG 1948, p. 188 and 479.
14. L. Vegard: Doppler Displacement of Auroral Hydrogen Lines and its Bearing on the Theory of Aurora and Magn. Disturbances, G. P. Vol. XVIII, No. 5, 1952.
15. L. Vegard: C. R. Vol. 230, p. 1884, 1950. Nature 165, p. 1012, 1950. Ann. d. Geophys, Vol. 6, p. 157, 1950.
16. L. Vegard and G. Kvifte: G. P. XVIII, No. 3, 1951.
17. L. Vegard: Transaction of the Congress of IUGG at Brussels 1951. Annales de geophys. Tome 8, fasc. 1, Jan. 1952.
18. L. Vegard: Proc. of Mixed Commis. on the Ionosphere from the Meeting at Camberra 1952.
19. L. Vegard and E. Tønsberg: G. P. Vol. XVIII, No. 8, 1952.
20. A. B. Meinel: a) Astrophys. Journ. Vol. 113, No. 1, 1951. b) Phys. Rev. Vol. 80, No. 6, p. 1096. Des. 15, 1950. c) C. R. 231, p. 1049, 1950.
21. C. W. Gartlein: Phys. Rev. 81, No. 3, p. 463, 1951. Nature 167, p. 277, 1951.
22. L. Vegard: G. P. Vol. XIX, No. 4, 1954.
23. A. B. Meinel: Astrophys. Journ. 112, No. 3, Nov. 1950.
24. J. W. Chamberlain, C. J. Fan, and A. B. Meinel: The Astrophys. Journ. Vol. 120, No. 3, p. 560, 1954.
25. L. Vegard: G. P. Vol. X, No. 4, 1933.
26. L. Vegard: G. P. Vol. XII, No. 5, 1938.
27. L. Vegard: Ann. d. geophys. Tome 6, p. 157, 1950.
28. L. Vegard: G. P. Vol. XIX, No. 4, 1954.
29. L. Vegard and H. Raastad. G. P. XVII, No. 7, 1950.
30. L. Vegard: Nature 170, p. 536, 1952.
31. L. Vegard: Nature 170, p. 1120, 1952.
32. L. Vegard and G. Kvifte: G. P. XIX, No. 2, 1954.
33. B. Rypdal and L. Vegard: G. P. XII, No. 12, 1939.
34. Helge Foss and L. Vegard: Det Norske Vid.-Akad. Oslo, Avh. I, No. 4, 1949.
35. A. B. Meinel: The Spectrum of the Airglow and the Aurora. Reports on Progress in Phys. Vol. 14, p. 121, 1951.
36. A. B. Meinel: Astrophys. Journ. Vol. 113, No. 3, 1951.
37. A. B. Meinel: Astrophys. Journ. Vol. 114, No. 3, Nov. 1951.
38. A. B. Meinel: Excitation Mechanisms in the Aurora. Mem. Soc. roy. des. sci. de Liège XII, I—II, 1952.
39. J. W. Chamberlain and A. B. Meinel: Reprint from Kuiper «The Earth as a Planet». Chicago 1954.
40. W. Petrie and R. Small: The Intensities of Ultraviolet Features of the Auroral Spectrum, Journ. of Geophys. Research. Vol. 57, No. 1, 1952.
41. W. Petrie and R. Small: The Auroral Spectrum

in the Wave-Length Range 3300—8900 Å. Scientific Report No. AR—7 University of Saskatchewan.
42. W. Petrie: Rotational Temperatures of Auroral Nitrogen Bands. Journ. of Atmospheric and Terrestrial Physics. Vol. 4. Nos. 1—2, p. 5, 1953.
43. W. H. Bennett and E. O. Hulburt: The Phys. Review, Vol. 95, No. 2, p. 315, 1954.
Journ. of Atmosperic and Terrestrial Physics. Vol. 5, p. 211, 1954.
44. L. Vegard: On the Determination of Temperature by means of Band Spectra. Det Norske Vid.-Akad. Oslo. Avh. I, 1934, No. 2.
45. L. Vegard, H. Th. Ringdal, and Arne Benedicks: The Determination of Temperature by means of Bands Taken with Spectrographs of small Dispersion. Det Norske Vid.-Akad. Oslo. Avh. I, 1934, No. 13.
46. J. Dufay, Junior Gauzit, Tchang Mao-Lin: Publ. de l'Observatoire de Lyon. T. III, Fasc. 3, 1941.
47. J. Dufay et Tcheng Mao-Lin: Publ. de l'Observatorie de Lyon. T. III, Fasc. 8, 1942.
48. C. W. Gartlein: The Appearance of Hydrogen in Auroral Spectra 1942—51. Extrait de la Société roy. de science de Liège, Tome XII, Fasc. I—II, 1952.
49. D. Barbier and D. R. Williams: Journ. of Geophys. Research Vol. 55, No. 4, Dec. 1950.
50. J. W. Chamberlain and N. J. Oliver: Journ. of Geophys. Research, Vol. 58, No. 4, Des. 1953.
51. N. O. Sayers: Meinel's Infra-Red Auroral Bands. Proc. Phys. Society, A Vol. LXV, p. 152, 1952.
52. J. W. Chamberlain: Excitation of Hydrogen in the Aurorae. The Astroph. Journ. Vol. 120, No. 2, 1954.
53. J. W. Chamberlain: On the Production of Auroral Arcs by Incident Protons. The Astroph. Journ. Vol. 120, No. 3, 1954.
54. A. B. Meinel: The Morphology of the Aurorae, Proc. Nat. Acad. of Sc. 40, No. 10, p. 943, 1954.
55. W. Petrie and R. Small: Canadian Journ. of Physics, 31, 911, 1953.
56. L. Vegard: Terr. Magn. 37, 380, 1932.
57. L. Vegard and E. Tønsberg: G. P. Vol. XI, No. 2, 1935.
58. L. Vegard and E. Tønsberg: G. P. Vol. XII, No. 3, 1938.
59. L. Vegard: G. P. Vol. XIX, No. 4, 1955.
60. L. Vegard: Proc. of the Brussels Meeting 1954 of the Mixed Commission on the Ionosphere.
Secrétariat général de L'U.R.S.I. Bruxelles 1955, pp. 99—102.
61. B. Rypdal and L. Vegard: The Excitation Functions of Nitrogen Bands and their Bearing on Auroral Problems. G. P. Vol. XII, No. 12, 1939.
62. Helge Foss and L. Vegard: Continued Investigations on the Excitation Functions of Nitrogen Bands. Det Norske Vid.-Akad. Oslo. Avh. I, No. 4, 1949.
63. M. E. Pillow: Intensity Distribution among Nitrogen Bands in the Auroral Spectrum.
Proc. of the Phys. Soc. A 67, p. 780, 1954.
64. M. E. Pillow: Intensities in Band Systems of O_2 etc. Proc. Phys. Soc. A 67, p. 847, 1954.
65. L. Vegard: On some Recently Detected Important Variations within the Auroral Spectrum.
Terr. Magn. March 1940, p. 4.
66. L. Vegard: G. P. Vol. XII, No. 14, 1940.
67. L. Vegard: The Origin of the Red Colour of the Aurora etc. Nature 117, 356, 1926.
68. L. Vegard and E. Tønsberg: Variations of the Intensity Distribution within the Auroral Spectrum. G. P. Vol. XI, No. 16, 1937.
69. L. Vegard: Nature 124, p. 947, 1929.
70. L. Vegard: Nature 137, p. 778, 1936, and 138, p. 930, 1936.
71. L. Vegard: Phil. Mag. 42, p. 47, 80, 81, 1921.

Explanation to Pl. I.

The spectrograms are taken with spectrograph «*V*»

Spectr.	Sort of Plate	Date of Exposure	Effective time of exposure	Remarks
1	Kodak 103a—F	10.11.51—15.1.52	ca. 4 hours	Towards magn. zenith
2	» » —F	27.1.1952	» 1 »	Towards magn. equator
3	» » —T	28.1—6.3.52	» 8 »	Various forms and directions
4	» » —O	18.3—25.3.52	» 5 »	Towards magn. Zenith
5	» » —C	25.9—18.12. 52	» 7 »	Towards magn. Zenith
6	» » —C	8—9.1.1953	» 5 »	Weak arcs mostly tow. N.
7	» » —F	13.1—24.1.53	» 7 »	A and D mostly weak, various directions
8	» » —C	28.1—29.1.53	» 2 »	Strong A and D mostly near Z. moonlight.

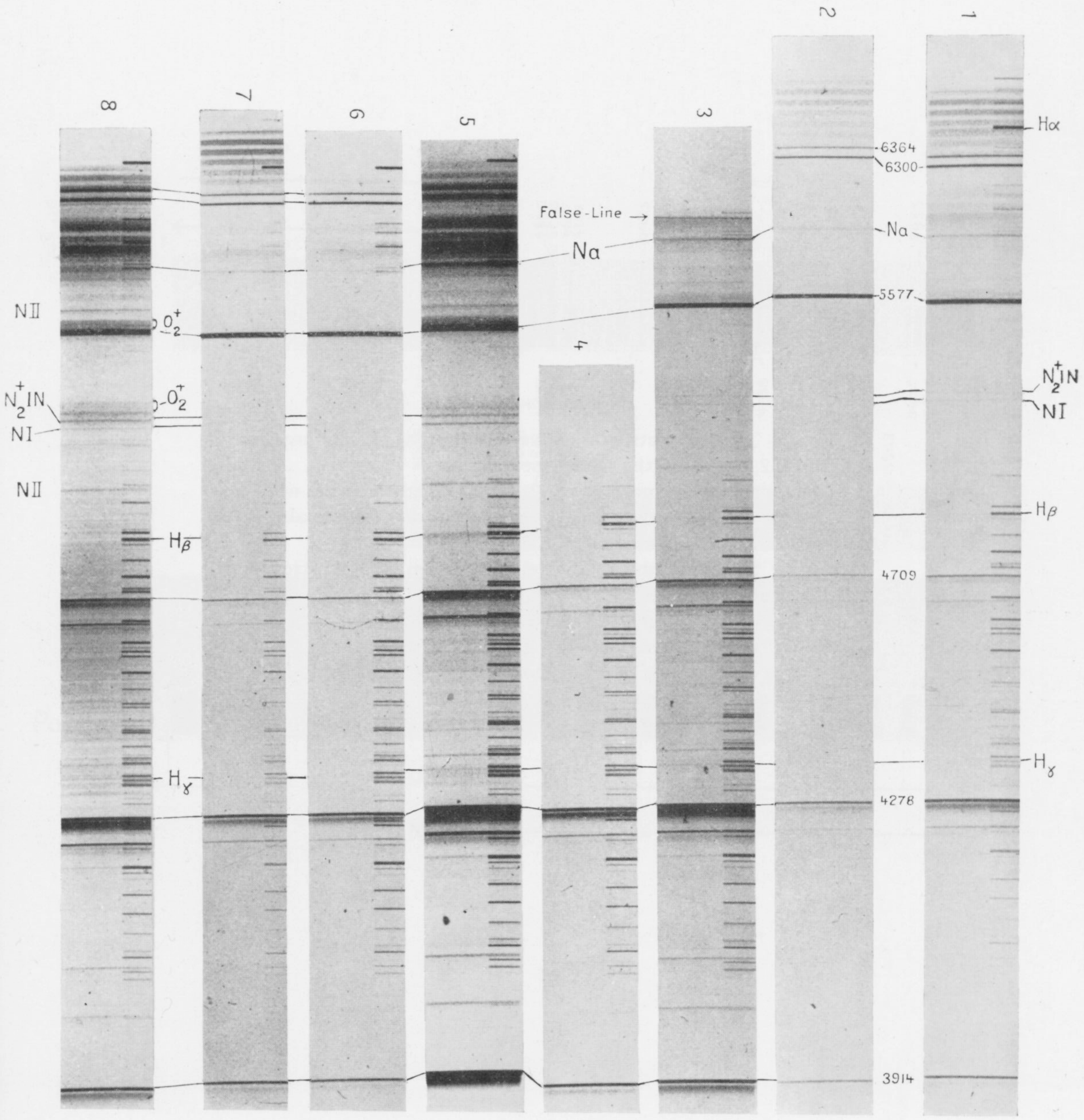
1
2
3
4
5
6
7
8
Hα
6364
6300
Na
False-Line
5577
N_2^+1N
NI
NII
O_2^+
Hβ
4709
Hγ
4278
3914

Explanation to pl. II.

These spectrograms were taken at Würzburg in 1912, all with the same spectrograph.

Spectrograms (a) and (b) were taken from the negative glow (electron excitation) and from the canalrays of an oxygen canal ray tube.

Spectrograms (c), (d), (e) were taken from a nitrogen canalray tube.

c: Nitrogen canal rays.

d: Nitrogen negative glow (swift electrons).

e: Nitrogen positive column (slow electrons).

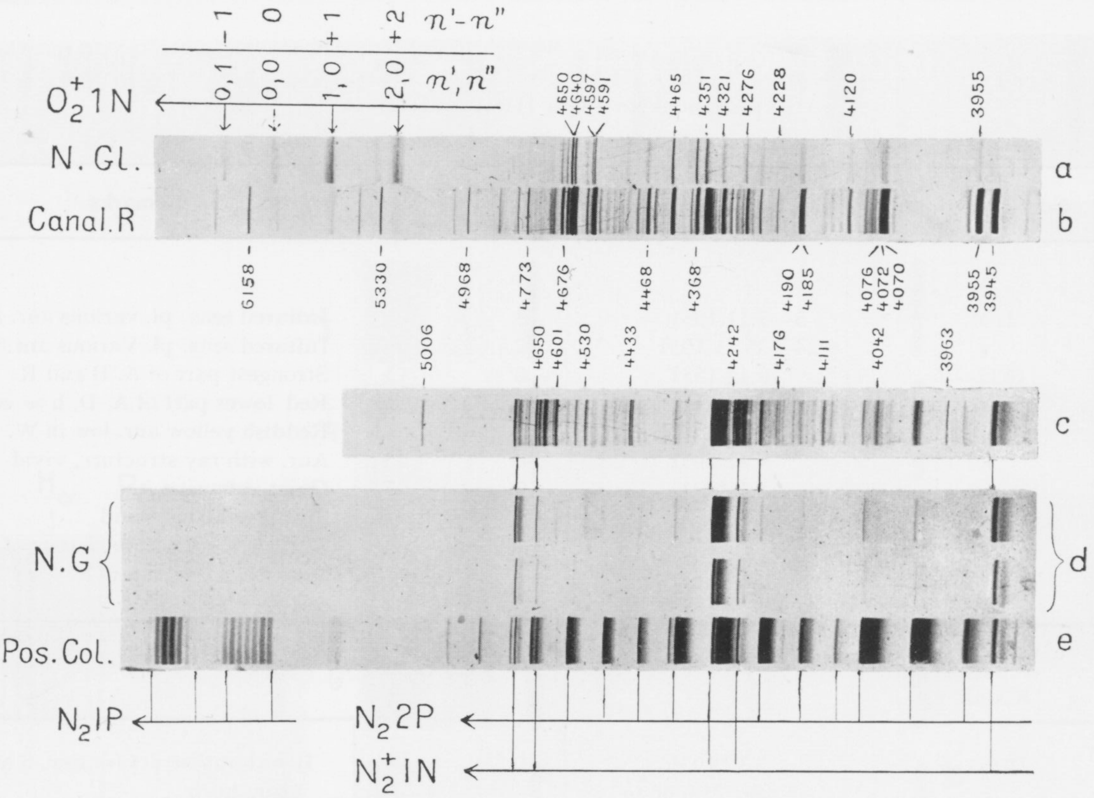

-1 0 +1 +2 n'-n''
0,1 0,0 1,0 2,0 n',n''
O2+ 1N
4650 4640 4597 4591 4465 4351 4321 4276 4228 4120 3955
N. Gl.
Canal.R
a
b
6158 5330 4968 4773 4676 4468 4368 4190 4185 4076 4072 4070 3955 3945
5006 4650 4601 4530 4433 4242 4176 4111 4042 3963
c
N.G
d
Pos. Col.
e
N2 1P
N2 2P
N2+ 1N

Explanations to Plate III A and III B.
Spectrograms taken at Tromsø with spectrograph «*F*».

Pl III A No.	Sort of Kodak pl.	Date	Exposure time		Remarks
			h	m	
1	I. M.	5—7.11.1951	3	00	Infrared sens. pl. various aur. forms
2	»	24—30,11.1951	2	00	Infrared sens. pl. Various aur. forms.
3	103a—F	8.12.1951	0	15	Strongest part of A, B and R
4	»	»	0	03	Red lower part of A, D, h = ca. 45°
5	»	»	0	03	Reddish yellow aur. low in W.
6	»	9.12.1951	0	03	Aur. with ray structure, vivid
7	»	4.1.1952	0	07	Quiet extensive A.
8	»	»	0	02	Strong corona, vivid
9	»	»	0	03	B with R. -structure,change of colour
10	»	»	0	02	Reddish, vivid aurora
11	»	»	0	03	»
Pl. III B No.	**Kodak**				
1	103a—F	3.12.1951 near 23 h 00 m	0	04	B with ray structure tow. S and SE, near, horiz.
2	»	»	0	05	R. near Z.
3	»	»	0	07	A towards N.
4	»	»	0	10	Tow. auroral rays.

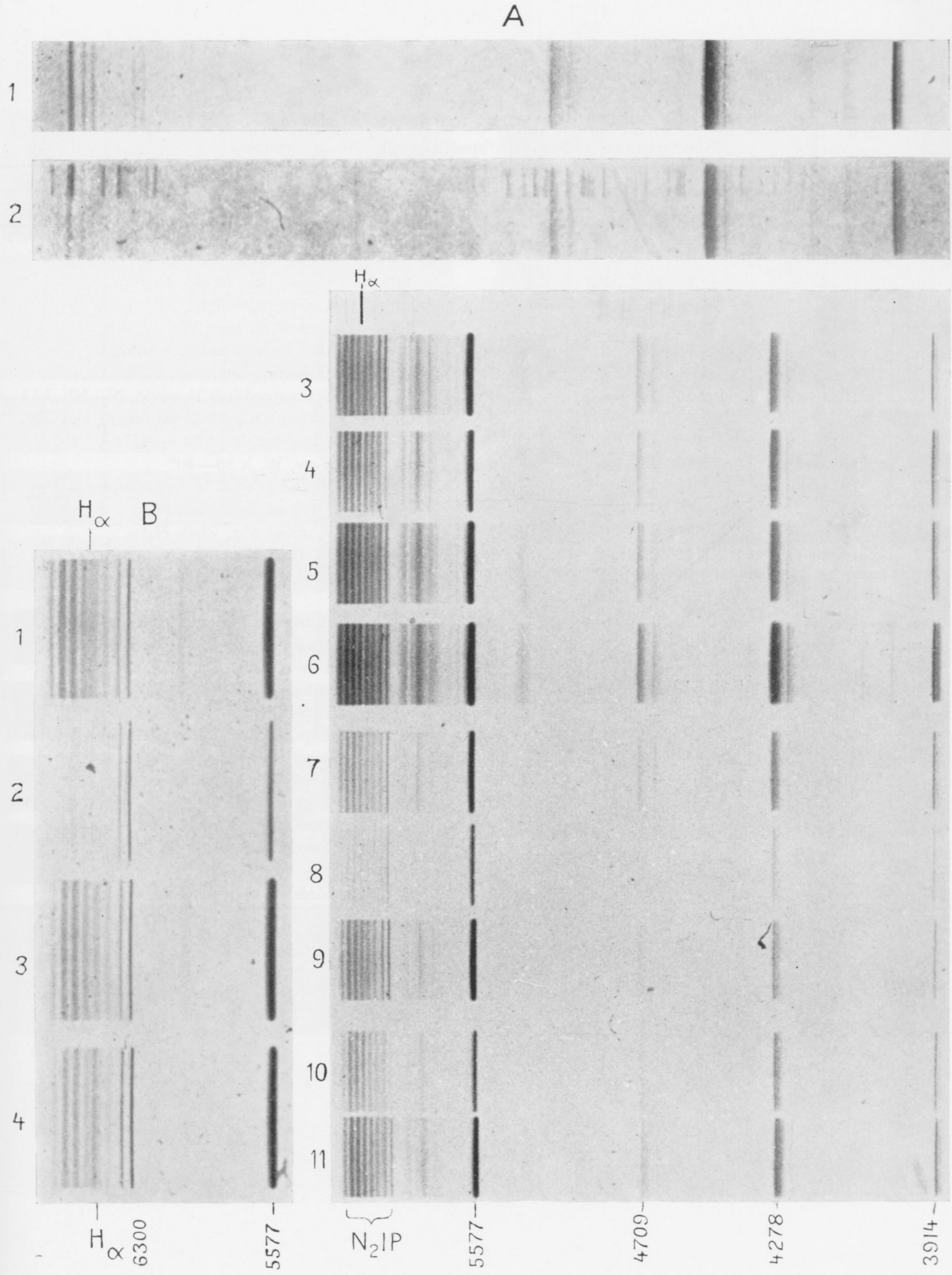
A
1
2
H_α
3
4
5
6
7
8
9
10
11
H_α B
1
2
3
4
H_α
6300
5577
N_2 1P
5577
4709
4278
3914

Explanations to Plate IV.

Spectrograms taken with spectrograph »*F*« at Tromsø.

Pl. IV No.	Sort of Kodak pl.	Date	Exposure time		Remarks
			h	m	
1	103a—E	27.1—20.2.1952	1	30	Upper part of R.
2	103a—E	15.3—21.3.	0	50	Lower part of R.
3	103a—C	29.9.1952	0	03	Top of R. tow. W.
4	103a—C	29.9.1952	0	02	Red lower border. Vivid
5	103a—C	29.9.1952	0	40	Pulsating aur. tow. E. h=ca.45°
6	103a—C	2.10 20(09—28)	0	19	Strong reddish B, vivid, N—NE, h15=45°
7	103a—C	3.10 20(32—41)	0	08	Strong D. with R-structure, red low. border, h — 30 — 45°
8	103a—F	7.10.1952	0	30	Tow. W. h 30—40°
9	103a—F	8.10.1952	1	00	A and B tow. W. — NW.
10	103a—F	25.—26.10 19.00—01.00	5	30	Various aur, weak $H\beta$
11	103a—F	26.—27.10 20.00—03.00	7	00	Various aur, weak $H\beta$
12	103a—C	8.11.52 20.08—23.00	1	24	A, D in N and N-W. h 30—60°
13	103a—C	14.11.52 21.58—22.45	0	47	Red aur.type A, tow. W.$H\alpha$, $H\beta$
14	103a—F	14.1.53 22.35—23.15	0	40	A near Z.
15	103a—F	15.1.53 21.45—00.00	2	15	Upper part of D, tow. W and E
16	103a—F	24.1. 20.05—20.45	0	40	Lower part of A.
17	103a—F	24.1. 20.47—22.00	0	48	A and D, various directions
18	103a—C	28.1. 17.10—17.25	0	15	B and D mostly upper part
19	103a—C	28.1. 17.28—19.28	0	25	Top of B with ray structure
20	103a—C	29.1. 17.45—18.10	0	25	A various directions h ≈ 30°
21	103a—C	29.1.	0	39	A with ray structure
22	103a—C	29.1.	0	20	Top of aur.
23	103a—C	29.1.	0	08	Bottom of A in W and NW
24	103a—C	24.3.53	0	10	Lower part of radiant aur
25	103a—C	24.3.53	0	03	Top of aur. with R.-structure
26	103a—C	24.3.53	0	15	Reddish pulsating aurora.

Plate IV.

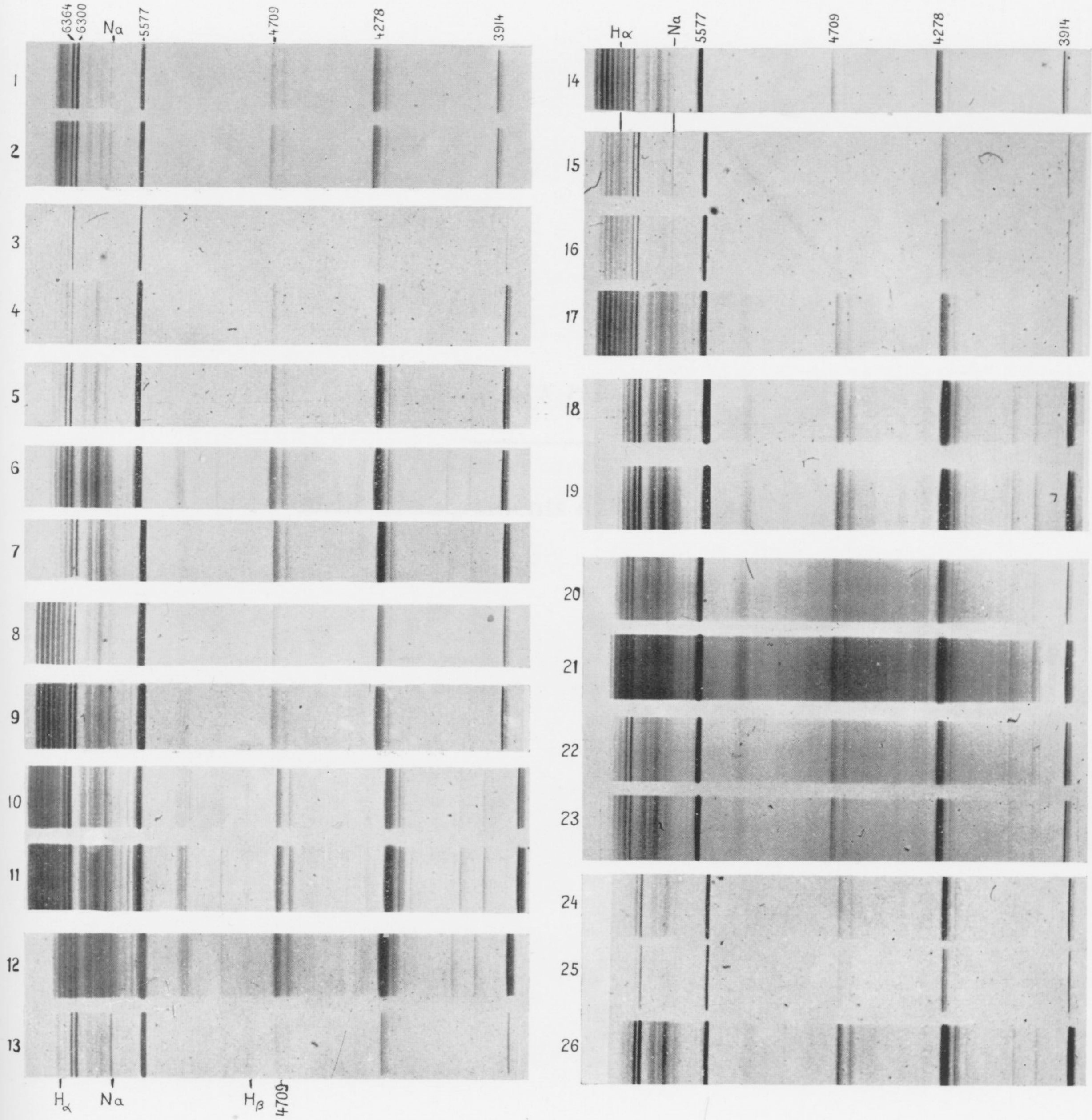
6364
6300
Nα
5577
4709
4278
3914
1
2
3
4
5
6
7
8
9
10
11
12
13
Hα
Nα
Hβ
4709
Hα
Na
5577
4709
4278
3914
14
15
16
17
18
19
20
21
22
23
24
25
26